Single Wheel Robot: Gyroscopical Stabilization on Ground and on Incline

by

Loi-Wah Sun

A dissertation submitted in partial
fulfillment of the requirements for the degree of
Master of Philosophy

in the Division of

Mechanical and Automation Engineering

of

The Chinese University of Hong Kong
Shatin, N.T.,
Hong Kong SAR,
China

22 Feb 2000

Single Wheel Robot: Gyroscopical Stabilization on Ground and on Incline

22 Feb 2000

Abstract

Single Wheel Robot: Gyroscopical Stabilization on Ground and on Incline

by

Loi-Wah Sun

A single wheel gyroscopically stabilized robot is a thin sharp-edged wheel with an actuation mechanism fitted inside the wheel domes that exploit gyroscopic forces for steering and stability. In order to enhance the static stability without losing dynamic stability of a single wheel, an angular momentum of a high spinning flywheel is imposed to achieve the stability in the lateral direction of the robot. At the same time, it performs a steering motion under the gyroscopical precession. It is subjected to a nonholonomic systems with rolling constraints under the non-slip condition. Increasing attention have been paid for a nonholonomic system as it cannot be stabilized to an equilibrium via any smooth time-invariant feedback. In this system, there are two kinds of nonholonomic constraints with different order in our system. Nonholonomic constraints arise from the existence of non-slip rolling condition, high coupling effect between the flywheel and the wheel and the underactuation in the roll direction of the robot. Its dynamics are described by a set of highly nonlinear coupled differential equations and it is unstable in the lateral direction. It is an inherently nonlinear, underactuated, nonholonomic and non-minimum phase system and it is significant to determine the complete study of the dynamics characteristic of the single wheel robot in a cluttered environment. In this thesis, the dynamics and controls of a single wheel robot rolling without slipping on ground and on incline are studied. The motion of a single wheel robot is analyzed using Lagrangian dynamics with no assumptions that the robot is constrained to remain vertical and performs along the horizontal plane. The effects of internal pendulum motion and the inclination angle of the plane are addressed. Linearizing the model around the perpendicular position to the surface, the state feedback controllers for stabilizing the robot from falling over on ground and on incline are proposed respectively. The backstepping control method is designed to balance the robot following a straight path with a general heading angle. The condition of rolling up of the robot on the inclined plane is investigated and different motion strategies are proposed for the robot when violation of the condition of rolling up. The feasibility of the method is then verified by simulation analysis.

摘要

单轮机器人：
地面与斜坡上基于陀螺仪的稳定方法

单轮陀螺仪稳定机器人采用具有刃状边缘的扁平式轮状结构，在拱形轮盖内安装有驱动机构，利用陀螺力进行机器人的方向操纵和保持稳定。为在不损失单轮动态稳定性的前提下增强其静态稳定性，利用一个高速旋转飞轮的转动惯量来获得机器人的横向稳定性。同时，在陀螺的运动过程中也产生一种行驶运动。在无滑动条件下，由于存在滚动约束，它属于一种众所周知的典型非完全约束系统。由于非完全约束系统不能通过平滑非时变反馈稳定于一个平衡点而受到更多的重视。在本文工作中，系统存在两种不同阶次的非完全约束。非完全约束来源于机器人存在无滑动滚动状态，飞轮和单轮间有强耦合效应，以及机器人滚动方向上欠缺驱动作用。机器人的动态过程由一组强耦合非线性微分方程所描述，且其横向是不稳定的。它是一个固有非线性，欠驱动，非完全约束和非最小相位系统。这促使我决定全面研究单轮机器人的动态特征。在研究工作中，考虑了单轮机器人在地面和斜坡上无滑动滚动状态时的动态过程和控制方法。在未假设机器人由于受到约束而保持垂直且工作于水平面上的前提下，采用拉格朗日动态法分析了单轮机器人的运动。论述了内部单摆运动和平面倾斜角的效应。分别提出了围绕表面垂直位置的模型线性化方法和用于稳定机器人避免其在地面和斜坡上跌倒的状态反馈控制器。设计了一种控制方法来稳定机器人使其按通常的前进方位角沿直线路径运动。计算了机器人滚上斜坡的条件，提出了当这些条件被违反时机器人的运动策略。通过仿真分析验证了该方法的灵活性。

Acknowledgments

Most of all I wish to thank Prof. Yangsheng Xu for his patient guidance and invaluable advice during my study. He allowed me much freedom to explore under his guidance. Though the studies were very hard, it is worth to do so. I would like to thank him from the bottom of my heart for his generous support and inspiration. Robotics is a real excitement to me.

I would like to express my gratitude to my thesis advisory committee members, Dr. Yun-Hui Liu and Dr. Jie Huang, for their helpful discussions and suggestions in the project. I would like to extend my sincere thank to Prof. Xiaoping Yun of Naval Postgraduate School for his insightful ideas and reviewed comments of my thesis.

I also owe a debt of gratitude for the invaluable suggestion, concern and encouragement to Dr. Hu-Long Pei and Dr. Bergerman Marcel. I would like to express my thanks to Mr. Wai-Kit Mok Allan, Mr. Yuk-Leung Lee Phillip, Mr. Yun-Yee Leung Martin and Mr. Hang Tong for their technical assistance.

My sincere gratitude is to my dear colleagues for helping me in various ways. I am very grateful to Mr. Kwok-Wai Au for having discussion and sharing his ideas with me. His valuable suggestions on my research are absolutely appreciated. I also gratefully acknowledge Mr. Wai-Keung Fung and Mr. Chi-Tin Yang for their unconditional assistance. Special thanks are to Mr. Wai-Kuen Yu Wilson, Mr. Ka-Keung Lee, Mr. Kwok-Ho Law Cedric, Mr. Tin-Tak Tseung for their kindly help and encouragement.

My thanks also due to staff members in Department of Mechanical and Automation, who have helped me but whose names have not been mentioned individually.

Last but not the least, my deep hearty thanks go to my family and all my friends for their support and concern throughout my studies.

Contents

List of Figures

List of Tables

Chapter 1

Introduction

1.1 Motivation

A single wheel gyroscopically stabilized robot originally was developed by Xu & B. Brown at Carnegie Mellon University since 1992 [7]. The concept of mobility they proposed is a sharp-edged wheel, with an actuation mechanism fitted inside the wheel domes. The robot itself uses a high spinning flywheel as a gyroscope for stabilizing the robot, and it also actuated by a spinning flywheel for steering and a drive motor for propulsion.

In this research work, the author deals with the system of dynamically stable but statically unstable. A nice example illustrating many features of dynamically stable but statically unstable systems is the bicycle. The bicycle always fall sideways when it is stationary. Consequently, the bicycle itself is assumed to be balanced by the action of its rider. Rider pedal so as to keep the bicycle upright. When riding a bicycle faster, it is more stable and could not fall over even. When he feels the vehicle falling, he steers into the direction of leaning and so traverses a curved trajectory of such a radius as to generate enough centrifugal force to correct the fall. The faster a bicycle moves the easier it is to ride. Also when a bicycle pushed and released riderless, it will stay up on its own, traveling in a long curve and finally collapsing. It can travel much more time without falling, comparing to it would take if static. Almost everyone have experience with bicycle and probably this common sense by observation, yet apparently not everyone knows how it works. The phenomenon it is describing can be explained in term of gyroscopic procession. The detail of description you can refer to Section 1.1.2.

It also falls into the class of systems which cannot be stabilized to an equilibrium via any smooth time-invariant feedback. Nonholonomic system defined as system in

which there are constraints on the velocities of the robots which cannot be integrated to give constraints which are exclusively a function of the configuration variables. For instant, systems with linear velocity constraints of the form $w_i(x)\dot{x} = 0$, $i = 1, \ldots, k$, however, it cannot be written as an algebraic constraint in the configuration space such as $h_i(x) \neq c_i$. A constraint is said to be nonholonomic or nonintegrable.

The static roll stability of bicycle should be sacrificed in order to enhance the dynamic roll stability. Nevertheless, its configuration conveys significant advantage over high speed operation of a mobile robot. If the vehicle moves in relative high speed, it has much difficult to roll over compared with the static stable system. The torques generated by the dynamic disturbances at the wheels, can be reduced for preventing upset the vehicle about the roll, pitch and yaw axes. The obstacle crossing ability of the vehicle may be enhanced. The dynamic effect consideration have much significance especially in high speed operation, weak gravity environment and great dynamic disturbance situation.

The new dynamic mobility which is unstable statically are proposed [7]. A single wheel, gyroscopically stabilized robot connected by a spinning flywheel through a manipulator at the wheel bearing. In order to augment static stability without loss of dynamic stability, the spinning flywheel is used to provide an angular momentum for lateral stability even when the wheel operated very slow or is idling. Its ideal is to take advantage of the dynamic stability of a single wheel, but augment it with a gyroscope to achieve static stability. A series of single wheel robots, whose family name is *Gyrover*, had been developed at Carnegie Mellon University. *Gyrover* comes from two words, *Gy*-roscopic and *rover* respectively. It means as a rover, which relies on gyroscopic action for dynamic stability, is delivered to a planet's surface for exploration and transportation. Three prototypes have been developed.

1.1.1 Literature review

There are precedents for single-wheel-like vehicles [15, 16, 19, 29]. In ancient time, the single wheel vehicles were designed as operator who was circling by the domes and he rides inside the vehicle. In the past of the western countries, a large wheel encircling the rider was created by R.C. Hemmings in 1869 [15], executing the dream of more peoples. A Velocipede, got patents for Hemmings, which used hand cranks for controlling. Later, Pallmer describes several single-wheel vehicles. A 1935 publication [29] he introduced the Gyroauto, which carried the riders between a pair of large, side-by-side wheels, and was claimed capable of a speed of 187 *kph*. Moreover, he describes Dyno-Wheel [29]. It is a concept having a bus-like chassis straddling a huge central wheel. The relative large

diameter of a single-wheel vehicle enhances its obstacle-crossing ability, smoothness of motion and rolling efficiency.

Many researchers took their effort on the dynamics and control of autonomous unicycle and bicycle [35, 36, 41]. An autonomous stabilized unicycle was studied by Schoonwinkel [35]. Consider a unicycle acts as three rigid bodies composed of a wheel, a frame and a rotary turntable. He modeled the motion of a unicycle operated by the human. And he separated the lateral and longitudinal dynamics by perturbated the yaw rate to specific quantities and constructed a autonomous stabilized robot.

The study of dynamics on inclined surfaces has a long history in Physics since the time of Galileo's experiments [9] and the work of Coulomb on friction in the 18th century. However, all of Galileo's theorems and propositions are only restricted for spheres rolling down an incline. Rui [31] proposed a controller for asymptotically path tracking of a rolling disk which is allowed to perturb from the vertical position. However, one strong assumption is that there is a torque generated directly acting on the roll direction of the disk for balancing.

Not until recently some researchers started to work with gyroscopical stabilization [2, 3, 5, 7, 27, 40, 44, 45, 47]. Gyroscopical stabilization of bicycle was studied by Beznos et al. [5]. It is consisting of two coupled gyroscopes spinning in the opposite directions. He linearized the system model, but the yaw dynamics of bicycle were not considered and the steering angle was decoupled from the dynamics. It was assumed to be a input for directly controlling of the steering front wheel. Besides, the motion was only restrict on the horizontal plane.

Our research group concentrated on this kind of concept [2, 3, 7, 27, 44, 45] and studied about the dynamics of the single wheel robot. Using constrained Lagrangian method, the kinematics constraints and system dynamics were determined. They provided the linearized model around the vertical position and investigated the controllability of non-minimum phase characteristic of the system. An algorithm was proposed for tracking the reference steering velocity by restricting the robot to an equilibrium lean angle which corresponds to that steering velocity.

They studied its nonholonomic constraints, its stabilizing effect of the flywheel to the system through simulation and tilting up of the flywheel on the robot by both of simulation and experiments. The work is of significant in understanding of utilizing this type of mobility with dynamically stability yet statically instability in the field and service application.

However, their work [2, 3, 7, 27, 44, 45] have suffered from some limitations; (1) The dynamic models developed previously assumes that the single wheel robot remains

strictly on the flat plane and it fails to represent the actual motions when the robot is perturbed from the vertical position and it rolls up a slope. (2) In the deviation of the robot dynamics, a single wheel robot in general should be considered as a single wheel, actuated through a spinning flywheel attached through a two-link manipulator at the wheel bearing and a drive motor, but for simplifying of the model, the previous approach assumed that the mass center of flywheel and the internal mechanism was assumed to be coincident with the center of the robot, and the horizontal offset between the plane of wheel and the moving body frame was neglected. The variation of this simplified model will be studied on the following chapter. Based on the linear, simplified model, all simulations were conducted on his dissertation. For steady motion of the robot, the pendulum motion of the internal mechanism was only to be neglected. The pendulum swinging motion was without under consideration as θ was assumed to be zero.

Tsai [40] developed robot dynamic model. The model of the single wheel robot was investigated as the control point of view. He applied Extended Kalman filter EKF to estimate the state vector of the Gyrover and the complete state too. The pendulum swinging motion considered in his work. The nonlinear dynamics equations of motion about the unstable equilibrium point was then linearized. The operation point stated that the robot is upright and gyro is horizontal. However, dynamics were not symbolically yet analytically. For instance, when non-minimum phase of the system was proved, the matrix was a number instead of symbol form. The observer-based controller experimental result was provided but the simulations result was missing.

For the work of Yu [48], the input selection of tilting up task of a simple wheel robot was determined. Sensitivity Analysis and Factor Analysis were proposed for selecting state inputs of the system. The Human Control Strategies (HCS) model was learned modeled human control input from the human point of view. And then the sensitivity analysis for input selecting based on the simplified model of Au, which is only limited to the model without l_1.

As those limitations stated before, it motivates the author to exploit the whole picture of dynamics of the single wheel robot research. The research work of the author reveals that dynamics of a single wheel gyroscopically stabilizing robot posses richer and more complicated dynamical aspects in comparison with the simplified systems proposed that the model develops without l_1 and θ. Many researchers have viewed wheeled robots with high maneuverability, capable of dynamic behavior, high speed traveling on rough terrain. The goal of our research group are concentrated on developing an automatic control for a single wheel robot on rough terrains. Essentially,

the single wheel robot is a novel concept for mobility that employs gyroscopic effect to stabilize a single wheel robot. The model established in this thesis is more general in the sense that it should not be difficult to describe the real robot in practical.

1.1.2 Gyroscopic precession

In this section, we would like to highlight the fundamentals of gyroscopic precession and the principles of steering of the single wheel robot. Now, we take a rolling coin as an example for explaining the fundamentals of gyroscopic precession.

Consider a coin rolling on the flat plane. After rolling for a while, the coin not only starts to fall over, but it also begins to turn. It is so interesting to see that a rolling coin actually turns in the direction that it is leaning. This phenomenon can be explained by the clenched fist rule and the right hand rule. The clenched fist rule: Hold the right hand so that the fist is tightly clenched with fingers curled and the thumb is straight and pointing away from the fingers. If we consider a rolling coin leans to the right hand side, the gravitational torque induced is: $\tau = r \times mg\cos\theta$. The fingers curled is used as the direction of gravitational torque and the straight thumb will point into the paper i.e the forward direction. The direction of the straight thumb is called as D_{grav}. As the coin is rolling, by the clenched fist rule, the curled fingers show the direction of spinning rate $\dot{\gamma}$ and then the straight thumb which points into the paper are represented by D_{spin}. The right hand rule: the forefinger and the middle finger represent D_{spin} and D_{gra} respectively. The thumb will show the axis of precession of the coin, by the clenched fist rule again, the direction of the curled fingers are the direction of precession rate. It is shown in the Figure 1.1.

It is the same phenomenon as riding a bike. A bicycle can be balanced by the action of its rider. The rider can steer the bike in the direction of fall when he/she wants to prevent the bike from falling. This theory is formalized mathematically. Because of its angular momentum, a spinning wheel tends to precess at right angles to an applied torque, according to the fundamental equation of gyroscopic precession [7]:

$$T = J\dot{\gamma} \times \Omega \tag{1.1}$$

where $\dot{\gamma}$ is the angular speed of the wheel, Ω is the wheel's precession rate, normal to the spin axis, J is the wheel polar moment of inertia about the spin axis, $J\dot{\gamma}$ is the angular momentum of the wheel and T is the applied torque, normal to the spin and precession axes. It is shown in the Figure 1.2. Therefore, when a rolling wheel leans to one side, rather than just fall over, the gravitationally induced torque causes the wheel

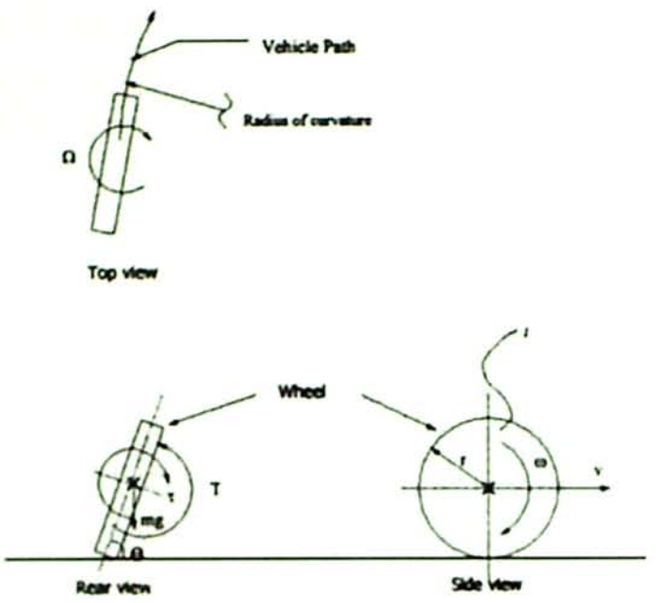

Figure 1.1: The principle of gyroscopic precession

Figure 1.2: The right hand rule

to precess so that it turns in the direction that it is leaning.

1.2 Thesis overview

In this Chapters of the thesis we discuss important problems related to the modeling, dynamics and control of a single wheel robot either in the horizontal plane or on inclines that have not yet been studied in the past. The outline of this thesis is as follow:

In Chapter two, we consider the dynamics and feedback control of a single wheel robot rolling without slipping on a rough horizontal plane; In general the single wheel robot system is considered as a sharp-edged wheel actuated by a spinning flywheel attached through a manipulator. The vertical offset of the actuation mechanism from the axis of the wheel was not been neglected. The general rolling single wheel robot system, when the pendulum swinging motion included, represents much richer dynamics and deserves attention. The derivation of the dynamical equations is similar to the development in Au [7, 27, 44, 45]. During the developing of the model, variable reduction of the dynamics itself was applied. We used state variables $[\alpha, \beta, \gamma \,\&\, \theta]$ to describe the whole systems. Its approaching of input selection is totally different from the work of Yu [48].

In this work, the author was concentrated to estimate the stabilizing of the robot around vertical position and the tilting up of flywheel on the robot when the internal mechanism are to swing inside the wheel. We are analysized these three kind of dynamic characteristics on rolling disk, simplified model of the robot (model proposed by Au) and modified model of the robot (the general model). The simplification of the model by Au is only applied when the robot reaches at the steady state. These models fail to represent the actual dynamics especially in the transient state. On the simulation analysis for the tilting up motion of flywheel, preliminary experimental results are shown for verifying the developed model. It is more general in the sense that model should not be difficult to extend for description of the real robot in practical. Despite of it, the dynamic models we developed previously fails to represent the actual motion when the robot is perturbed from the vertical position and it rolls up a slope. It was because that the robot remains strictly on the flat plane.

In Chapter three, the dynamics of a robot rolling without slipping on an inclined plane are established. The general model of the single wheel robot on incline is studied. The new dynamics of a single wheel robot without slipping on an inclined plane were also investigated. We pay much attention for study the gyroscopical stabilization of the robot on inclined plane when the dynamics of a robot rolling without slipping on an inclined plane are established.

We first derived the kinematics and dynamics of a rolling disk without slipping on

the inclined plane. After that we developed the model of the single wheel robot which is considered as a combination of three rigid body components: a wheel, an internal mechanism and a flywheel. The general model of the single wheel robot on incline is established. For model simplification, the flywheel is located at the center of the wheel and the swinging effect is terminated. It is because the extension of the general single wheel robot system on an inclined plane is extremely complicated. The equation of motion of a single wheel robot on an inclined plane differs significantly from that on horizontal plane. On an incline, some components of the gravity forces act on the system. The motion of a single wheel robot is analyzed using Lagrangian dynamics with no assumption that the robot is constrained to remain vertical. We then linearized the dynamic model around the position perpendicular to the surface.

In Chapter four, we proposed a feedback controller for stabilization of the robot from falling over on an inclined plane , which based on the linear model. Moreover, the backstepping control was designed to balance the robot following a straight path with a general heading angle. The feasibility and efficiency of the method is then validated by simulation study.

In the Chapter five, we addressed the condition of rolling up of the robot on an inclined plane from the system dynamics itself. Furthermore, we developed a measure that Safety Factor is actually a performance index which measures the robot's ability successfully to roll up a slope from its at rest. And then, we suppose some method for planning of rolling up by tracking the robot's motion in different motion strategies.

Chapter 2

Dynamics of the robot on ground

In this chapter, we investigate the dynamics and control of a single wheel robot when it rolls without slipping on a horizontal plane. Using the constrained generalized Lagrangian formulation, general form of dynamical equations of a single wheel robot is derived. We linearize the dynamical model around the vertical position. The stabilizing effect of the robot as its upright and the tilting up of flywheel on the robot are determined respectively. We then study dynamics characteristic of a single wheel robot on the basis of the dynamical equations. The effect of swinging motion is estimated. We summarize that the elimination of the pendulum motion from the dynamics by Au [2, 3, 7, 27, 44, 45] is only applied to the robot which is reached at the steady state. Moreover, the modified model of the single wheel robot is validated by the preliminary experimental results. The dynamic analysis of some important parameters is also determined.

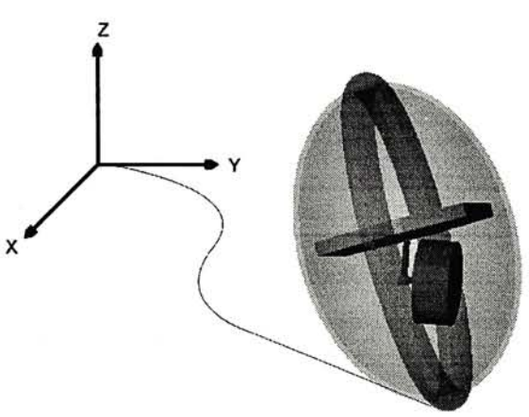

Figure 2.1: A single wheel robot rolls on ground

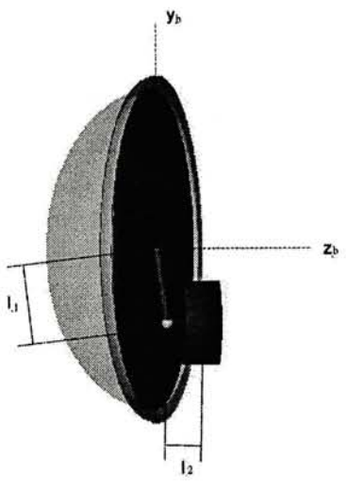

Figure 2.2: Top view of a single wheel robot

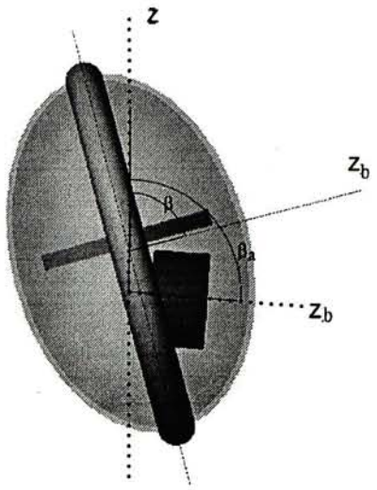

Figure 2.3: Front view of a single wheel robot

2.1 System model re-derivation

We developed dynamical model of a single wheel robot using the constrained Lagrangian method, as well as kinematics constraints [44]. However, so far no attempt has been considered the internal pendulum swinging of the robot. A single wheel robot consists of a rim and two polycarbonates domes that carry the drive shaft. Around this shaft swings the main body of the Gyrover, this motion is so called pendulum swinging. Past research on the Gyrover [2, 3, 7, 27, 44, 45] assumed that the pendulum motion of the internal mechanism is sufficiently small to be neglected when the robot reaches in the steady state. And then the parameter of θ should be taken out from the dynamics. On the contrary, at the transient state, there are significant coupling effects between the steering (gyro-tilt) and propulsion (pendulum swinging). The system will possibly come to singularity without considering pendulum swinging motion properly.

Now we discuss with the model derivation of a single wheel robot on ground. In Figures 2.1, 2.2 and 2.3 show that a single wheel robot, is a sharp-edged wheel actuated by a two-link manipulator, with a spinning disk (gyro) attached at the end of the second link. Figure 2.2 shows that the first link of length l_1 represents the vertical offset of the actuation mechanism from the axis of the single wheel robot. And the second link of length l_2 represents the horizontal offset of the spinning flywheel. There is no offset between the axis of tilt & gyro rotor and the middle plane of whole structure on the robot. The l_2 is set to be zero. It means that the flywheel's center of mass coincides with that of the internal mechanism. A summary of the definition of model variables is

Table 2.1: Variable definition

α	Precession angles of the wheel measured about the vertical axis
β	Lean angles of the wheel
β_a	Tilt angle between the link l_1 and z_a-axis of the flywheel
γ, γ_a	Spin angles of the wheel and the flywheel, respectively
θ	Angle between link l_1 and x_B-axis of the wheel
m_w, m_i, m_f	Mass of the wheel, internal mechanism and flywheel respectively
m	Total mass of the robot
R, r	Radius of the wheel and the flywheel respectively
I_{xw}, I_{yw}, I_{zw}	Moment of inertia of the wheel about x, y and z axes
I_{xf}, I_{yf}, I_{zf}	Moment of inertia of the flywheel about x, y and z axes
μ_s, μ_g	Friction coefficient in yaw and pitch directions, respectively
u_1, u_2	Drive motor torque and the tilt motor torque, respectively

shown in Table 2.1. The coordinates frames of the system are divided into three major frames:

1. The inertial frame $\Sigma_O XYZ$, whose XY plane is anchored to the flat surface and Z is vertical position,

2. The body coordinate frame $\Sigma_B X_b Y_b Z_b$, whose origin is located at the center of the single wheel, and whose z-axis represents the axis of rotation of the wheel,

3. The flywheel coordinates frame $\Sigma_D X_d Y_d Z_d$, whose center is located at the center of the flywheel, and whose z-axis represents the axis of rotation of the flywheel. Note that Y_b is always parallel to Y_d.

We have derived the general dynamical equation of a single wheel robot using the constrained generalized Lagrangian formulation, showed as detailed in [45]. Those velocity constraints are

$$\dot{X} = R(\dot{\gamma}C_\alpha + \dot{\alpha}C_\alpha C_\beta - \dot{\beta}S_\alpha S_\beta) \tag{2.1}$$

$$\dot{Y} = R(\dot{\gamma}S_\alpha + \dot{\alpha}C_\beta S_\alpha + \dot{\beta}C_\alpha S_\beta) \tag{2.2}$$

$$\dot{Z} = R\dot{\beta}C_\beta \quad \Rightarrow \quad Z = RS_\beta \tag{2.3}$$

Equations (2.1) and (2.2) are nonintegrable and hence are nonholonomic while Equation (2.3) is integrable.

The dynamics equations of a single wheel robot are

$$\bar{M}(q)\ddot{q} + \bar{N}(q, \dot{q}) = Bu \tag{2.4}$$

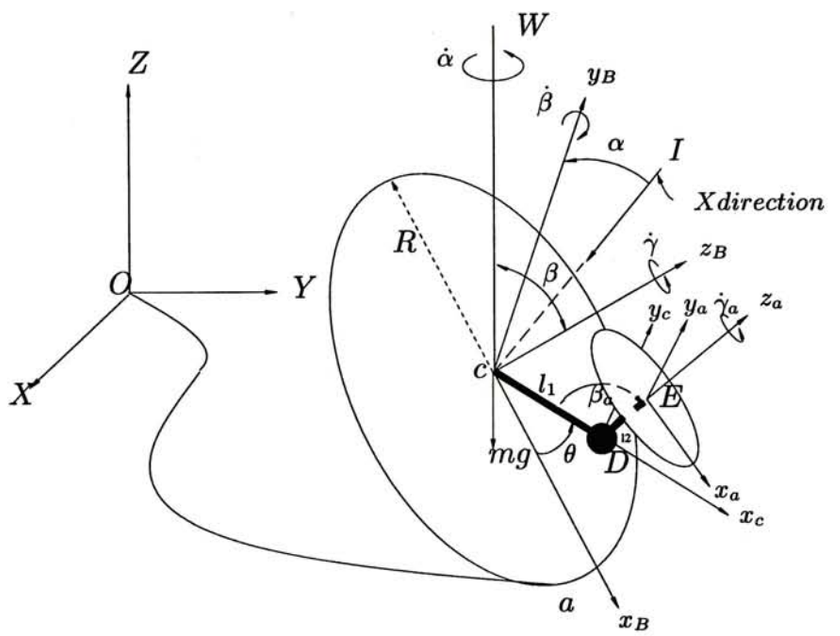

Figure 2.4: Definition of coordinate frames and system variables of the robot model

$$\bar{M} = \begin{bmatrix} \bar{M}_{11} & 0 & \bar{M}_{13} & 0 & \bar{M}_{15} \\ 0 & \bar{M}_{22} & 0 & \bar{M}_{24} & \bar{M}_{25} \\ \bar{M}_{13} & 0 & \bar{M}_{33} & 0 & \bar{M}_{35} \\ 0 & \bar{M}_{24} & 0 & \bar{M}_{44} & 0 \\ \bar{M}_{15} & \bar{M}_{25} & \bar{M}_{35} & 0 & \bar{M}_{55} \end{bmatrix}, \quad B = \begin{bmatrix} 0 & 0 & 1 & 0 & k \\ 0 & 0 & 0 & 1 & 0 \end{bmatrix}^T$$

where,

$$\begin{aligned}
\bar{M}_{11} &= I_{xf} + I_{xw} + I_{xw}C_\beta^2 + mR^2C_\beta^2 + I_{xf}\left(C_{\beta_a}^2C_\beta^2 - C_\beta C_{\beta_a}C_\theta S_\beta S_{\beta_a} + C_\theta^2 S_\beta^2 S_{\beta_a}^2\right) - 2l_1 m_a RC_\theta C_\beta^2 \\
\bar{M}_{13} &= \left(2I_{xw} + mR^2 - l_1 m_a RC_\theta\right) C_\beta \\
\bar{M}_{15} &= l_1 m_a C_\beta \left(1 - RC_\theta\right) \\
\bar{M}_{22} &= I_{xf} + I_{xw} + mR^2 + m_a l_1^2 C_\theta^2 - 2m_a l_1 RC_\theta S_\beta^2 \\
\bar{M}_{24} &= I_{xf}C_\theta \\
\bar{M}_{25} &= -l_1 m_a RS_{2\beta}S_\theta \\
\bar{M}_{33} &= 2I_{xw} + mR^2 \\
\bar{M}_{35} &= -l_1 m_a RC_\theta \\
\bar{M}_{55} &= l_1^2 m_a \\
\bar{N}_1 &= \{2I_{xf}C_\beta S_\beta(C_\theta^2 - 1) + 2I_{xf}(C_{\beta_a}C_\theta S_\beta^2 S_{\beta_a} + C_\beta C_\theta^2 S_\beta S_{\beta_a}^2 - C_\beta C_{\beta_a}^2 S_\beta - C_\beta^2 C_{\beta_a}C_\theta S_{\beta_a}) \\
&\quad -(I_{xw} + mR^2)S_{2\beta} + m_a l_1^2 C_\beta C_\theta S_\beta + 4m_a l_1 RC_\beta C_\theta S_\alpha^2 S_\beta + 2I_{xf}C_\beta S_\beta S_\theta^2\}\dot{\alpha}\dot{\beta} \\
&\quad +2I_{xf}\{C_{\beta_a}C_\theta^2 S_\beta^2 S_{\beta_a}^2 + C_\beta C_\theta S_\beta S_{\beta_a}^2 - C_\beta C_{\beta_a}^2 C_\theta S_\beta - C_\beta^2 C_{\beta_a}S_{\beta_a}\}\dot{\alpha}\dot{\beta}_a \\
&\quad -l_1 m_a RS_\theta \dot{\alpha}\dot{\gamma} + \{-l_1 m_a RC_\beta S_\theta + l_1^2 m_a C_\beta C_\theta S_\theta + I_{xf}C_{\beta_a}S_\beta S_{\beta_a}S_\theta + I_{xf}C_\beta C_\theta S_{\beta_a}^2 S_\theta\}\dot{\beta}^2 \\
&\quad \{-\frac{1}{4}l_1^2 m_a C_{2\beta}S_\theta + 2l_1 m_a RC_\beta^2 S_\theta + l_1^2 m_a C_\theta S_\theta + 2I_{xf}C_\beta C_{\beta_a}S_\beta S_{\beta_a}S_\theta - 2I_{xf}C_\theta S_\beta^2 S_{\beta_a}^2 S_\theta\}\dot{\alpha}\dot{\theta}
\end{aligned}$$

$$
\begin{aligned}
&+\{-I_{xf}C_{\beta}S_{\theta}C_{2\beta_a}+2I_{xf}C_{\beta_a}C_{\theta}S_{\beta}S_{\beta_a}S_{\theta}\}\dot{\beta}\dot{\beta}_a+\{-2I_{xf}C_{\beta_a}S_{\beta}-2I_{xf}C_{\beta}C_{\theta}S_{\beta_a}\}\dot{\beta}\dot{\gamma}_a\\
&+\{2l_1^2m_aC_{\theta}^2-I_{xf}C_{\beta}C_{\beta_a}C_{\theta}S_{\beta_a}+I_{xf}C_{\theta}^2S_{\beta}S_{\beta_a}^2-I_{xf}S_{\beta}S_{\beta_a}^2S_{\theta}^2\}\dot{\beta}\dot{\theta}+l_1m_aRC_{\beta}S_{\theta}\dot{\theta}^2\\
&\{-2I_{xf}C_{\beta_a}C_{\theta}S_{\beta}-2I_{xf}C_{\beta}S_{\beta_a}\}\dot{\beta}_a\dot{\gamma}_a-2I_{xw}S_{\beta}\dot{\beta}\dot{\gamma}-I_{xf}S_{\beta}C_{\theta}\dot{\beta}_a\dot{\theta}-2S_{\beta}S_{\theta}S_{\beta_a}\dot{\theta}\dot{\gamma}_a\\
\bar{N}_2 \;=\;&\{(I_{xw}+mR^2)\,S_{\beta}C_{\beta}+I_{xf}\,(C_{2\beta_a}S_{\beta}C_{\beta}+C_{\theta}C_{2\beta}S_{2\beta_a})-2l_1m_aRC_{\theta}S_{\beta}C_{\beta}+l_1^2m_aS_{\theta}C_{\theta}\\
&+l_1^2m_aS_{\theta}C_{\theta}^2\}\dot{\alpha}^2+\{-l_1^2m_aS_{\beta}+l_1^2m_aS_{\beta}C_{2\theta}-2l_1m_aRC_{\theta}S_{\beta}\}\dot{\alpha}\dot{\theta}+mgRC_{\beta}-gl_1m_aC_{\beta}C_{\theta}\\
&+\{2I_{xw}S_{\beta}+mR^2S_{\beta}-l_1m_aRC_{\theta}S_{\beta}\}\dot{\alpha}\dot{\gamma}+I_{xf}C_{\beta}S_{\theta}\dot{\alpha}\dot{\beta}_a+2I_{xf}\{C_{\beta_a}S_{\beta}+C_{\beta}C_{\theta}S_{\beta_a}\}\dot{\alpha}\dot{\gamma}_a\\
&+\{(S_{2\beta_a}C_{2\theta})I_{xf}-I_{xf}S_{\theta}C_{\theta}+2m_al_1RS_{\theta}-2l_1^2m_aS_{\theta}C_{\theta}\}\dot{\theta}\dot{\beta}-I_{xf}S_{\beta_a}C_{\theta}\dot{\theta}\dot{\gamma}_a-I_{xf}S_{\theta}\dot{\beta}_a\dot{\theta}\\
&+2l_1m_aRS_{\beta}C_{\beta}C_{\theta}\dot{\theta}^2-I_{xf}S_{\theta}C_{\beta_a}\dot{\gamma}_a\dot{\beta}_a\\
\bar{N}_3 \;=\;&l_1m_aRS_{\theta}(\dot{\alpha}^2+\dot{\theta}^2+2C_{\beta}\dot{\alpha}\dot{\theta})-2\{I_{xw}+mR^2-l_1m_aRC_{\theta}\}S_{\beta}\dot{\alpha}\dot{\beta}\\
\bar{N}_4 \;=\;&I_{xf}\{C_{\beta_a}(C_{\beta}^2-C_{\theta}^2S_{\beta}^2)S_{\beta_a}\}\dot{\alpha}^2-S_{\theta}\dot{\beta}\dot{\theta}-C_{\theta}S_{\beta}\dot{\alpha}\dot{\theta}-2S_{\theta}^2S_{\beta_a}C_{\beta_a}\dot{\beta}^2+2S_{\theta}C_{\beta_a}\dot{\beta}\dot{\gamma}_a\\
&+\{-C_{\beta}+C_{\beta}C_{\beta_a}^2-C_{\beta}S_{\beta_a}^2-2C_{\beta_a}C_{\theta}S_{\beta}S_{\beta_a}\}S_{\theta}\dot{\alpha}\dot{\beta}+2\{C_{\beta_a}C_{\theta}S_{\beta}+C_{\beta}S_{\beta_a}\}\dot{\alpha}\dot{\gamma}_a\\
\bar{N}_5 \;=\;&gl_1m_aS_{\beta}S_{\theta}+\{-l_1m_aRC_{2\beta}S_{\beta}+l_1^2m_aC_{\theta}S_{\theta}+\frac{1}{2}\,(I_{xf}C_{2\beta_a}C_{\theta}S_{\theta}-I_{xf}C_{\theta}S_{\theta})\}\dot{\beta}^2+\frac{1}{8}\{I_{xf}S_{2\theta}\\
&+(1-4R)\,C_{2\beta}S_{\theta}-2I_{xf}S_{2\beta}S_{\theta}-2I_{xf}S_{2\beta}S_{2\beta_a}S_{\theta}-4Rl_1m_aS_{\theta}-2l_1^2m_aS_{2\theta}S_{2\theta}-I_{xf}C_{2\beta}S_{2\theta}\\
&-2I_{xf}C_{2\beta}S_{\beta}^2S_{2\theta}\}\dot{\alpha}^2+I_{xf}C_{\theta}S_{\beta}\dot{\alpha}\dot{\beta}_a-l_1m_aRC_{\beta}S_{\theta}\dot{\alpha}\dot{\gamma}+2I_{xf}C_{\theta}S_{\beta_a}\dot{\beta}\dot{\gamma}_a-2I_{xf}S_{\beta}S_{\theta}S_{\beta_a}\dot{\gamma}\dot{\gamma}_a\\
&+I_{xf}S_{\theta}\dot{\beta}\dot{\beta}_a+\Big\{\frac{1}{2}S_{\beta}\Big(I_{xf}C_{2\beta_a}+2l_1m_a(1+2RC_{\theta})-(I_{xf}+2l_1^2m_a)C_{2\theta}\Big)+\frac{1}{2}I_{xf}C_{\beta}C_{\theta}S_{2\beta_a}\Big\}\dot{\alpha}\dot{\beta}
\end{aligned}
$$

$\bar{M}(q) \in \mathbb{R}^{5\times5}$ is the inertial matrix of the single wheel robot which is a positive definite. And $\bar{N}(q,\dot{q}) \in \mathbb{R}^{5\times1}$ is nonlinear term. The generalized variable and inputs variables are represented by $q = [\alpha, \beta, \gamma, \beta_a, \theta]^T$ and $u = [u1, u2]^T$ respectively. The configuration of the single wheel robot can be described by five generalized coordinates $[\alpha, \beta, \gamma, \beta_a, \theta]^T$.

The single wheel robot has more degrees of freedom than a rolling disk, owing to the swinging motion of the link l_1 and the tilting motion of the flywheel. The flywheel's angular momentum produces lateral stability when the wheel is stopped or moving slowly. A tilt mechanism enables tilting the flywheel's axis about the roll axis with respect to the wheel. Because the flywheel acts as an inertial reference in attitude, the immediate effect of the tilt action is to cause the wheel leaning left or right, which in turn causes the wheel to steer in the direction of leaning. Torques generated by a drive motor, reacting against the suspended internal mechanism which pendulum swings as well as produce thrust for acceleration and braking. The turning (steering) of the wheel is the result of gyroscopic procession about the yaw axis, caused by roll torques as explained before, in the Section 1.1.2. Because the wheel have large angular momentum of flywheel in order to provide a good low speed or static stability. The flywheel spins very fast. The spin motor cannot generate an enough torque for sudden change of angular velocity. It is reluctance to change the spinning rate of flywheel so the angular velocity of the flywheel is set to be constant. It is not used for the control purposes. In this case, the control of a single wheel robot is achieved by two generalized

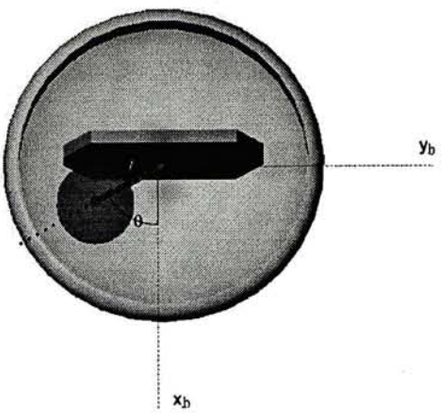

Figure 2.5: Side view of a single wheel robot

inputs:(1) the drive torque (u_1) for propulsion $\dot{\gamma}$ as well as swinging pendulum $\dot{\theta}$, (2) the tilt torque (u_2) for tilting the flywheel for lateral stability.

The system dynamics can be decoupled by the tilting variable β_a. Similar as the case of decoupling the steering variable from the bicycle dynamics shown in [5],[12]. As $\dot{\beta}_a$ denotes as a new input u_{β_a}, the dynamics model in Equations (2.4) re-determined.

The dynamic model of the robot on ground (*System[1]*) is

$$\begin{aligned} \tilde{M}(\tilde{q})\ddot{\tilde{q}} + \tilde{N}(\tilde{q},\dot{\tilde{q}}) &= \tilde{B}\tilde{u}. \\ \dot{\beta}_a &= u_{\beta_a} \end{aligned} \tag{2.5}$$

with $\tilde{q} = [\alpha, \beta, \gamma, \theta]^T$,

$$\tilde{M} = \begin{bmatrix} \tilde{M}_{11} & 0 & \tilde{M}_{13} & \tilde{M}_{14} \\ 0 & \tilde{M}_{22} & 0 & \tilde{M}_{24} \\ \tilde{M}_{13} & 0 & \tilde{M}_{33} & \tilde{M}_{34} \\ \tilde{M}_{14} & \tilde{M}_{24} & \tilde{M}_{34} & \tilde{M}_{44} \end{bmatrix} = \begin{bmatrix} \bar{M}_{11} & 0 & \bar{M}_{13} & \bar{M}_{15} \\ 0 & \bar{M}_{22} & 0 & \bar{M}_{25} \\ \bar{M}_{13} & 0 & \bar{M}_{33} & \bar{M}_{35} \\ \bar{M}_{15} & \bar{M}_{25} & \bar{M}_{35} & \bar{M}_{55} \end{bmatrix}$$

$$\tilde{B} = \begin{bmatrix} 0 & 0 & 1 & 0 \\ \tilde{B}_1 & \tilde{B}_2 & 0 & \tilde{B}_4 \end{bmatrix}^T, \tilde{N} = \left[\tilde{N}_1, \tilde{N}_2, \tilde{N}_3, \tilde{N}_4\right]^T, \tilde{u} = [u_1, u_{\beta_a}]$$

$$\begin{aligned} \tilde{N}_1 = \; & \{2I_{xf}C_\beta S_\beta(C_\theta^2 - 1) + 2I_{xf}(C_{\beta_a}C_\theta S_\beta^2 S_{\beta_a} + C_\beta C_\theta^2 S_\beta S_{\beta_a}^2 - C_\beta C_{\beta_a}^2 S_\beta - C_\beta^2 C_{\beta_a} C_\theta S_{\beta_a}) \\ & -(I_{xw} + mR^2)S_{2\beta} + m_a l_1^2 C_\beta C_\theta S_\beta + 4m_a l_1 R C_\beta C_\theta S_\alpha^2 S_\beta + 2I_{xf}C_\beta S_\beta S_\theta^2\}\dot{\alpha}\dot{\beta} \\ & -l_1 m_a R S_\theta \dot{\alpha}\dot{\gamma} + \{-l_1 m_a R C_\beta S_\theta + l_1^2 m_a C_\beta C_\theta S_\theta + I_{xf}C_{\beta_a}S_\beta S_{\beta_a}S_\theta + I_{xf}C_\beta C_\theta S_{\beta_a}^2 S_\theta\}\dot{\beta}^2 \\ & \{-\frac{1}{4}l_1^2 m_a C_{2\beta} S_\theta + 2l_1 m_a R C_\beta^2 S_\theta + l_1^2 m_a C_\theta S_\theta + 2I_{xf}C_\beta C_{\beta_a} S_\beta S_{\beta_a} S_\theta - 2I_{xf}C_\theta S_\beta^2 S_{\beta_a}^2 S_\theta\}\dot{\alpha}\dot{\theta} \\ & +\{2l_1^2 m_a C_\theta^2 - I_{xf}C_\beta C_{\beta_a} C_\theta S_{\beta_a} + I_{xf}C_\theta^2 S_\beta S_{\beta_a}^2 - I_{xf}S_\beta S_{\beta_a}^2 S_\theta^2\}\dot{\beta}\dot{\theta} + l_1 m_a R C_\beta S_\theta \dot{\theta}^2 \end{aligned}$$

$$
\begin{aligned}
& +\{-2I_{xf}C_{\beta_a}S_{\beta} - 2I_{xf}C_{\beta}C_{\theta}S_{\beta_a}\}\dot{\beta}\dot{\gamma}_a - 2I_{xw}S_{\beta}\dot{\beta}\dot{\gamma} - 2S_{\beta}S_{\theta}S_{\beta_a}\dot{\theta}\dot{\gamma}_a \\
\tilde{N}_2 \;=\; & \{\left(I_{xw}+mR^2\right)S_{\beta}C_{\beta} + I_{xf}\left(C_{2\beta_a}S_{\beta}C_{\beta} + C_{\theta}C_{2\beta}S_{2\beta_a}\right) - 2l_1m_aRC_{\theta}S_{\beta}C_{\beta} + l_1^2m_aS_{\theta}C_{\theta} \\
& +l_1^2m_aS_{\theta}C_{\theta}^2\}\dot{\alpha}^2 + \{-l_1^2m_aS_{\beta} + l_1^2m_aS_{\beta}C_{2\theta} - 2l_1m_aRC_{\theta}S_{\beta}\}\dot{\alpha}\dot{\theta} + mgRC_{\beta} - gl_1m_aC_{\beta}C_{\theta} \\
& +\{2I_{xw}S_{\beta} + mR^2S_{\beta} - l_1m_aRC_{\theta}S_{\beta}\}\dot{\alpha}\dot{\gamma} + 2I_{xf}\{C_{\beta_a}S_{\beta} + C_{\beta}C_{\theta}S_{\beta_a}\}\dot{\alpha}\dot{\gamma}_a - I_{xf}S_{\beta_a}C_{\theta}\dot{\theta}\dot{\gamma}_a \\
& +\{(S_{2\beta_a}C_{2\theta})I_{xf} - I_{xf}S_{\theta}C_{\theta} + 2m_al_1RS_{\theta} - 2l_1^2m_aS_{\theta}C_{\theta}\}\dot{\theta}\dot{\beta} + 2l_1m_aRS_{\beta}C_{\beta}C_{\theta}\dot{\theta}^2 \\
\tilde{N}_3 \;=\; & l_1m_aRS_{\theta}(\dot{\alpha}^2 + \dot{\theta}^2 + 2C_{\beta}\dot{\alpha}\dot{\theta}) - 2\{I_{xw} + mR^2 - l_1m_aRC_{\theta}\}S_{\beta}\dot{\alpha}\dot{\beta} \\
\tilde{N}_4 \;=\; & gl_1m_aS_{\beta}S_{\theta} + \{-l_1m_aRC_{2\beta}S_{\beta} + l_1^2m_aC_{\theta}S_{\theta} + \frac{1}{2}\left(I_{xf}C_{2\beta_a}C_{\theta}S_{\theta} - I_{xf}C_{\theta}S_{\theta}\right)\}\dot{\beta}^2 + \frac{1}{8}\{I_{xf}S_{2\theta} \\
& +\left(1-4R\right)C_{2\beta}S_{\theta} - 2I_{xf}S_{2\beta}S_{\theta} - 2I_{xf}S_{2\beta}S_{2\beta_a}S_{\theta} - 4Rl_1m_aS_{\theta} - 2l_1^2m_aS_{2\theta}S_{2\theta} - I_{xf}C_{2\beta}S_{2\theta} \\
& -2I_{xf}C_{2\beta}S_{\beta}^2S_{2\theta}\}\dot{\alpha}^2 - l_1m_aRC_{\beta}S_{\theta}\dot{\alpha}\dot{\gamma} + 2I_{xf}C_{\theta}S_{\beta_a}\dot{\beta}\dot{\gamma}_a - 2I_{xf}S_{\beta}S_{\theta}S_{\beta_a}\dot{\gamma}\dot{\gamma}_a \\
& +\Big\{\frac{1}{2}S_{\beta}\Big(I_{xf}C_{2\beta_a} + 2l_1m_a(1+2RC_{\theta}) - (I_{xf}+2l_1^2m_a)C_{2\theta}\Big) + \frac{1}{2}I_{xf}C_{\beta}C_{\theta}S_{2\beta_a}\Big\}\dot{\alpha}\dot{\beta} \\
\tilde{B}_1 \;=\; & -2I_{xf}\{C_{\beta_a}C_{\theta}^2S_{\beta}^2S_{\beta_a} + C_{\beta}C_{\theta}S_{\beta}S_{\beta_a}^2 - C_{\beta}C_{\beta_a}^2C_{\theta}S_{\beta} - C_{\beta}^2C_{\beta_a}S_{\beta_a}\}\dot{\alpha} + I_{xf}S_{\beta}C_{\theta}\dot{\theta} \\
& -\{-I_{xf}C_{\beta}S_{\theta}C_{2\beta_a} + 2I_{xf}C_{\beta_a}C_{\theta}S_{\beta}S_{\beta_a}S_{\theta}\}\dot{\beta} + 2I_{xf}\{C_{\beta_a}C_{\theta}S_{\beta} + C_{\beta}S_{\beta_a}\}\dot{\gamma}_a \\
\tilde{B}_2 \;=\; & -I_{xf}C_{\beta}S_{\theta}\dot{\alpha} + I_{xf}S_{\theta}C_{\beta_a}\dot{\gamma}_a + I_{xf}S_{\theta}\dot{\theta} \\
\tilde{B}_4 \;=\; & -I_{xf}C_{\theta}S_{\beta}\dot{\alpha} - I_{xf}S_{\theta}\dot{\beta}
\end{aligned}
$$

Equations (2.5) show the reduced dynamic model of the single wheel robot after decoupling the tilting variable β_a , with new matrices $\tilde{M}(\tilde{q}) \in \mathbb{R}^{4\times4}$ and $\tilde{N}(\tilde{q},\dot{\tilde{q}}) \in \mathbb{R}^{4\times1}$. Note that if the lean angle β is set to be $0°$ or $180°$, the inertial matrix $\tilde{M}$ will become singular as in the case of the rolling disk. Also, the lean angle β does not couple with the rolling angle γ and the steering angle α in acceleration level, while they are coupling in velocity level through the cross terms $\dot{\alpha}$ and $\dot{\beta}$. It is different from typical underactuated systems such as the underactuated manipulators because most of them are subjected on acceleration coupling. More discussions are given in the next chapter.

2.1.1 Linearized model

We at first linearize the dynamic model around its upright position. The system should be linearized around the vertical position such as $\beta = 90° + \delta\beta, \beta_a = \delta\beta_a, \dot{\beta} = \delta\dot{\beta}, \theta = \delta\theta, \dot{\beta}_a = u_{\beta_a}, \dot{\gamma} = \Omega_0 + \Omega$. In our derivation of linearized model we make the following assumptions:

- all the components are rigid
- the wheel rolls without slipping
- the ground is flat enough
- there is friction on the contact between the wheel and the ground, and on the drive motor and transmission

- the angular velocity of the gyro keeps remain constant
- the wheel remains in contact with the ground
- the term $\delta\dot{\beta}, \delta\dot{\beta}_a, \dot{\alpha}, \dot{\theta}$ are sufficiently small
- the terms $\dot{\gamma}_a\dot{\beta}, \dot{\gamma}\dot{\alpha}$ are much large enough compared with $\dot{\beta}\dot{\gamma}, \dot{\beta}\dot{\alpha}, \dot{\alpha}^2$.

The linearized model is given by

$$2I_{xw}\delta\dot{\beta}\Omega_0 + 2I_{xf}\delta\dot{\beta}\dot{\gamma}_a + 2I_{xf}\dot{\gamma}_a u_{\beta_a} - \mu_s\dot{\alpha} = (I_{xf} + I_{xw})\ddot{\alpha} \quad (2.6)$$

$$(mR - l_1 m_a)gm\delta\beta - 2I_{xf}\dot{\gamma}_a\dot{\alpha} - (2I_{xw} + mR^2 - l_1 m_a R)\Omega_0\dot{\alpha} = (I_{xf} + I_{xw} + mR^2 + m_a l_1^2 - 2m_a l_1 R)\delta\ddot{\beta} \quad (2.7)$$

$$(2I_{xw} + mR^2)\dot{\Omega} = -\mu_g\Omega + u_1 \quad (2.8)$$

$$-l_1 m_a R\dot{\Omega} + l_1^2 m_a\ddot{\theta} = \tilde{R}u_1 \quad (2.9)$$

The key point for the stabilization of the robot is the coupling effect between the yaw and roll motions while no actuator direct drive the control of the roll motion. For the low yaw rate, $\ddot{\alpha} = \ddot{\beta} = \ddot{\gamma} = \ddot{\theta} = 0, \dot{\beta} = \dot{\beta}_a = \dot{\theta} = 0, u_1 = u_{\beta_a} = 0$.

$$\dot{\alpha}_s = \frac{(l_1 m_a C_\theta - mR)gC_\beta}{(2I_{xf}S_\beta + mR^2 S_\beta - l_1 m_a R C_\theta S_\beta)\dot{\gamma} + (C_{\beta_a}S_\beta + C_\beta C_\theta S_{\beta_a})2I_{xf}\dot{\gamma}_a} \quad (2.10)$$

If β is not equal to 90°, the wheel turns according to the Equation (2.10). The control method for the stabilization of a single wheel robot is to propose an algorithm for tracking the reference steering velocity by stabilizing the robot to an equilibrium lean angle which corresponds to that steering velocity.

2.2 A state feedback control

In this section, the control properties of the system are determined. From Equations (2.6),(2.7),(2.8) & (2.9), it is clear to notice that $\ddot{\alpha}$ is affected by u_{β_a} and $\dot{\Omega}$ & $\ddot{\theta}$ are affected by u_1 while $\ddot{\beta}$ is only indirectly affected by u_{β_a}, u_1. As Ω and θ are independent of the roll and yaw dynamics. We then combine Equations (2.6) and (2.7) into one subsystem and Equations (2.8) and (2.9) into other subsystem.

Define state variables $x_1 = \delta\beta, x_2 = \delta\dot{\beta}, x_3 = \dot{\alpha}, x_4 = \theta, x_5 = \dot{\theta}, x_6 = \Omega$, state equations form

$$\dot{x} = f(x) + g(x)u \quad (2.11)$$

where

$$\begin{cases} \dot{x}_1 &= x_2 \\ \dot{x}_2 &= a_{21}x_1 + a_{23}x_3 \\ \dot{x}_3 &= a_{22}x_3 + a_{32}x_2 + bu_\beta \end{cases} \quad \text{and} \quad \begin{cases} \dot{x}_4 &= x_5 \\ \dot{x}_5 &= c_2u_1 \\ \dot{x}_6 &= c_3x_6 + u_1 \end{cases} \tag{2.12}$$

For

$$\begin{aligned} a_{21} &= \frac{(mR - l_1m_a)g}{I_{xf} + I_{xw} + mR^2 + m_al_1^2 - 2m_al_1R} \\ a_{23} &= \frac{-(2I_{xw} + mR^2 - l_1m_aR)\Omega_0 - 2I_{xf}\dot{\gamma}_a}{I_{xf} + I_{xw} + mR^2 + m_al_1^2 - 2m_al_1R} \\ a_{32} &= \frac{2I_{xf}\dot{\gamma}_a}{I_{xw} + I_{xf}} \\ a_{22} &= \frac{-\mu_s}{I_{xw} + I_{xf}} \\ c_2 &= \frac{R}{l_1} \\ c_3 &= -\frac{\mu_g}{2I_{xw} + mR^2} \\ b &= \frac{2I_{xf}\dot{\gamma}_a}{I_{xw} + I_{xf}} \end{aligned}$$

The angular velocity of flywheel keeps remain at very high speed 16000 *rpm*. We select u_β such that $\beta, \dot{\beta}$ & $\dot{\alpha}$ converge to zero. The input u_β should be chose as

$$u_\beta = -k_1\beta - k_2\dot{\beta} - k_3\dot{\alpha}$$

And then we select

$$u_1 = \frac{-k_4\theta - k_5\dot{\theta}}{c_2}$$

The rolling speed of the wheel converges to Ω_0. If $\mu_g > a > 0$, as a is a constant, we can select that u_β & u_1 such that all state variables $(\beta, \dot{\beta}, \dot{\alpha}, \theta, \dot{\theta}, \Omega)$ will converge to zero. It is a closed loop for controlling system dynamics.

2.3 Dynamic characteristics of the system

In this section, we study the controllability, observability and non-minimum phase characteristics of the system. Let

$$\begin{aligned}
\mathbb{C} &= [B\,|AB|\,A^2B] \\
&= \begin{bmatrix} 0 & 0 & a_{23}b \\ 0 & a_{23}b & a_{22}^2 b \\ b & a_{22}b & a_{32}a_{23} + a_{22}^2 \end{bmatrix} \\
&= a_{23}^2 b^3 \\
&= \left(\frac{(2I_{xw} + mR^2 - l_1 m_a R)\Omega_0 + 2I_{xf}\dot{\gamma}_a}{I_{xf} + I_{xw} + mR^2 + m_a l_1^2 - 2m_a l_1 R}\right)^2 \left(\frac{2I_{xf}\dot{\gamma}_a}{I_{xw} + I_{xf}}\right)
\end{aligned}$$

If $\dot{\gamma}_a \neq 0$, the rank is 3. The system is controllable when the spinning rate of flywheel is not equal to zero. And the system is observable when $\dot{\gamma}_a \neq 0$. As

$$\begin{aligned}
\mathbb{Q} = \begin{bmatrix} C \\ CA \\ CA^2 \end{bmatrix} &= \begin{bmatrix} 0 & 0 & 1 \\ 0 & a_{32} & a_{22} \\ a_{21}a_{32} & a_{22}a_{32} & a_{32}a_{23} + a_{22}^2 \end{bmatrix} \\
&= -a_{21}a_{32}^2 \\
&= \left(\frac{(mR - l_1 m_a)g}{I_{xf} + I_{xw} + mR^2 + m_a l_1^2 - 2m_a l_1 R}\right)\left(\frac{2I_{xf}\dot{\gamma}_a}{I_{xw} + I_{xf}}\right)^2
\end{aligned}$$

The system exhibits non-minimum phase behaviour when the steering velocity $\dot{\alpha}$ is the output of the system. Consider the system in state space form, $\dot{x} = Ax + Bu, \quad y = C^T x$. We note from linear control that the input/output behaviour of the system can be expressed in the companion form.

$$\begin{aligned}
y &= c^T (sI - A)^{-1} bu \\
\mathbb{H}(s) &= c^T (sI - A)^{-1} b \\
&= \frac{(s^2 - a_{21})b}{s^3 - a_{22}s^2 + (a_{23}a_{32} - a_{21})s + a_{21}a_{22}}
\end{aligned}$$

There is a zero of the transfer function $\mathbb{H}(s)$ on the right-half plane. Therefore, the control design objective for non-minimum phase systems should not be perfect tracking or asymptotic tracking.

Table 2.2: Parameters used in simulation and experiments

Wheel	:	$m = 1.25kg,\ R = 17cm$
Internal mechanism:		$m_i = 4.4kg,$
Flywheel	:	$m_f = 2.4kg,\ r = 5cm$
Manipulator	:	$l_1 = 10cm$
Friction coefficients:		$\mu_s = 1Nm/(rad/s),\ \mu_g = 0.01Nm/(rad/s)$

2.4 Simulation study

The realistic geometric/mass parameters are shown in Table 2.2. The single wheel robot balanced around the vertical position. In Figure 2.6, it shows that the lean angle β converges to 90°. At the same time, $\dot{\alpha}, \dot{\beta}, \dot{\theta}$ & u_g become zero. The robot reaches to an equilibrium state. The pendulum motion stops. And the swinging angle θ is very small and the robot moves along the straight line as steering angle $\alpha = 30°$.

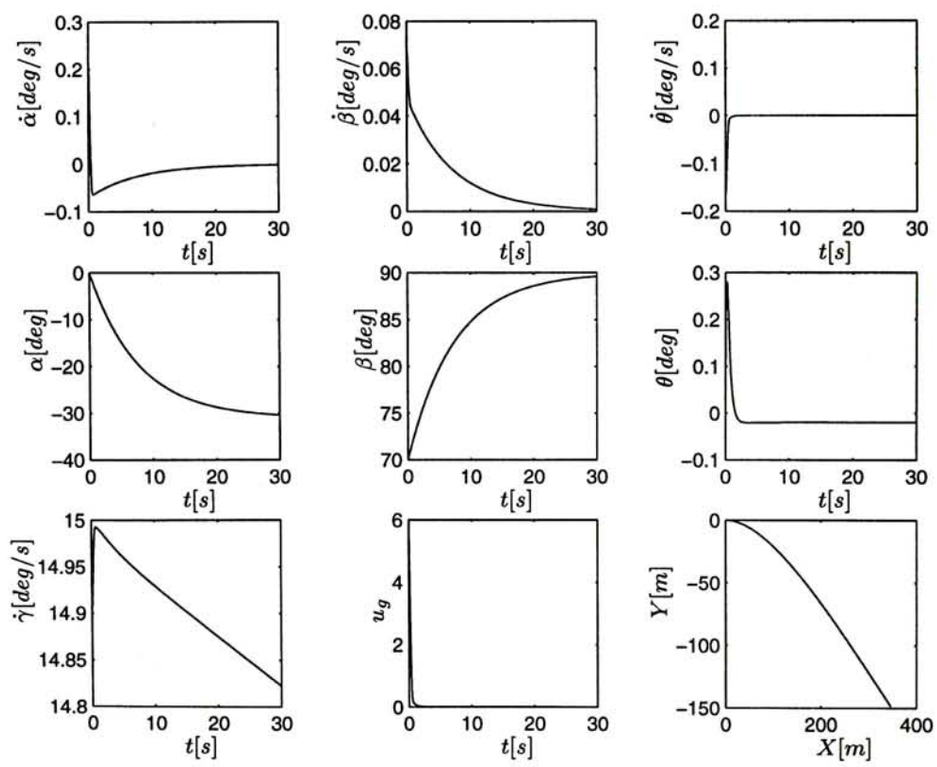

Figure 2.6: The simulation results of the robot on ground

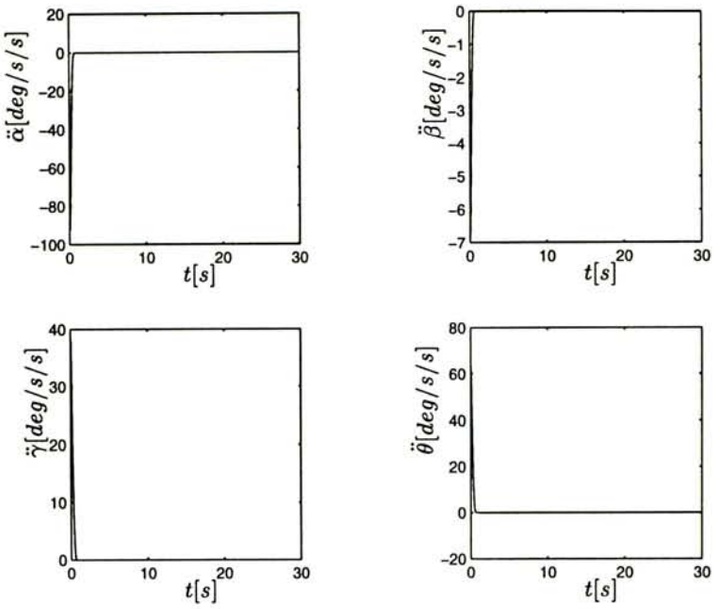

Figure 2.7: Acceleration of the robot

In Figure 2.7, angular acceleration of the robot in yaw, pitch, roll and swing directions become zero. In Figure 2.8, the flywheel turns to be $-30°$ with respect to the vertical and keeps steady at that point. The orientation of the flywheel with respect to the wheel keeps remain unchanged.

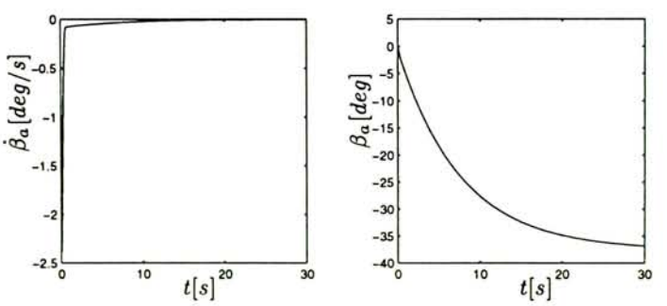

Figure 2.8: The rate of change of lean angle and lean angle itself of the flywheel

2.4.1 The self-stabilizing dynamics effect of the single wheel robot

In this section, we make a comparison of the self-stabilizing dynamic property between the rolling disk and the single wheel robot on the ground.

In the dissertation of Au [2], the self-stabilizing dynamic property of the single wheel robot was investigated and varied by the experiment result. It is shown as Figures 2.9 and 2.10. The robot kept in balance without fall out, due to the gyroscopic torque. It is generated by the coupling motion between the roll and yaw motions, for balancing the gravitational torque.

However, we must pay attention that the model of the single wheel robot by Au [2, 45] had much simplified; The mass center of flywheel and the internal mechanism are coincident with the center of the robot. The pendulum motion was assumed to be neglected. The system model of robot proposed by Au is called as "the simplified one" from now on. We study the self-stabilizing dynamics of the single wheel robot again. The new model of the robot including l_1 are under investigation, it is called as "the modified one".

The stabilizing effect of the flywheel are demonstrated by the change of lean angle. In Figure 2.9b, it is clear that decreasing of lean angle β for a rolling disk without the flywheel is more rapidly than that of the single wheel robot either the simplified or the modified one, as shown in Figures 2.10b and 2.16b. In Figures 2.10a-c and 2.16a-c, under the influence of friction in the yaw direction, the steering rate $\dot{\alpha}$ and the leaning rate $\dot{\beta}$ converge and it tends to a steady state equilibrium as shown in Equation (2.10). The oscillation occurs in the rolling disk is much significant than that robot. This verifies that the stabilizing effect of flywheel on the robot take places. In the Figure 2.16, at the transient state, the effect of swinging motion cannot be neglected. The pendulum swings sinusoidual. The rate of change θ is formed as Cosine function.

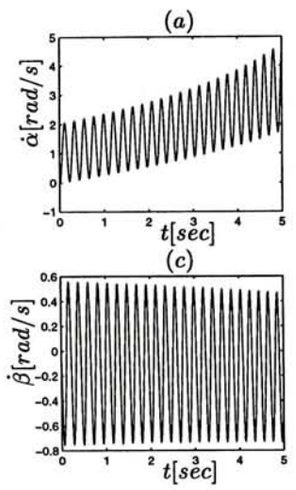

Figure 2.9: The simulation results of a rolling disk without flywheel.

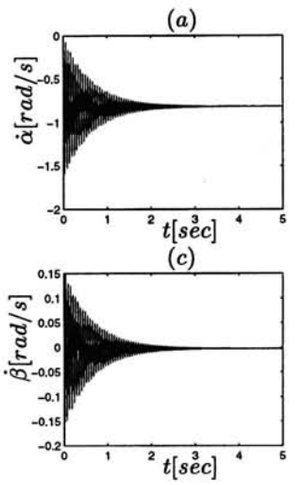

Figure 2.10: The simulation results of the simplified robot.

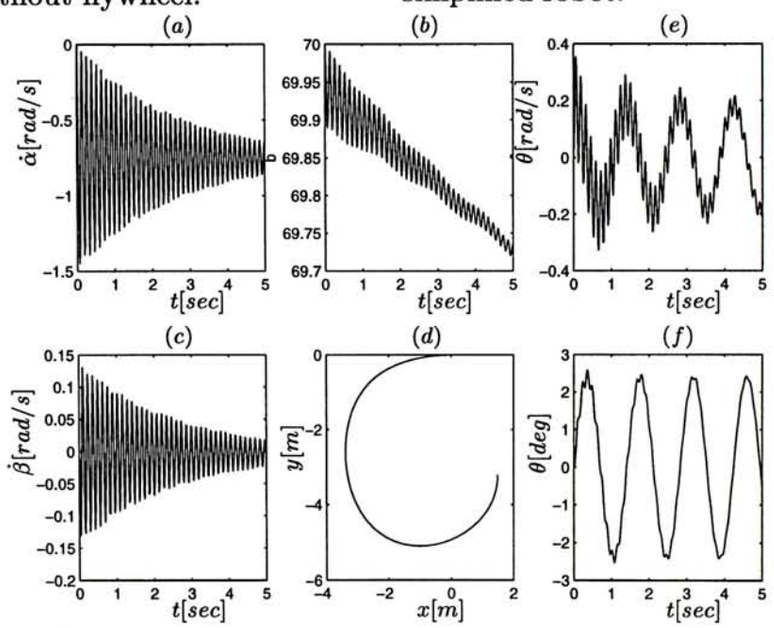

Figure 2.11: The simulation results of the modified robot

2.4.2 The Tilting effect of flywheel on the robot

In this section, the tilting effect of flywheel on the robot is investigated. When the flywheel's orientation is not longer to be fixed with respect to the wheel, the tilting effect of the flywheel on the robot implies.

Based on the conservation of angular momentum, when the tilt angle of flywheel β_a turns, the whole robot will lean in the opposite direction of tilting in order to maintain a constant angular momentum. Simulation and experiment results done by Au [2] are shown as Figure 2.12 and Figure 2.13. The same initial conditions are considered for all cases of tilting up of flywheel. The simulation results shown as Figures 2.12, 2.14 & 2.15 and experiment result as Figure 2.13 are under the same initial conditions as follow:

$$\begin{cases} \beta = 90°, \beta_a = \alpha = 0°, \\ \dot{\beta} = \dot{\alpha} = \dot{\beta}_a = 0\ rad/s, \dot{\gamma} = 15\ rad/s, \\ \alpha = 0°. \end{cases}$$

Both Figures 2.12, 2.13 & 2.14 and 2.15 show that while the tilt angle of flywheel β_a rotates 30° counterclockwise during 2.4 second to 2.7 second, the lean angle β leans in clockwise direction. The tilt angle β_a rotates in 73 deg/s counterclockwise while 2.4 second.

In the experiment, the transient response of lean angle β is more critical than the simulations. The small oscillation comes from the vibration of the mechanism inside the wheel especially the swinging motion. The phenomenon cannot be explained by Au, it was because that l_1 and the pendulum motion reduced from the model he proposed. The swinging motion will become very significant in the transient state, it must not be neglected otherwise it makes the system which comes to singularity.

In the Figures 2.14, the rate of steering and leaning change very rapidly. It occurs due to the pendulum motion of the robot. After some adjustment for the parameters of manipulator for the robot, the performance of the robot becomes better and the pendulum swings less. For 2.7 second, the tilt angle remains unchanged and then the lean angle β and steering rate $\dot{\alpha}$ converge to steady state solution in both simulations and experiments.

In the experiment, we have not found any high frequency oscillations perhaps because the sensor response and the sampling time are much slower than the high frequency oscillations. The simulation result Figures 2.15b-c are much similar to the experimental result in Figure 2.13b-c than Figure 2.12b-c.

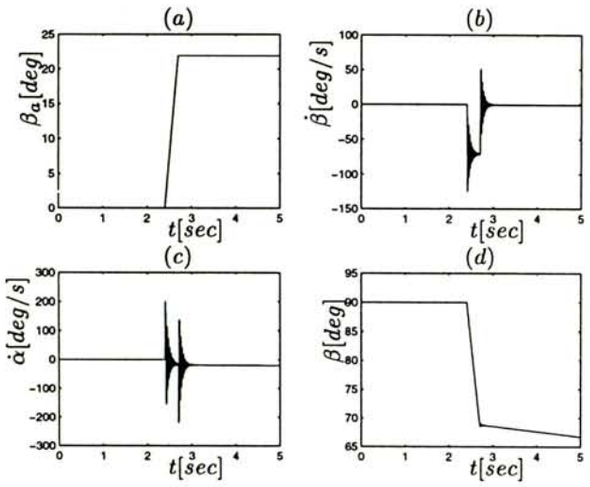

Figure 2.12: The simulation results of the simplified model with $\dot{\beta}_a = 73\ deg/s$

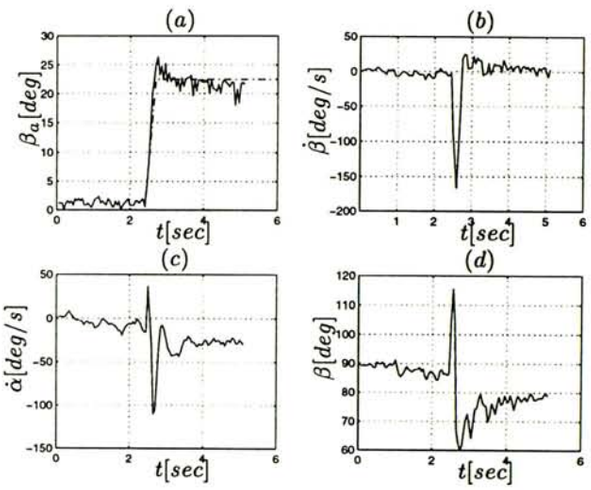

Figure 2.13: The experiment results of the robot with $\dot{\beta}_a = 73\ deg/s$

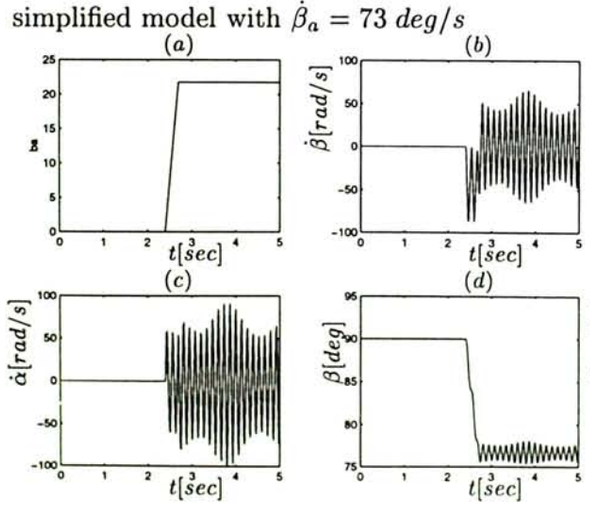

Figure 2.14: The simulation results of the modified model with oscillation.

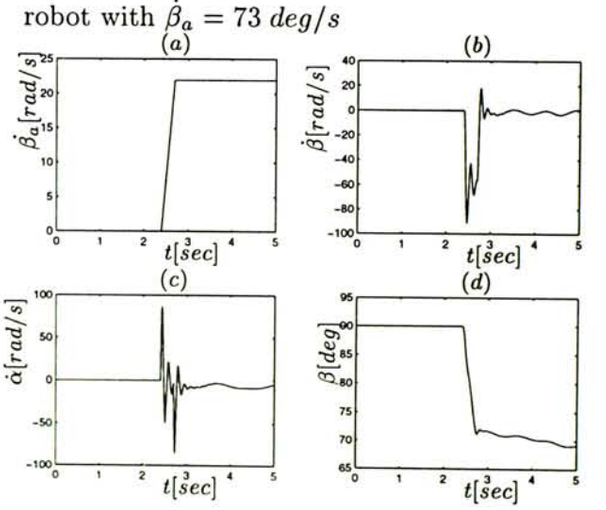

Figure 2.15: The simulation results of the modified model.

Table 2.3: Lengths of manipulator used

	Case i	Case j	Case k	Case l
length, l_1	0.033m	0.05m	0.067m	0.083m

2.5 Dynamic parameters analysis

Stability represents a robot's ability to produce lateral stability using gyroscopical force. In this section, we address the sensitivity of stability of a single wheel robot with respect to the geometric parameters of the robot. The effect of length of manipulator and moment of inertia of the robot are under investigation.

2.5.1 Swinging pendulum

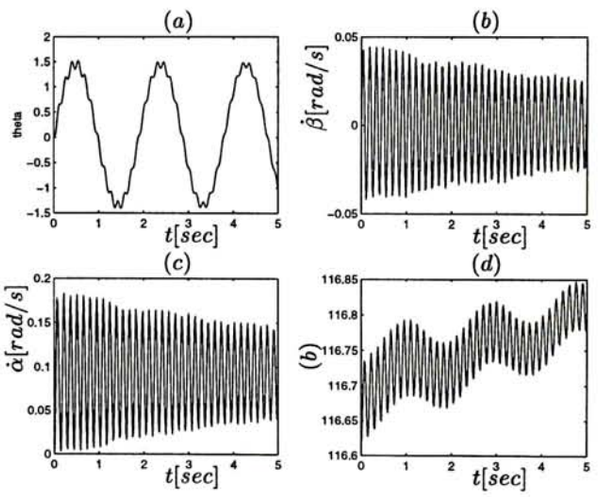

Figure 2.16: Swinging pendulum motion occurs

The parameter l_1 investigated now. One of the most basic questions in the study of swinging pendulum is simply "What happen if the length of the manipulator l_1 increases in causing pendulum motion?" In Figures 2.17 and 2.18, the effect of length of manipulator on the robot are shown. When the length of manipulator used as Table 2.3, it showed that the amplitude of oscillation for velocities of the robot become smaller when the length of manipulator increases. The moment of swinging become less as the length of manipulator increase. Physically, the length of manipulator should be limit as $0 < l_1 \leq r_w - r_f$.

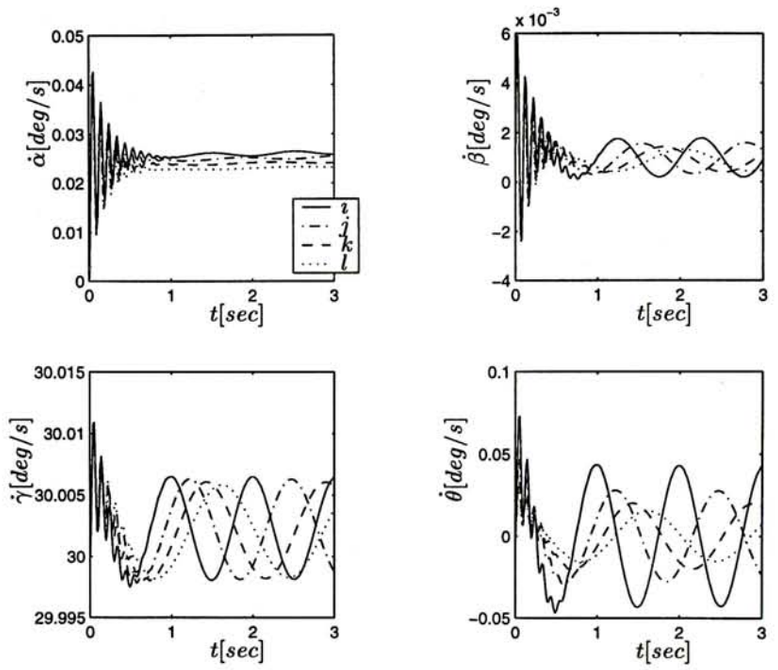

Figure 2.17: Change of velocities of the robot for different lengths of manipulator

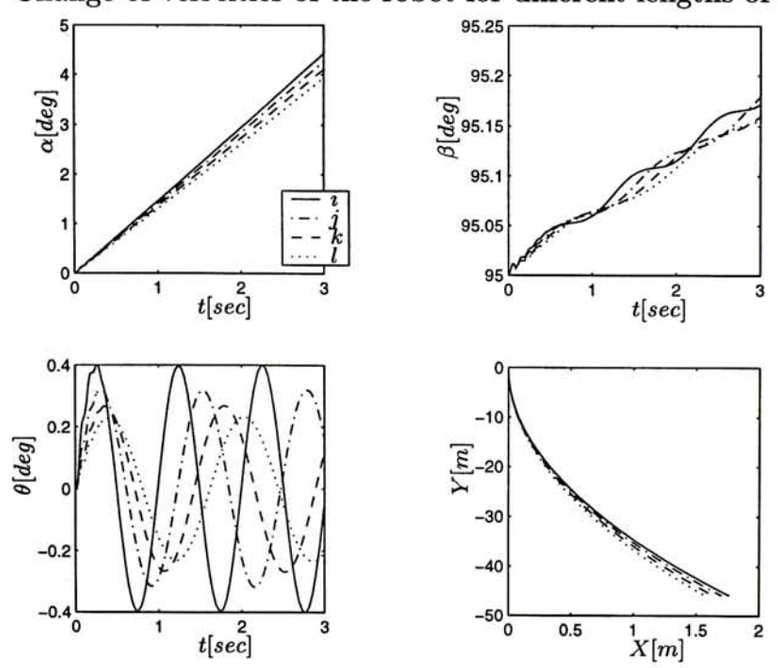

Figure 2.18: Change of Swing angle, lean angle, steering angle and trajectory of the robot for different lengths of manipulator

Table 2.4: Radius ratios between the flywheel and wheel

Case	Radius ratio,r_f/r_w	M.I of flywheel,I_{xf}	M.I of wheel,I_{xw}
$a-1$	$\frac{0.05}{0.17} = 0.2940$	0.003	0.0181
$b-1$	$\frac{0.05}{(0.17)(2)} = 0.1470$	0.003	0.0723
$c-1$	$\frac{0.05}{(0.17)(4)} = 0.0735$	0.003	0.2890
$d-1$	$\frac{0.05}{(0.17)(6)} = 0.0368$	0.003	0.6502

2.5.2 Analysis of radius ratios

We investigate the inertia of flywheel with respect to the stability of the robot. It is divided into two parts: radius ratios between the flywheel and wheel and mass ratios between the flywheel and wheel. In this two sections, we will study the radius ratios and mass rations between the flywheel and wheel respectively. We study the effect of length ratio between the radius of domes and the radius of flywheel on the stabilization of the robot.

Imagine that if the plastic domes become bigger and bigger, we would like to discuss the performance of the robot when same flywheel are anchored on the robot. For the case of $a-1$, we use the same parameters as Table 2.2, however, the radius of wheel dome is multiplied by two, four and six for cases $b-1$, $c-1$ and $d-1$ respectively. The radius ratio for cases $a-1$, $b-1$, $c-1$ and $d-1$ are shown as Table 2.4. The initial conditions for simulation is as follow:

$$\begin{cases} \beta = 80°, \beta_a = \alpha = 0°, \\ \dot{\beta} = \dot{\alpha} = \dot{\beta}_a = 0\ rad/s, \dot{\gamma} = 15\ rad/s, \\ \alpha = 0°. \end{cases}$$

The rate of change of steering angle $\dot{\alpha}$ and the rate of change of leaning angle $\dot{\beta}$ of the robot for different radius ratios are shown as Figures 2.19 and 2.20. The $\dot{\alpha}$ and $\dot{\beta}$ converge exponentially for all cases. And the rate of convergence of $\dot{\alpha}$ and $\dot{\beta}$ for case $a-1$ are the fastest, compared with all three cases.

The spectrum for $\dot{\alpha}$ of the robot are plotted by using the discrete Fourier Transform Function. In Figures 2.21 and 2.22, the magnitude plots and phase plots for cases $a-1$, $b-1$, $c-1$ and $d-1$ are presented.

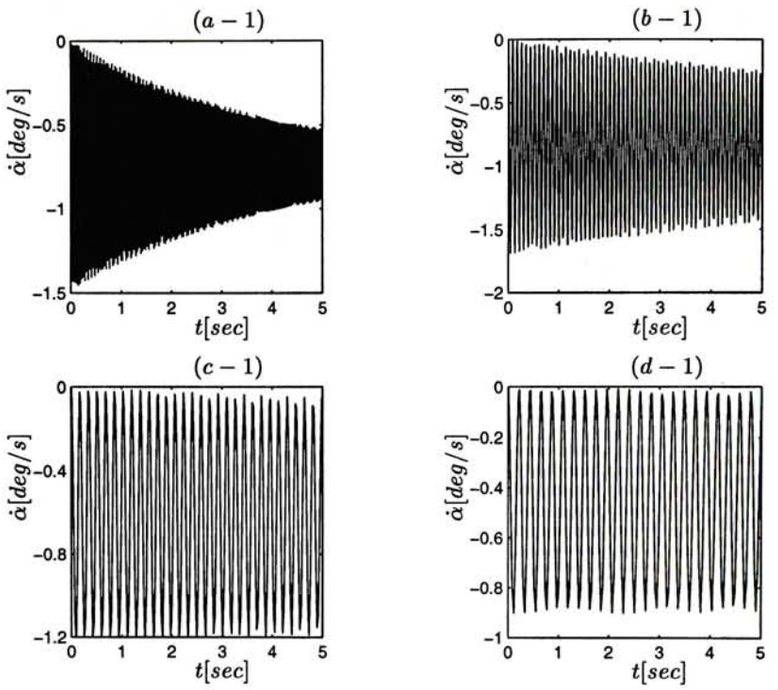

Figure 2.19: $\dot{\alpha}$ of the robot for different radius ratios

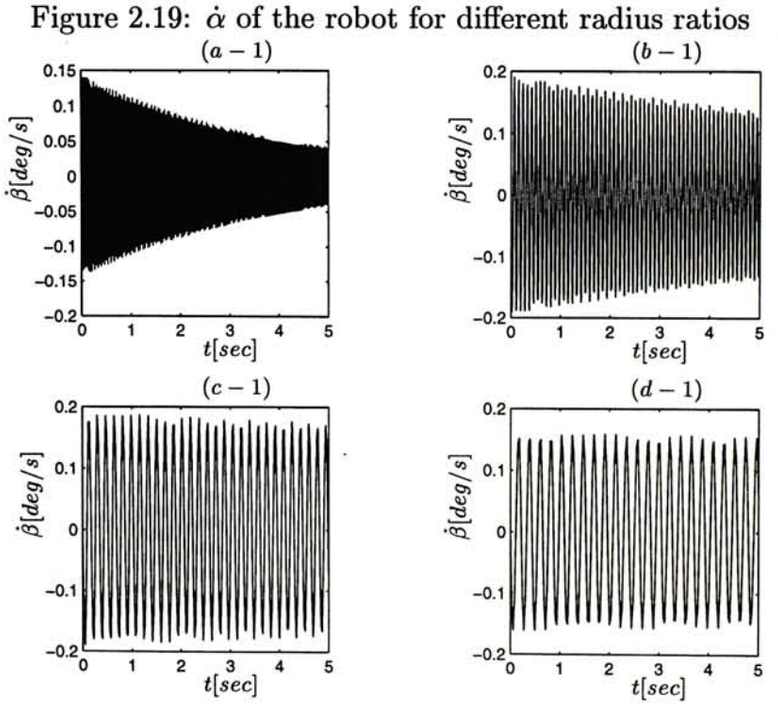

Figure 2.20: $\dot{\beta}$ of the robot for different radius ratios

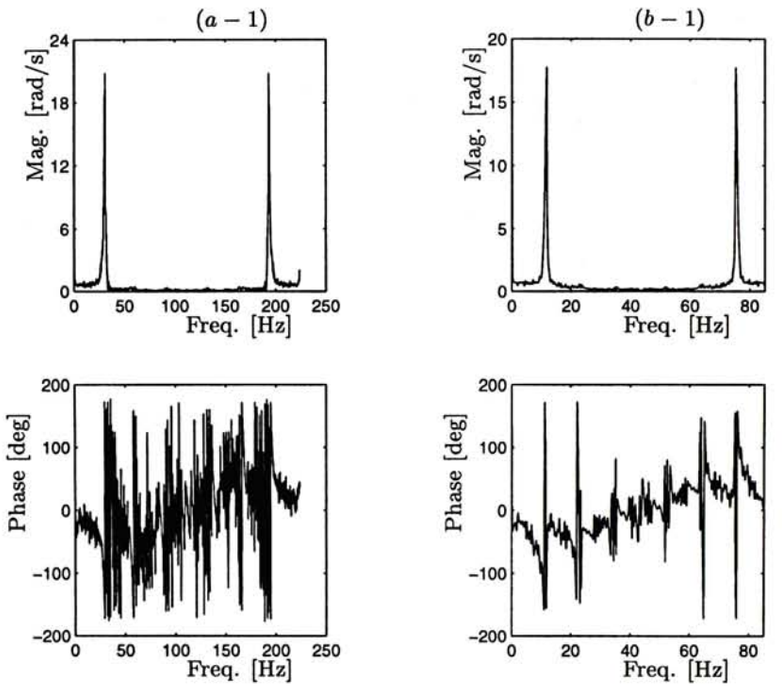

Figure 2.21: Magnitude plots and phase plots for case $a-1$ and $b-1$

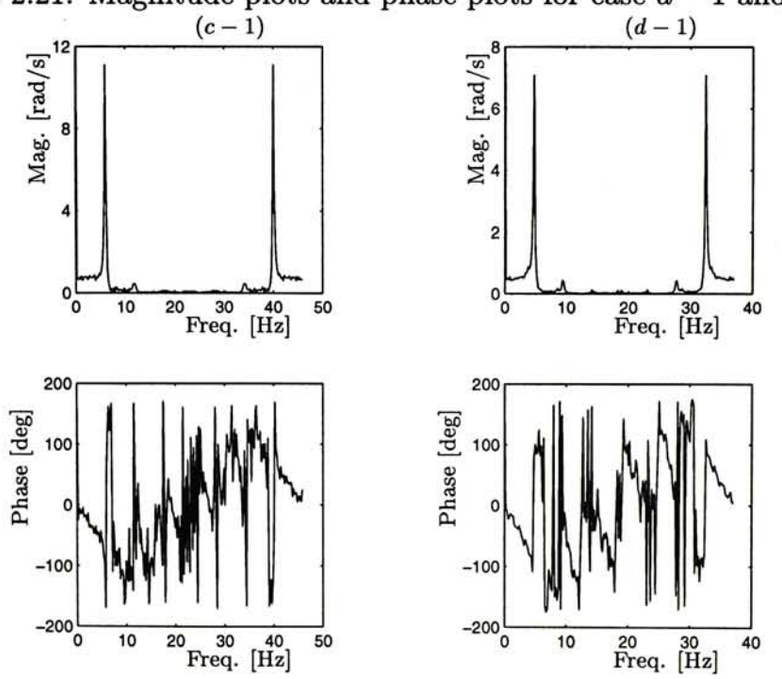

Figure 2.22: Magnitude plots and phase plots for case $c-1$ and $d-1$

Table 2.5: The frequency and magnitude responses for different radius ratios

Case	Steering rate $\dot{\alpha}$		Leaning rate $\dot{\beta}$	
	Magnitude [rad/s]	Frequency [Hz]	Magnitude [rad/s]	Frequency [Hz]
$a-1$	23.65	30	7.00	30
$b-1$	17.7	12	6.94	12
$c-1$	11.1	6	5.69	6
$d-1$	7.0	4.8	4.15	4.8

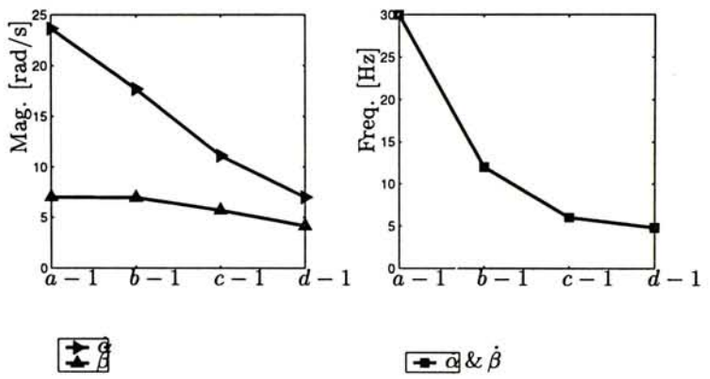

Figure 2.23: The frequent and magnitude response for different radius ratios

We summarize the analysis of radius ratios in Table 2.5 and Figure 2.24. When the length ratio $\frac{r_f}{r_w}$ reduces by increasing the radius of wheel r_f, the magnitude response of steering rate and leaning rate are decreasing from case $a-1$ to $d-1$ with different gradient. Moreover, the frequency response for both of steering rate and leaning rate are also decreasing. It is because that when the same flywheel used on the robot with increasing radius of wheel. The effect of flywheel on the robot become less. On the same hands, we should turn the flywheel more in order to provide some leaning rate of the robot for steering if the wheel is larger.

2.5.3 Analysis of mass ratios

We study the effect of mass ratio between the domes and the flywheel on the stabilization of the robot. Same method as the analysis of length ratio in the previous section, we summarize the analysis of mass ratios in Table 2.7 and Figure 2.24. When the mass ratio $\frac{m_f}{m_w}$ become larger by increasing the mass of flywheel r_f, the magnitude response of steering rate and leaning rate change little from case $a21$ to $f-2$. The frequency response for both of steering rate and leaning rate increase significantly. It is because that

Table 2.6: Mass ratio between the flywheel and wheel

Case	Mass ratio,m_f/m_w	M.I of flywheel,I_{xf}	M.I of wheel,I_{xw}
$a-2$	$\frac{1.2}{1.25}=0.96$	0.0015	0.0181
$b-2$	$\frac{2.4}{1.25}=1.92$	0.0030	0.0181
$c-2$	$\frac{4.8}{1.25}=3.84$	0.0060	0.0181
$d-2$	$\frac{9.6}{1.25}=7.68$	0.0120	0.0181
$e-2$	$\frac{14.4}{1.25}=11.52$	0.0180	0.0181
$f-2$	$\frac{19.2}{1.25}=15.32$	0.0240	0.0181

Table 2.7: The frequency and magnitude responses for different mass ratios

	Steering rate $\dot{\alpha}$		Leaning rate $\dot{\beta}$	
Case	Magnitude [rad/s]	Frequency [Hz]	Magnitude [rad/s]	Frequency [Hz]
$a-2$	25.24	19.373	9.2	19.373
$b-2$	23.65	30	7	30
$c-2$	22.65	47.6	6.8	47.6
$d-2$	22.4	68.573	6.6	68.573
$e-2$	22	81	6	81
$f-2$	21	90	6	90

the angular momentum generated into the wheel are larger if more massive flywheel spins with same angular velocity. The stability on the robot enhances.

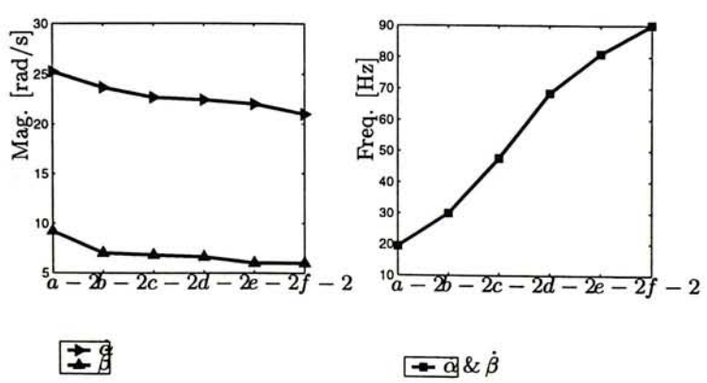

Figure 2.24: The frequent and magnitude response for different mass ratios

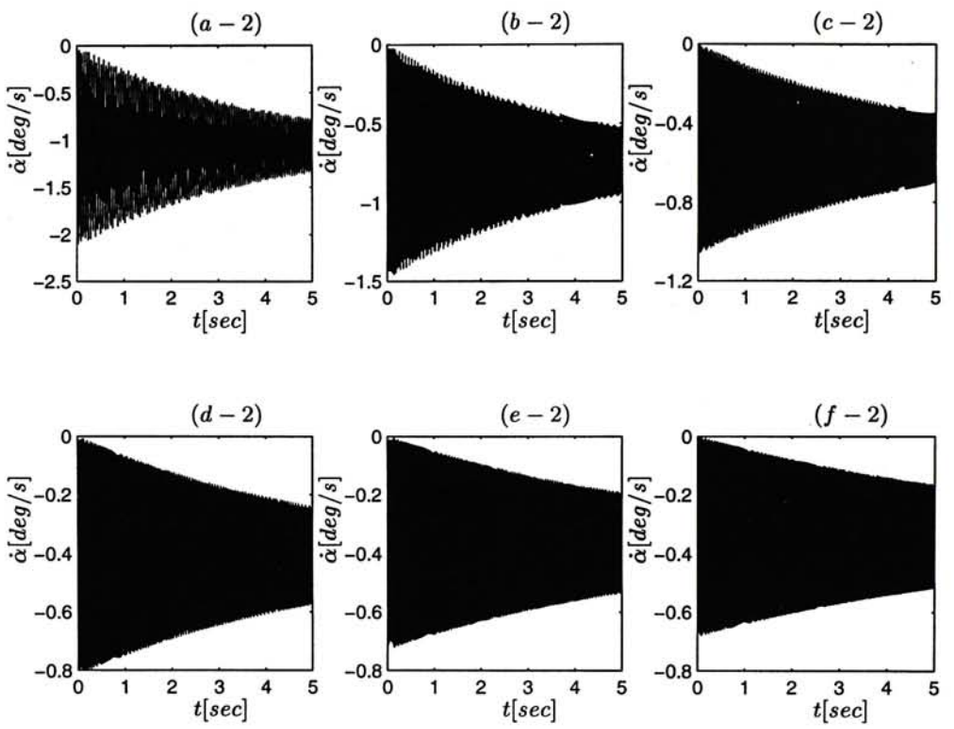

Figure 2.25: $\dot{\alpha}$ of the robot for different mass ratios

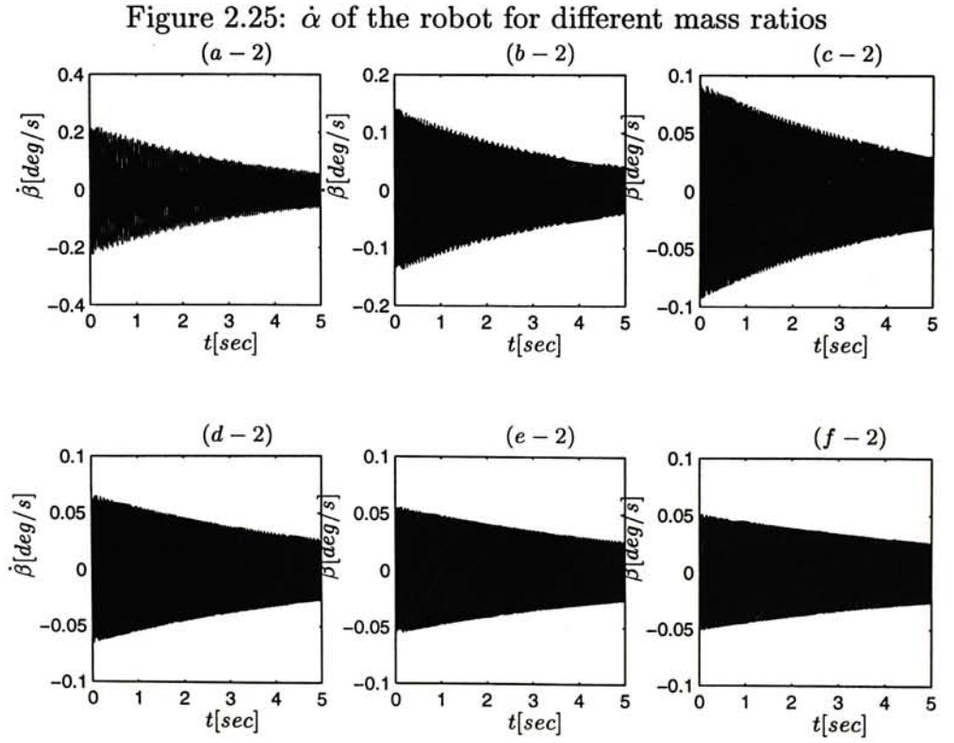

Figure 2.26: $\dot{\beta}$ of the robot for different mass ratios

Chapter 3

Dynamics of the robot on incline

In this chapter, we derive the dynamics of a rolling disk and a single wheel robot on an inclined plane respectively. The motion of a single wheel robot is analyzed using Lagrangian dynamics with no assumption that the robot is constrained to remain vertical and performed along the horizontal plane. The model should not be restricted only on the flat ground as the robot supposed it can be perturbed on the rough terrains. The equation of motion of a single wheel robot on an inclined plane differs significantly from that on horizontal plane. On an inclined plane, some components of the gravity forces act on the system.

3.1 Modeling of rolling disk on incline

Consider a disk rolls without slipping along an inclined plane with an inclination angle φ as shown in Figure 3.1. Assume that the disk is rigid with radius R. The dynamic model can be developed using the Constrained Lagrangian Method. It is different with the derivation in [31], [45] & the Previous Section 2.1. The gravity term decomposes into different directions. Let $\Sigma_O XYZ$ be a fixed inertial frame whose XY plane is anchored to the flat surface and Z is vertical position to the surface. Let the body coordinate frame $\Sigma_B X_b Y_b Z_b$ whose origin is located at the center of the disk, and whose z-axis represents the axis of rotation of the disk. The configuration of the system can be described by six generalized coordinates $[X, Y, Z, \alpha, \beta, \gamma]^T$, where X, Y, Z represent the coordinates of the center of mass of the disk with respect to the inertial frame $\Sigma_O XYZ$, α is the steering angle measured from the Z axis, β is the leading angle measured from the Z axis to the Z_b axis, γ is the spinning angle along Z_b axis. Let $[\hat{\mathbf{i}}, \hat{\mathbf{j}}, \hat{\mathbf{k}}]$ and $[\hat{\mathbf{l}}, \hat{\mathbf{m}}, \hat{\mathbf{n}}]$ to be the unit vectors of the coordinate system Σ_O and Σ_B respectively. The

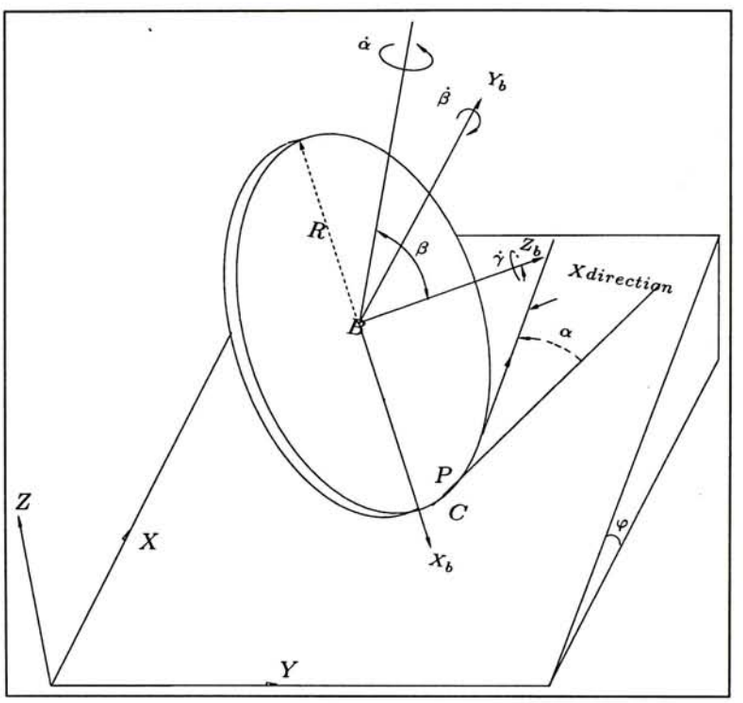

Figure 3.1: System variables of a rolling disk on incline

transformation between these two coordinate frames Σ_O and Σ_B is given by

$$\begin{bmatrix} \hat{\mathbf{l}} \\ \hat{\mathbf{m}} \\ \hat{\mathbf{n}} \end{bmatrix} = \begin{bmatrix} C_\alpha C_\beta & S_\alpha & C_\alpha S_\beta \\ -S_\alpha C_\beta & C_\alpha & -S_\alpha S_\beta \\ -S_\beta & 0 & C_\beta \end{bmatrix} \begin{bmatrix} \hat{\mathbf{i}} \\ \hat{\mathbf{j}} \\ \hat{\mathbf{k}} \end{bmatrix}$$

where $sin(x)$ and $cos(x)$ are simplified by S_x and C_x respectively and the subscript represents the angle of the trigonometical function. The angular velocity of the disk with respect to the inertia frame Σ_O,

$$\begin{aligned} \omega_B &= \dot{\alpha}\hat{\mathbf{m}} + \dot{\beta}\hat{\mathbf{j}} + \dot{\gamma}\hat{\mathbf{k}} \\ &= -\dot{\alpha}S_\beta\hat{\mathbf{i}} + \dot{\beta}\hat{\mathbf{j}} + (\dot{\gamma} + \dot{\alpha}C_\beta)\hat{\mathbf{k}} \end{aligned} \tag{3.1}$$

The constraints require that the disk rolls without slipping on the surface, i.e., the velocity of the contact point on the disk is zero at any instant, $v_P = 0$. Then we express v_C as

$$v_C = \omega_B \times r_{B/P} + v_P \tag{3.2}$$

where $r_{B/P} = -R\hat{\mathrm{I}}$ representing the vector from the frame P to B. Substituting Equation (3.6) in Equation (3.7), those velocity constraints are formulated,

$$\dot{X} = -R(\dot{\gamma}S_\alpha + \dot{\alpha}C_\beta S_\alpha - \dot{\beta}C_\alpha S_\beta) \tag{3.3}$$

$$\dot{Y} = -R(\dot{\gamma}C_\alpha + \dot{\alpha}C_\alpha C_\beta - \dot{\beta}S_\alpha S_\beta) \tag{3.4}$$

$$\dot{Z} = R\dot{\beta}C_\beta \quad \Rightarrow \quad Z = RS_\beta \tag{3.5}$$

Equations (3.8) and (3.9) are nonintegrable and hence are nonholonomic, while Equation (3.10) is integrable. As the disk rolls without slipping, the locus of points of contact defines a smooth curve in the surface plane. Let (X_c, Y_c) denote the coordinates of the point C on this locus that coincides with a point of contact P of the disk.

$$\begin{aligned} X_c &= X_b + RS_\alpha C_\beta \\ Y_c &= Y_b + RC_\alpha C_\beta \end{aligned}$$

There are six variables with two velocity constraints, so the system has 3 DOF's. We use five generalized coordinates $q = [X, Y, \alpha, \beta, \gamma]^T$ to describe the system. The XY represent the coordinates of the center of mass B with respect to the inertial system ΣXYZ, α is the steering angle measured from the X axis to the contact line, $\beta \in (-\frac{\pi}{2}, \frac{\pi}{2})$ is the leaning angle measured from the Z axis to the z axis, and γ is the rolling angle of the disk itself along z axis. The moment of inertia of the disk along X_b axis is I_x.

The kinetic energy $\mathcal{L}$ and potential energy of the system $\mathcal{P}$ are determined

$$\begin{aligned} \mathcal{L} &= \frac{1}{2}m\left(\dot{X}^2 + \dot{Y}^2 + \dot{Z}^2\right) + \frac{1}{2}(\frac{1}{2}I_x)(\omega_x^2 + \omega_y^2) + \frac{1}{2}I_x\omega_z^2 \\ &= \frac{1}{2}\left[m\dot{X}^2 + m\dot{Y}^2 + mr^2\dot{\beta}^2C_\beta^2 + (\frac{1}{2}I_x)\dot{\alpha}^2S_\beta^2 + (\frac{1}{2}I_x)\dot{\beta}^2 + I_x(\dot{\alpha}C_\beta + \dot{\gamma}^2)\right] \\ \mathcal{P} &= mg[RS_\beta C_\varphi + YS_\varphi] \end{aligned}$$

As a Lagrangian,

$$\mathcal{L} = \mathcal{K} - \mathcal{P}, \qquad q = [X, Y, \alpha, \beta, \gamma]^T, \quad \frac{d}{dt}(\frac{\delta L}{\delta \dot{q}}) - \frac{\delta L}{\delta q} = \tau$$

Using of Lagrange undetermined multiplier λ method, the force constraints must be grouped in this form $\sum \lambda_k a_{kj}\dot{q}_j = 0$. The equations of motion of a rolling disk can be

determined below

$$\begin{aligned}
m\ddot{X} &= \lambda_1 \\
m\ddot{Y} + mgS_\varphi &= \lambda_2 \\
\lambda_1 RS_\alpha + \lambda_2 RC_\alpha &= 2I_x(\ddot{\alpha}C_\beta + \ddot{\gamma} - \dot{\alpha}\dot{\gamma}S_\beta) \\
\lambda_1 RS_\alpha C_\beta + \lambda_2 RC_\alpha C_\beta &= I_x(\ddot{\alpha}(1 + C_\alpha^2) - 2\dot{\alpha}\dot{\beta}S_\beta C_\beta + 2\ddot{\gamma}C_\beta - 2\dot{\beta}\dot{\gamma}S_\beta) \\
C - \lambda_1 RC_\alpha S_\beta + \lambda_2 RS_\alpha S_\beta &= (mR^2C_\alpha^2 + I_x)\ddot{\beta} - mR^2\dot{\beta}^2C_\beta \\
&\quad + mgRC_\beta + I_x\dot{\alpha}^2C_\beta S_\beta + 2I_x\dot{\alpha}\dot{\gamma}S_\beta
\end{aligned}$$

Differential of two nonholonomic constraints equations, we have

$$\begin{aligned}
\ddot{X} &= R[-\ddot{\alpha}C_\beta S_\alpha - \ddot{\gamma}S_\alpha - \dot{\alpha}^2C_\beta C_\alpha - \dot{\gamma}\dot{\alpha}C_\alpha + \ddot{\beta}C_\alpha S_\beta + \dot{\beta}^2C_\alpha C_\beta] \\
\ddot{Y} &= R[-\ddot{\alpha}C_\beta C_\alpha - \ddot{\gamma}C_\alpha + \dot{\alpha}^2C_\beta S_\alpha + \dot{\gamma}\dot{\alpha}S_\alpha - \ddot{\beta}S_\alpha S_\beta + \dot{\beta}^2S_\alpha C_\beta]
\end{aligned}$$

We eliminate the Lagrange multipliers by obtaining $\ddot{X}, \ddot{Y}$ and then they were substituted back into the dynamic equations. A minimum set of differential equations are found i.e. Normal form of the system. The dynamic equation of the entire system is given by

$$M(q)\ddot{q} + N(q, \dot{q}) = Gu$$

where $M(q) \in \mathbb{R}^{3\times3}$ and $N(q, \dot{q}) \in \mathbb{R}^{3\times1}$ are the inertia matrix and the nonlinear terms respectively.

$$M = \begin{bmatrix} I_x + (mR^2 + I_x)C_\beta^2 & 0 & (mR^2 + 2I_x)C_\beta \\ 0 & mR^2 + I_x & 0 \\ (mR^2 + 2I_x)C_\beta & 0 & (mR^2 + 2I_x) \end{bmatrix}$$

$$\begin{aligned}
q &= [\alpha, \beta, \gamma]^T, \quad G = [0, 1, 0]^T, \qquad u = \tau \\
N &= \left[N_1, N_2, N_3\right]^T \\
N_1 &= -gmRC_\alpha C_\beta S_\varphi - (I_x + mR^2)S_{2\beta}\dot{\alpha}\dot{\beta} - 2I_x S_\beta \dot{\beta}\dot{\gamma} \\
N_2 &= mgrC_\beta C_\varphi - gmRS_\alpha S_\beta S_\varphi + (mR^2 + I_x)S_\beta C_\beta \dot{\alpha}^2 + (mR^2 + I_x)S_\beta \dot{\alpha}\dot{\gamma} \\
N_3 &= -gmRC_\alpha S_\varphi - 2(mR^2 + I_x)S_\beta \dot{\alpha}\dot{\beta}
\end{aligned}$$

3.1.1 Disk rolls up on an inclined plane

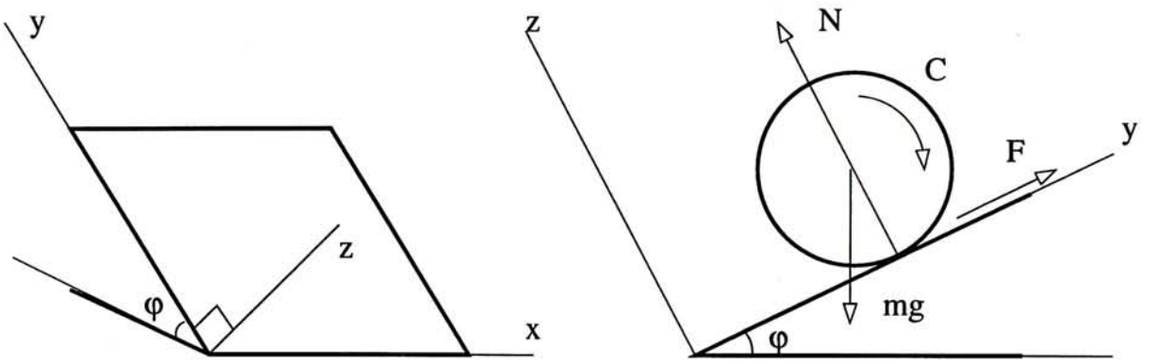

Figure 3.2: Disk rolls on slope

Consider a thin disk of radius r, remaining vertical and rolling up an inclined plane without slipping. The nonslip condition of the disk's motion, i.e., roll without slipping, imposes the following nonholonomic constraint equation:

$$\begin{aligned} dy &= rd\gamma \\ \dot{y} &= r\dot{\gamma} \end{aligned}$$

It seen very common on daily. If the disk starts from a certain position and rolls along two different paths, so that the final position and the point of contact between the disk and the ground are the same in each case, but the two final values for coordinates α and γ may be different. It is meanth that this constraint equation is not integrable, so is commonly called nonholonomic constraint. On the other hands, if there is a holonomic constraint, α and γ were functions of x and y, and then the final values of α and γ would have been the same. The centre of the disk is subject to the holonomic constraint $z = r$ and the disk is to remain vertical, i.e., it is subject to the holonomic constraint, lean angle $\beta = 0$. Force constraints are in the form $\sum a_j dq_j = 0$ by using Lagrange undetermined multipliers λ. And virtual work principle is applied. The torque C applied to the shaft $\delta W = C\delta\gamma$.

$$\begin{aligned} \delta\acute{W} &= \delta W + \sum(\lambda_k \sum a_j dq_j) \\ &= C\delta\gamma + \lambda dy - \lambda r d\gamma \end{aligned}$$

Assuming that the disk remains normal to the plane surface. We can write the La-

grangian as

$$\mathcal{L} = \frac{1}{2}m\dot{y}^2 + \frac{1}{2}I\dot{\gamma}^2 - mg(y\sin\varphi + r\cos\varphi)$$

Using Lagrangian equation method

$$\frac{d}{dt}\left(\frac{\delta\mathcal{L}}{\delta\dot{q}}\right) - \frac{\delta\mathcal{L}}{\delta q} = \delta\dot{W}$$

Deriving the equations of motion of the rolling disk for $q = [y, \gamma]^T$,

$$\begin{aligned} m\ddot{y} + mg\sin\varphi &= \lambda \\ I\ddot{\gamma} &= C - \lambda r \end{aligned}$$

Substituting,

$$\begin{aligned} \lambda &= \frac{mrC + mgI\sin\varphi}{mr^2 + I} \\ \ddot{y} &= \frac{rC - mr^2 g\sin\varphi}{mr^2 + I} \\ \ddot{\gamma} &= \frac{C - mrg\sin\varphi}{mr^2 + I} \end{aligned}$$

From the Free Body Diagram,

$$m\ddot{y} = F - mg\sin\varphi$$

Take moment at centre of the disk,

$$\begin{aligned} I\ddot{\gamma} &= C - Fr \\ F &= \lambda \\ Power &= Mw = C\dot{\gamma} \end{aligned}$$

3.2 Modeling of single wheel robot on incline

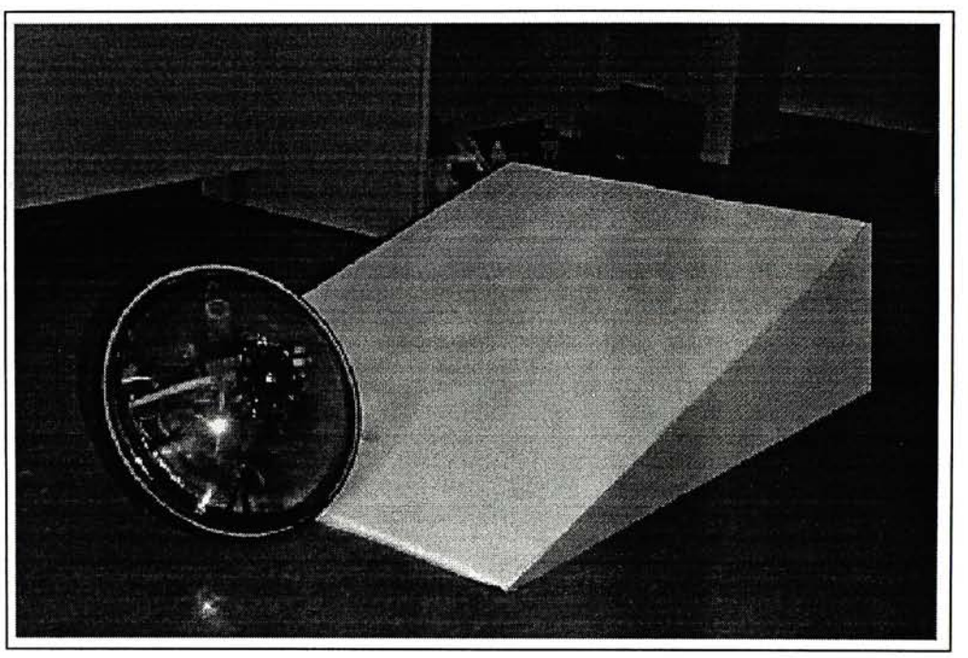

Figure 3.3: Photograph of Gyrover on an inclined plane

Consider a single wheel robot is a sharp-edged wheel actuated by a two-link manipulator, with a spinning disk(gyro) attached at the end of the second link. In the Figure 2.2 shows that the first link of length l_1 represents the vertical offset of the actuation mechanism from the axis of the single wheel robot. And the second link of length l_2 represents the horizontal offset of the spinning flywheel. There is no offset between the axis of tilt & gyro rotor and the middle plane of whole structure on the robot. The l_2 is set to be zero. It means that the flywheel's center of mass coincides with that of the internal mechanism. A summary of the definition of model variables is shown in Table 2.1.

The coordinates frames of the system are divided into three major frames.

1. The fixed inertial frame $\Sigma_O XYZ$, whose XY plane is anchored to the flat surface of an inclined plane and Z is a position perpendicular to the surface.

2. The body coordinate frame $\Sigma_B X_b Y_b Z_b$, whose origin is located at the center of the single wheel, and whose z axis represents the axis of rotation of the wheel.

3. The flywheel coordinates frame $\Sigma_D X_d Y_d Z_d$, whose center is on the center of mass of the flywheel itself, and whose z-axis represents the axis of rotation of the flywheel. Note that Y_b is always parallel to Y_d.

The configuration of the system can be described by eight generalized coordinates $[X, Y, Z, \alpha, \beta, \gamma, \beta_a, \theta]^T$, where X, Y, Z represent the cartesian coordinates of the center of mass (C.M) of the system with respect to the inertial frame $\Sigma_O XYZ$, α is the steering angle measured from the Z axis, β is the leading angle measured from the Z axis to the Z_b axis, γ is the spinning angle along Z_b axis and β_a is the leading angle measured from the Z_b axis to the Z_d axis. θ is the swing angle between link l_1 and X_b-axis of the wheel. $sin(x)$ and $cos(x)$ are simplified by S_x and C_x respectively throughout this paper and the subscripts represent the angles of the trigonometry. The rotation matrix from Σ_O to Σ_B is $R_B^O = R_Z(\alpha)R_Y(\beta)$. The rotation matrix from Σ_B to Σ_D is $R_D^B = R_Z(\theta)R_Y(\beta_a + 90°)$.

3.2.1 Kinematic constraints

Let $[\hat{\mathbf{i}}, \hat{\mathbf{j}}, \hat{\mathbf{k}}]$ and $[\hat{\mathbf{l}}, \hat{\mathbf{m}}, \hat{\mathbf{n}}]$ to be the unit vectors of the coordinate system Σ_O and Σ_B respectively. The transformation between these two coordinate frames Σ_O and Σ_B is given by

$$\begin{bmatrix} \hat{\mathbf{i}} \\ \hat{\mathbf{j}} \\ \hat{\mathbf{k}} \end{bmatrix} = \begin{bmatrix} C_\alpha C_\beta & -S_\alpha & C_\alpha S_\beta \\ S_\alpha C_\beta & C_\alpha & S_\alpha S_\beta \\ -S_\beta & 0 & C_\beta \end{bmatrix} \begin{bmatrix} \hat{\mathbf{l}} \\ \hat{\mathbf{m}} \\ \hat{\mathbf{n}} \end{bmatrix}$$

The kinematics constraint is presented. We define v_A and ω_B to denote the velocity of the center of mass of the single wheel and its angular velocity with respect to the inertia frame Σ_O. Then, we have

$$\omega_B = -\dot{\alpha} S_\beta \hat{\mathbf{l}} + \dot{\beta} \hat{\mathbf{m}} + (\dot{\gamma} + \dot{\alpha} C_\beta) \hat{\mathbf{n}} \tag{3.6}$$

The constraints require that the wheel rolls without slipping on the surface, i.e, the velocity of the contact point on the disk is zero at any instant, $v_c = 0$. Then we express v_A as

$$v_A = \omega_B \times r_{AC} + v_c \tag{3.7}$$

where $r_{AC} = -R\hat{l}$ representing the vector from the frame C to A. Substituting Equation (3.6) in Equation (3.7), those velocity constraints are formulated,

$$\dot{X} = R(\dot{\gamma} S_\alpha + \dot{\alpha} C_\beta S_\alpha + \dot{\beta} C_\alpha S_\beta) \tag{3.8}$$

$$\dot{Y} = -R(\dot{\gamma} C_\alpha + \dot{\alpha} C_\alpha C_\beta - \dot{\beta} S_\alpha S_\beta) \tag{3.9}$$

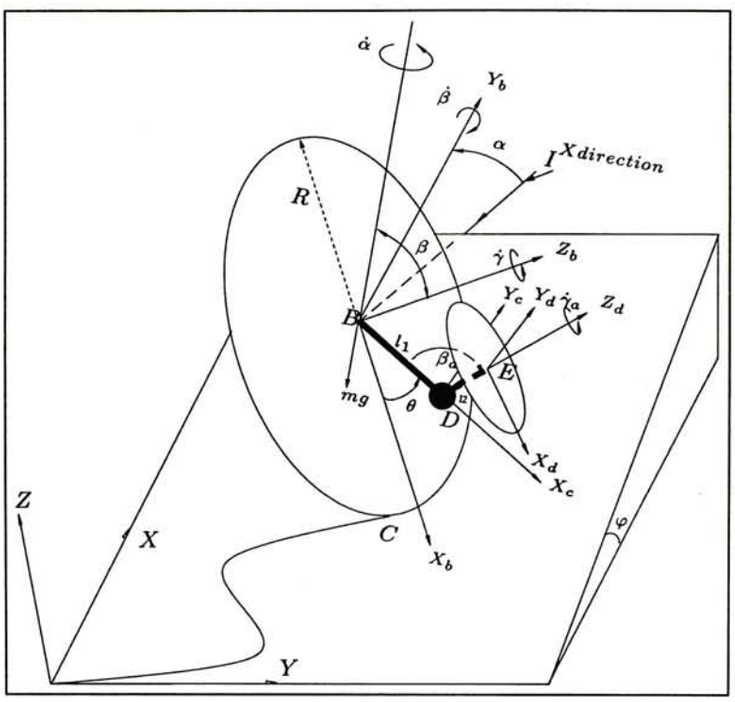

Figure 3.4: System variables of the single wheel robot on incline

$$\dot{Z} = R\dot{\beta}C_\beta \quad \Rightarrow \quad Z = RS_\beta \tag{3.10}$$

Equations (3.8) and (3.9) are nonintegrable and hence are nonholonomic, while Equation (3.10) is integrable. Therefore, the robot can be represented by seven independent variables $(X, Y, \alpha, \beta, \gamma, \beta_a, \theta)$ instead of eight.

3.2.2 Equations of motion

The robot dynamics is presented. We study the equation of motion by the Lagrangian $\mathcal{L} = \mathcal{T} - \mathcal{P}$ of the system, where $\mathcal{T}$ and $\mathcal{P}$ are the kinetic energy and potential energy of the system respectively. We divide the system into three main parts: wheel, internal mechanism, and spinning flywheel.

A wheel

The kinetic energy of a wheel is

$$\begin{aligned}
\mathcal{T}_w &= \frac{1}{2}m_w[\dot{X}^2 + \dot{Y}^2 + \dot{Z}^2] + \frac{1}{2}[I_{xw}\omega_x^2 + I_{xw}\omega_y^2 + 2I_{xw}\omega_z^2] \\
&= \frac{1}{2}m_w[\dot{X}^2 + \dot{Y}^2 + (R\dot{\beta}C_\beta)^2] + \frac{1}{2}[I_{xw}(\dot{\alpha}S_\beta)^2 + I_{xw}\dot{\beta}^2 + 2I_{xw}(\dot{\alpha}C_\beta + \dot{\gamma})^2]
\end{aligned}$$

The potential energy of a wheel is

$$\mathcal{P}_w = m_w g(RS_\beta C_\varphi + YS_\varphi)$$

An internal mechanism and spinning flywheel

The coordinates of the origin of the flywheel is

$$\begin{bmatrix} x_f \\ y_f \\ z_f \end{bmatrix} = \begin{bmatrix} X_B \\ Y_B \\ Z_B \end{bmatrix} + R_B^O \begin{bmatrix} l_1 C_\theta \\ l_1 S_\theta \\ 0 \end{bmatrix}$$

Let $\mathcal{T}_f^t$ denote the translational kinetic energy of the flywheel and the internal mechanism.

$$\mathcal{T}_f^t = \frac{1}{2}(m_i + m_f)[\dot{x_f}^2 + \dot{y_f}^2 + \dot{z_f}^2]$$

Let ω_f be the angular velocity of flywheel w.r.t Ω_O. We then have

$$\omega_f = R_B^E \omega_B + \begin{bmatrix} 0 \\ \dot{\beta}_a \\ \dot{\gamma}_a \end{bmatrix}$$

The transformation from Σ_B to Σ_E is

$$R_B^E = \begin{bmatrix} C_\theta S_{\beta_a} & -S_\theta S_{\beta_a} & -C_{\beta_a} \\ S_\theta & C_\theta & 0 \\ C_\theta C_{\beta_a} & -C_{\beta_a} S_\theta & S_{\beta_a} \end{bmatrix}$$

The rotational kinetic energy of the flywheel is given by

$$\mathcal{P}_f = (m_i + m_f)g(RS_\beta C_\varphi + YS_\varphi - l_1 C_\theta S_\beta C_\varphi)$$

The Lagrangian of the system thus is

$$\mathcal{L} = [\mathcal{T}_w + (\mathcal{T}_f^t + \mathcal{T}_f^r)] - (\mathcal{P}_w + \mathcal{P}_f)$$

Using the constrained Lagrangian method, the dynamic equation is determined.

The general model of the single wheel robot on an inclined plane is given by

$$M_7(q)\ddot{q} + N_7(q,\dot{q}) = A^T\lambda + Bu \tag{3.11}$$

where $M_7(q) \in \mathbb{R}^{7\times7}$ and $N_7(q,\dot{q}) \in \mathbb{R}^{7\times1}$ are the inertia matrix and the nonlinear terms respectively. B is the input matrix.

$$A(q) = \begin{bmatrix} 1 & 0 & -RS_\alpha C_\beta & -RC_\alpha S_\beta & -RS_\alpha & 0 & 0 \\ 0 & 1 & RC_\beta C_\alpha & -RS_\alpha S_\beta & RC_\alpha & 0 & 0 \end{bmatrix}$$

$$B = \begin{bmatrix} 0 & 0 & 0 & 0 & 1 & 0 & k \\ 0 & 0 & 0 & 0 & 0 & 1 & 0 \end{bmatrix}^T, u = [u_1, u_2]^T$$

$$q = [X, Y, \alpha, \beta, \gamma, \beta_a, \theta]^T, \lambda = [\lambda_1, \lambda_2]^T$$

The configuration of the system can be described by seven generalized coordinates $[X, Y, \alpha, \beta, \gamma, \beta_a, \theta]^T$, where X, Y, Z represent the coordinates of the center of mass of the system with respect to the inertial frame $\Sigma_O XYZ$, α is the steering angle measured from the Z axis, β is the leading angle measured from the Z axis to the Z_b axis, γ is the spinning angle along Z_b axis and β_a is the leading angle measured from the Z_b axis to the Z_d axis.

The nonholonomic constraints can be formed as $A(q)\dot{q} = 0$. The model is also underactuated as there are only two control torques available on the system. One is drive torque (u_1) and the other is the tilt torque (u_2). The nonholonomic constraints are only restrict to the motion of the wheel only, so all elements of the last two columns of the matrix A are zero. It is noted that the last two columns represent the motion variables of the flywheel. The input torques drive the tilt angle of the flywheel (β_a), the rotating angle of the wheel (γ) and the swinging angle of the pendulum (θ). It imposed that there are three rows with nonzero elements on the matrix B.

3.2.3 Model simplification

A minimum set of differential equations, i.e., Normal form is obtained when the Lagrange multipliers eliminated. The generalized variables X and Y are eliminated and the number of generalized coordinates become five i.e., $q = [\alpha, \beta, \gamma, \beta_a, \theta]^T$ and $n = 5$. By relationship transformation $\dot{q} = C(q)\dot{(q)}_2$ where $q_1 = [X, Y]^T$ and $q_2 = [\alpha, \beta, \gamma, \beta_a, \theta]^T$.

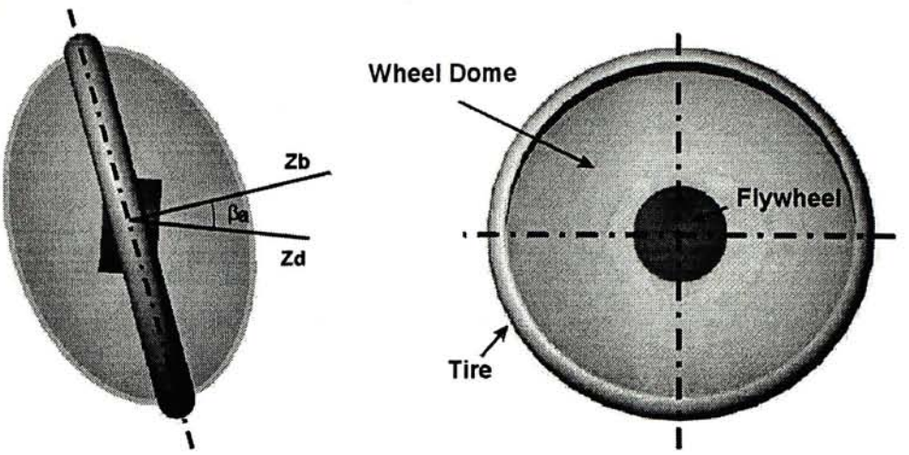

Figure 3.5: Front and side view of a single wheel robot

Then

$$\ddot{q} = C(q)\ddot{q}_2 + \dot{C}(q)\dot{q}_2$$

Therefore,

$$C^T(q)M(q)C(q)\ddot{q}_2 = C^T(q)[Bu - N(q, C(q)\dot{q}_2) - M(q)\dot{C}(q)\dot{q}_2]$$

where $C^T(q)M(q)C(q)$ is 5×5 a symmetric Positive Definite (P.D) matrix function. Then, the single wheel robot is considered as a rolling disk with a massive, high spinning concentric flywheel, which is shown in Figure 3.5. The l_1 is set to be zero as the gyroscopical stabilization is considered. The pendulum should be neglected if the robot reaches at the steady state. The θ will eliminate from the system dynamics. The number of generalized coordinates of the system will become three i.e., i.e., $q = [\alpha, \beta, \gamma, \beta_a]^T$ and $n = 4$. The system becomes

$$\begin{bmatrix} m_{11} & 0 & m_{13} & 0 \\ 0 & m_{22} & 0 & m_{24} \\ m_{13} & 0 & m_{33} & 0 \\ 0 & m_{24} & 0 & m_{44} \end{bmatrix} \begin{bmatrix} \ddot{\alpha} \\ \ddot{\beta} \\ \ddot{\gamma} \\ \ddot{\beta}_a \end{bmatrix} + N(q, \dot{q}) = \begin{bmatrix} 0 & 0 \\ 0 & 0 \\ 1 & 0 \\ 0 & 1 \end{bmatrix} u$$

where

$$\begin{aligned} m_{11} &= I_{xf} + I_{xw} + I_{xf}C^2_{\beta+\beta_a} + (I_{xw} + mR^2)C^2_{\beta} \\ m_{13} &= (2I_{xw} + mR^2)C_{\beta} \\ m_{22} &= I_{xf} + I_{xw} + mR^2 \end{aligned}$$

$$
\begin{aligned}
m_{33} &= 2I_{xw} + mR^2 \\
m_{24} &= m_{44} = I_{xf}
\end{aligned}
$$

$$
\begin{aligned}
N_1 &= -gmRC_\alpha C_\beta S_\varphi - (I_{xw} + mR^2)S_{2\beta}\dot{\alpha}\dot{\beta} - 2I_{xw}S_\beta\dot{\beta}\dot{\gamma} - 2I_{xf}S_{\beta+\beta_a}\dot{\gamma}_a\dot{\beta} \\
&\quad -I_{xf}S_{2(\beta+\beta_a)}\dot{\alpha}\dot{\beta} - 2I_{xf}S_{\beta+\beta_a}\dot{\beta}_a\dot{\gamma}_a - I_{xf}S_{2(\beta+\beta_a)}\dot{\beta}_a\dot{\alpha} \\
N_2 &= gmRC_\beta C_\varphi - gmRS_\alpha S_\beta S_\varphi + (I_{xw} + mR^2)C_\beta S_\beta\dot{\alpha}^2 \\
&\quad +(2I_{xw} + mR^2)S_\beta\dot{\alpha}\dot{\gamma} + 2I_{xf}S_{\beta+\beta_a}\dot{\alpha}\dot{\gamma}_a + I_{xf}S_{\beta+\beta_a}\dot{\alpha}^2 \\
N_3 &= -2(I_{xw} + mR^2)S_\beta\dot{\beta}\dot{\alpha} - gmRC_\alpha S_\varphi \\
N_4 &= 2I_{xf}S_{\beta+\beta_a}\dot{\alpha}\dot{\gamma}_a + I_{xf}S_{\beta+\beta_a}C_{\beta+\beta_a}\dot{\alpha}^2
\end{aligned}
$$

We further simplify the model by decoupling the tilting variable β_a from Equation 3.11. For position control of the Gyro, β_a is directly controlled by the tilt motor. The tilt actuator has an adequate torque to track the desired $\beta_a(t)$ trajectory exactly. It is similar to the case of decoupling the steering variable from the bicycle dynamics shown in [5]. Consider $\dot{\beta}_a$ as a new control input u_{β_a}, the number of generalized coordinates become three i.e., $q = [\alpha, \beta, \gamma]^T$ and $n = 3$.

The dynamic model of the robot on incline (*System[2]*) is

$$
\hat{M}_3(\hat{q})\ddot{\hat{q}} + \hat{N}(\hat{q}, \dot{\hat{q}}) = \hat{B}u, \quad \hat{q} = [\alpha, \beta, \gamma]^T \tag{3.12}
$$

where $\hat{M}_3(\hat{q}) \in \mathbb{R}^{3\times3}$ and $\hat{N}(\hat{q}, \dot{\hat{q}}) \in \mathbb{R}^{3\times1}$ are the inertia matrix and the nonlinear terms respectively. $\hat{B}$ is the input matrix. u is the input variable. u_1 is the drive torque and u_{β_a} is the tilt variable.

$$
\begin{aligned}
\hat{N} &= \left[\hat{N}_1, \hat{N}_2, \hat{N}_3\right]^T, \hat{B} = \begin{bmatrix} 0 & 0 & 1 \\ \hat{B}_{12} & 0 & 0 \end{bmatrix}^T, u = [u_1, u_{\beta_a}]^T \\
\hat{N}_1 &= -gmRC_\alpha C_\beta S_\varphi - (I_{xw} + mR^2)S_{2\beta}\dot{\alpha}\dot{\beta} - 2I_{xw}S_\beta\dot{\beta}\dot{\gamma} - 2I_{xf}S_{\beta+\beta_a}\dot{\gamma}_a\dot{\beta} \\
&\quad -I_{xf}S_{2(\beta+\beta_a)}\dot{\alpha}\dot{\beta} \\
\hat{N}_2 &= gmRC_\beta C_\varphi - gmRS_\alpha S_\beta S_\varphi + (I_{xw} + mR^2)C_\beta S_\beta\dot{\alpha}^2 \\
&\quad +(2I_{xw} + mR^2)S_\beta\dot{\alpha}\dot{\gamma} + 2I_{xf}S_{\beta+\beta_a}\dot{\alpha}\dot{\gamma}_a + I_{xf}S_{\beta+\beta_a}\dot{\alpha}^2 \\
\hat{N}_3 &= -2(I_{xw} + mR^2)S_\beta\dot{\beta}\dot{\alpha} - gmRC_\alpha S_\varphi \\
\hat{B}_{21} &= -2I_{xf}S_{\beta+\beta_a}\dot{\beta}_a\dot{\gamma}_a - I_{xf}S_{2(\beta+\beta_a)}\dot{\beta}_a\dot{\alpha}
\end{aligned}
$$

The model of a single wheel robot on the ground [45], assuming that the angle of inclination $\varphi = 0$, is a subset of this model. From the roll dynamics, the gravity term $gmRC_\beta C_\varphi - gmRS_\alpha S_\beta S_\varphi$ is dominant if the robot is stabilized at the position perpendicular to the surface of an inclined plane i.e., $\beta \to 90°$. On the other hands, the system dynamics becomes singularity if $\beta \to 0$. Therefore, the robot is difficult to balance when it moves on the surface of an inclined plane.
This type of robot possesses the typical characteristic when it reaches the equilibrium state. When the rate of change of yaw direction is small, and $\ddot{\alpha} = \ddot{\beta} = \ddot{\gamma} = 0, \dot{\alpha} = \dot{\beta} = 0, \alpha = 0, u_{\beta_a} = 0, \beta = 90°$, the pitch dynamic can be considered as $u_1 = -gmRS_\varphi$. The extra drive torque is used to maintain the robot without falling over on an inclined plane when it reaches an equilibrium state.

3.2.4 Linearized model

Due to the fact that when the robot is climbling up on an inclined plane, it is in a configuration perpendicular to the plane most of the time. Therefore, it is reasonable to linearize the model around the lean angle $\beta = 90°$. We now linearize the robot at the position perpendicular to the surface. We assume that $\beta = 90° + \delta\beta, \beta_a = \delta\beta_a, \dot{\beta} = \dot{\delta\beta}, \dot{\beta}_a = u_{\beta_a}$ and the term $\dot{\delta\beta}, \dot{\delta\beta}_a, \dot{\alpha}$ are sufficiently small and the terms $\dot{\gamma}_a\dot{\beta}, \dot{\gamma}\dot{\alpha}$ are sufficiently large compared with $\dot{\beta}\dot{\gamma}, \dot{\beta}\dot{\alpha}, \dot{\alpha}^2$. The linearized model is given by

$$\begin{aligned}
(I_{xf} + I_{xw})\ddot{\alpha} &= -gmRC_\alpha S_\beta S_\varphi + 2I_{xw}\dot{\delta\beta}\dot{\gamma} \\
&\quad +2I_{xf}\dot{\delta\beta}\dot{\gamma}_a + 2I_{xf}\dot{\gamma}_a u_{\beta_a} - \mu_s\dot{\alpha} \\
(I_{xf} + I_{xw} + mR^2)\ddot{\delta\beta} &= gmR\delta\beta C_\varphi - gmRS_\alpha S_\varphi - 2I_{xf}\dot{\gamma}_a\dot{\alpha} \\
&\quad -(2I_{xw} + mR^2)\dot{\gamma}\dot{\alpha} \\
(2I_{xw} + mR^2)\ddot{\gamma} &= -gmRC_\alpha S_\varphi + u_1 - \mu_g\dot{\gamma}
\end{aligned} \tag{3.13}$$

It is clear to notice that $\ddot{\alpha}$ is affected by u_{β_a} and $\ddot{\gamma}$ is affected by u_1, while $\ddot{\beta}$ is only indirectly affected by u_{β_a} and u_1. The key point for stabilizing the robot is the coupling effect between the yaw and roll motions as no actuator directly drives the control of the roll motion.

Chapter 4

Control of the robot on incline

In this chapter, we linearize the dynamic model of the single wheel robot around the position perpendicular to the surface. And then a linear state feedback controller is proposed to stabilize the robot from falling over on incline. And then the backstepping control method is designed to balance the robot following a straight path with a general heading angle. The feasibility of the method proposed is then verified by simulation analysis.

4.1 A state feedback control

The robot is stabilized without falling over and then rolls up on an incline.
Define state variables $x = [\delta\beta, \delta\alpha, \delta\dot{\beta}, \dot{\alpha}]^T$,the state equations form of (*System[2]*) is given by

$$\dot{x} = Ax + Bu, A = \begin{pmatrix} 0 & 0 & 1 & 0 \\ 0 & 0 & 0 & 1 \\ a_{31} & a_{32} & 0 & a_{34} \\ a_{41} & 0 & a_{43} & a_{44} \end{pmatrix}, B = \begin{pmatrix} 0 \\ 0 \\ 0 \\ b \end{pmatrix} \tag{4.1}$$

$$\begin{cases} \dot{x}_1 &= x_3 \\ \dot{x}_2 &= x_4 \\ \dot{x}_3 &= a_{31}x_1 + a_{32}x_2 + a_{34}x_4 \\ \dot{x}_4 &= a_{41}x_1 + a_{43}x_3 + a_{44}x_4 + bu_{\beta_a} \end{cases} \tag{4.2}$$

For

$$a_{31} = \frac{gmRC_\varphi}{I_{xf} + I_{xw} + mR^2}$$

$$
\begin{aligned}
a_{32} &= \frac{-gmRS_\varphi}{I_{xf}+I_{xw}+mR^2} \\
a_{34} &= \frac{-(2I_{xw}+mR^2)\dot{\gamma}-2I_{xf}\dot{\gamma}_a}{I_{xw}+I_{xf}+mR^2} \\
a_{41} &= \frac{-gmRS_\varphi}{I_{xw}+I_{xf}} \\
a_{43} &= \frac{2I_{xw}\dot{\gamma}+2I_{xf}\dot{\gamma}_a}{I_{xw}+I_{xf}} \\
a_{44} &= -\frac{\mu_s}{I_{xw}+I_{xf}} \\
b &= \frac{2I_{xf}\dot{\gamma}_a}{I_{xw}+I_{xf}}
\end{aligned}
$$

The angular velocity of flywheel keeps remain constant such as $\dot{\gamma}_a$=-16000 rpm. Consider the system with the following control law

$$
\begin{aligned}
u_\beta &= -k_1\delta\beta - k_2\delta\alpha - k_3\dot{\delta\beta} - k_4\dot{\delta\alpha} \\
u_1 &= -k_5\Omega
\end{aligned}
$$

u_β would be selected such that $\delta\beta, \delta\alpha, \dot{\delta\beta}$ & $\dot{\delta\alpha}$ converge to zero.

The rolling speed of the wheel converges to Ω_0. We can select that u_β & u_1 such that all state variables $\delta\beta, \delta\alpha, \dot{\delta\beta}$ & $\dot{\delta\alpha}, \Omega$) will converge to zero. Therefore, the robot is stabilized to the position perpendicular to the surface ($\beta = 90°$) and the heading angle become zero ($\alpha = 0$). At the same time, the rate of steering and leaning convert to zero ($\dot{\alpha} = 0, \dot{\beta} = 0$.

The controllability of the system is investigated. Let $\mathbb{C} = [B\,|AB|\,A^2B]$

$$
\begin{aligned}
&= \begin{bmatrix}
0 & 0 & a_{34}b & a_{32}b + a_{44}a_{34}b \\
0 & b & a_{44}b & a_{34}a_{43}b + a_{44}^2 b \\
0 & a_{34}b & a_{32}b + a_{44}a_{34}b & a_{31}a_{34}b + a_{32}a_{44}b + a_{34}^2 a_{43}b + a_{34}a_{44}^2 b \\
b & a_{44}b & a_{34}a_{43}b + a_{44}^2 b & a_{41}a_{34}b + a_{32}a_{43}b + a_{44}a_{43}a_{34}b + a_{34}a_{43}a_{44}b + a_{44}^2 b
\end{bmatrix} \\
&= b^4\left(a_{34}a_{44}(a_{32} + a_{44}a_{34})\right)
\end{aligned}
$$

If $\dot{\gamma}_a \neq 0$, the rank is 4. The system is controllable when the spinning rate of flywheel is not equal to zero.

The characteristic equation of the system is given by

$$
s^4 + (bk_4 - a_{44})s^3 + (k_2 b + a_{31})s^2 + (a_{31}a_{44} - bk_4 a_{31})s - a_{31}k_2 b
$$

Table 4.1: Parameters (1) used for simulation of robot on incline

Table 4.1: System parameters (1)	
Robot wheel:	$m = 15.0kg, R = 17cm, I_{xw} = 0.0289kgm^2$
Flywheel:	$I_{xf} = 0.0063kgm^2$
Friction coeff.:	$\mu_s = 1Nm/(rad/s), \mu_g = 0.1Nm/(rad/s)$
A climbling angle:	$\varphi = 20°$

The necessary conditions of the feedback gains are

$$k_1 > 0, k_2 > 0, k_3 > 0, k_4 < \frac{a_{44}}{b}$$

4.1.1 Simulation study

The geometric/mass parameters is summarized in the Table 4.1. The initial conditions are

$$\dot{\alpha} = \dot{\beta} = \dot{\beta}_a = 0\,\text{rad/s}, \dot{\gamma} = -15\,\text{rad/s}, \dot{\gamma}_a = -16000\,rpm$$
$$\alpha = \gamma = 0°, \beta = 80°, \beta_a = 0°,\ X = Y = 0$$

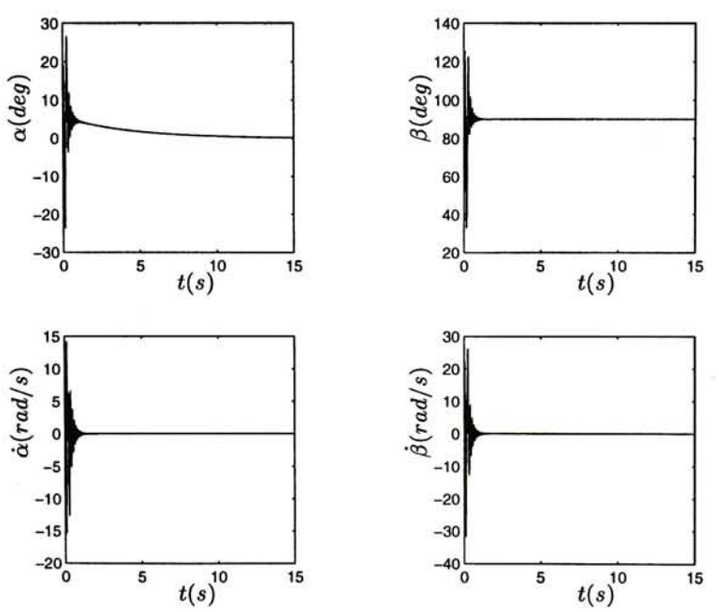

Figure 4.1: System State variables $x = [\delta\beta, \delta\alpha, \delta\dot{\beta}, \dot{\alpha}]^T$

In the Figure 4.1, state variables $(\delta\beta, \delta\dot{\beta}, \dot{\alpha})$ of the robot converge to zero at t=2s.

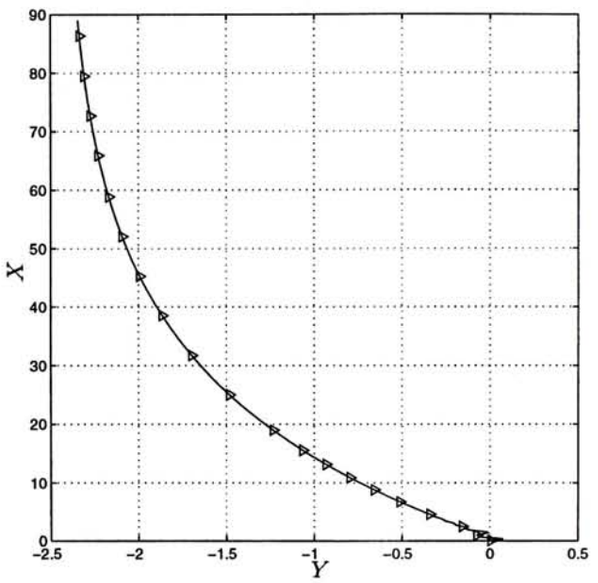

Figure 4.2: Path of the robot on an incline with $\varphi = 20°$

The rate of steering and leaning convert to zero. The $\beta = 90°$ becomes zero while the robot is stabilized to the position perpendicular to the surface. However, the $\delta\alpha$ converges to zero until t=14s. The heading angle become zero ($\alpha = 0$). At the same time, the robot track with the line parallel to Y-axis of the the surface. It is shown in the Figure 4.2 In the Figure 4.3, the rolling velocity of the robot becomes -35 rad/s. And the Torque $\tau = -10Nm$ is applied to overcome some components of gravity force of the robot on incline. In the previous section, we addressed the characteristic of (*System[2]*), when the robot reaches the equilibrium state, the extra drive torque is used to maintain the robot without falling over on an inclined plane. It is considered as $\tau = -gmRS_{\varphi}$.

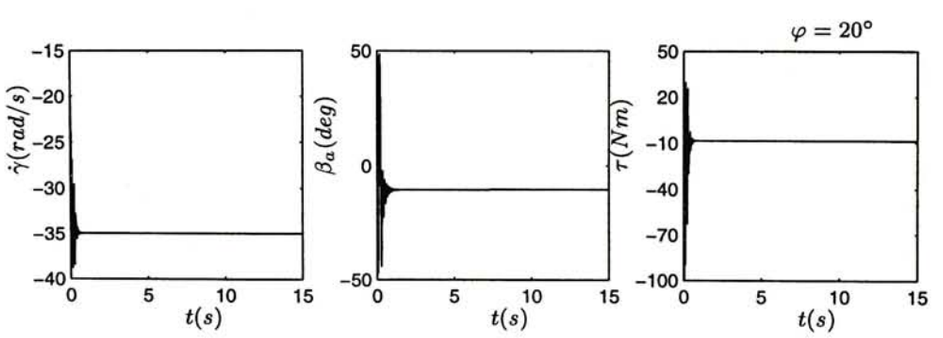

Figure 4.3: History of γ, β_a, τ

4.2 Backstepping-based control

The backstepping feedback control was used in nonholonomic systems [22]. The backstepping feedback is proposed in this section. The problem we are concerned is stabilization of the nonholonomic systems in a chained form. Consider $x = [\delta\beta, \dot{\alpha}, \dot{\delta\beta}]^T$, Equations (3.13) can be written

$$\begin{aligned} \dot{x}_1 &= x_3 \\ \dot{x}_2 &= f_{21}x_1 + f_{22}x_2 + f_{23}x_3 + g_{21}u_{\beta_a} \\ \dot{x}_3 &= f_{31}x_1 + f_{32}x_2 + g_{32} \end{aligned} \tag{4.3}$$

where

$$\begin{aligned} f_{21} &= \frac{-gmrS_\varphi C_\alpha}{I_{xf} + I_{xw}} \\ f_{22} &= \frac{\mu_s}{I_{xf} + I_{xw}} \\ f_{23} &= \frac{2(I_{xw}\dot{\gamma} + I_{xf}\dot{\gamma}_a)}{I_{xf} + I_{xw}} \\ f_{31} &= \frac{gmRC_\varphi}{I_{xf} + I_{xw} + mR^2} \\ f_{32} &= \frac{-(2I_{xw} + mR^2)\dot{\gamma} - 2I_{xf}\dot{\gamma}_a}{I_{xf} + I_{xw} + mR^2} \\ g_{21} &= \frac{2I_{xf}\dot{\gamma}_a}{I_{xf} + I_{xw}} \\ g_{32} &= \frac{-gmRS_\alpha S_\varphi}{I_{xf} + I_{xw} + mR^2} \end{aligned}$$

Theorem 1 *Consider the system (3.13) under the following control law are defined*

$$\begin{aligned} u_{\beta_a} &= \frac{-f_{21}x_1 - f_{22}x_2 - f_{23}x_3 + \dot{\alpha}_2 - k_3(x_2 - \frac{\eta}{f_{32}})}{g_{21}} \\ \dot{\alpha}_2 &= \frac{-(1 + f_{31})\dot{x}_1 - k_1\dot{x}_3 - k_2(x_3 + k_1x_1)}{f_{32}} \\ \eta_2 &= -(1 + f_{31})x_1 - g_{32} + k_1^2x_1 - k_2(x_3 + k_1x_1) \end{aligned}$$

Assuming that the initial condition $x_i(0) \neq 0$, the system converges (perpendicular position to the surface)

Proof. Under the change of coordinates, system (4.3) becomes

$$\begin{aligned} \dot{x}_1 &= \tilde{x}_3 + \alpha_3 \\ \dot{\tilde{x}}_2 &= \dot{x}_2 - \dot{\alpha}_2 \\ &= f_{21}x_1 + f_{22}x_2 + f_{23}x_3 + g_{21}u_{\beta_a} - \dot{\alpha}_2 \\ \dot{\tilde{x}}_3 &= f_{31}x_1 + f_{32}x_2 + g_{32} - \dot{\alpha}_3 \end{aligned} \tag{4.4}$$

We now search for the control law u_{β_a} for stabilization of Equations (4.3), using the backstepping approach. The first step is to find an adequate control x_3 which stabilizes x_1. In the next step, we define two new variables α_3 and $\tilde{x}_3$ and then look for a suitable Lyapunov function V_2 for the first two of Equations (4.4) and a virtual control x_2. Then we define two variables α_2 and $\tilde{x}_2$ and the augment V_2 to obtain an adequate function V_3 which leads to the control input u_{β_a} that stabilizes $\tilde{x}_2$.
Under the system (4.3), we first choose x_3 such that $x_3 = -k_1x_1$ with $k_1 > 0$.

Let

$$\begin{aligned} \alpha_3 &= -k_1x_1 \\ \tilde{x}_3 &= x_3 - \alpha_3 \\ \dot{x_1} &= \tilde{x}_3 + \alpha_3 \\ \dot{\tilde{x}}_3 &= \dot{x}_3 - \dot{\alpha}_3 \\ &= f_{31}x_1 + f_{32}x_2 + g_{32} - \dot{\alpha}_3 \end{aligned}$$

The Lyapunov's function is

$$\begin{aligned} V_2 &= \frac{1}{2}x_1^2 + \frac{1}{2}\tilde{x}_3^2 > 0 \\ \dot{V}_2 &= x_1\dot{x}_1 + \tilde{x}_3\dot{\tilde{x}}_3 \\ &= x_1(\tilde{x}_2 + \alpha_3) + \tilde{x}_3(f_{31}x_1 + f_{32}x_2 + g_{32} - \dot{\alpha}_3) \\ &= x_1\alpha_3 + \tilde{x}_3(x_1 + f_{31}x_1 + f_{32}x_2 + g_{32} - \dot{\alpha}_3) \end{aligned}$$

Consider $f_{32}x_2 = -(1+f_{31})x_1 - g_{32} + \dot{\alpha}_3 - k_2\tilde{x}_3 = \eta_2$. We know $\dot{V}_2 = -k_1x_1^2 - k_2\tilde{x}_3^2 < 0$. Then consider

$$\begin{aligned} \alpha_2 &= \frac{\eta_2}{f_{32}} \quad \text{as} \quad f_{32} \neq 0 \\ \tilde{x}_2 &= x_2 - \alpha_2 \\ \dot{x}_1 &= \tilde{x}_3 + \alpha_3 \end{aligned}$$

$$\begin{aligned}\dot{\tilde{x}}_2 &= \dot{x}_2 - \dot{\alpha}_2 \\ &= f_{21}x_1 + f_{22}x_2 + f_{23}x_3 + g_{21}u_{\beta_a} - \dot{\alpha}_2 \\ \dot{\tilde{x}}_3 &= f_{31}x_1 + f_{32}x_2 + g_{32} - \dot{\alpha}_3\end{aligned}$$

The Lyapunov's function is

$$\begin{aligned}V_3 &= \frac{1}{2}x_1^2 + \frac{1}{2}\tilde{x}_3^2 + \frac{1}{2}\tilde{x}_2^2 > 0 \\ \dot{V}_3 &= x_1\dot{x}_1 + \tilde{x}_3\dot{\tilde{x}}_3 + \tilde{x}_2\dot{\tilde{x}}_2 \\ &= -k_1x_1^2 - k_2\tilde{x}_3^2 + \tilde{x}_2(f_{21}x_1 + f_{22}x_2 + f_{23}x_3 + g_{21}u_{\beta_a} - \dot{\alpha}_2)\end{aligned}$$

Choose a suitable u_{β_a} to make $\dot{V}_3$ be negative definite. Consider $g_{21}u_{\beta_a} = -f_{21}x_1 - f_{22}x_2 - f_{23}x_3 + +\dot{\alpha}_2 - k_3\tilde{x}_2$. Then

$$\dot{V}_3 = -k_1x_1^2 - k_2\tilde{x}_3^2 - k_3\tilde{x}_2^2 < 0$$

The feedback control is

$$\begin{aligned}u_{\beta_a} &= \frac{-f_{21}x_1 - f_{22}x_2 - f_{23}x_3 + \dot{\alpha}_2 - k_3(x_2 - \frac{\eta}{f_{32}})}{g_{21}}, g_{21} \neq 0 \\ \text{where } \dot{\alpha}_2 &= \frac{-(1+f_{31})\dot{x}_1 - k_1\dot{x}_3 - k_2(x_3 + k_1x_1)}{f_{32}}, f_{32} \neq 0 \\ \eta_2 &= -(1+f_{31})x_1 - g_{32} + k_1^2x_1 - k_2(x_3 + k_1x_1)\end{aligned}$$

This ensures that the system converges (perpendicular position to the surface), such that

$$\delta\beta = 0, \dot{\delta\beta} = \dot{\alpha} = 0, \ddot{\delta\beta} = \ddot{\alpha} = \ddot{\gamma} = 0, \alpha = \text{constant}$$

4.2.1 Simulation study

The following geometric/mass parameters from the real system throughout our following simulations is summarized in the Table 4.2. We investigated the system when $\dot{\gamma}_a \neq 0$. It is clear that the spinning flywheel provide a large angular momentum. The initial conditions are

$$\begin{aligned}\dot{\alpha} = \dot{\beta} = \dot{\beta}_a = 0\,\text{rad/s}, \dot{\gamma} = -15\,\text{rad/s}, \dot{\gamma}_a = 1600\,rpm \\ \alpha = 5°, \gamma = 0°, \beta = 80°, \beta_a = 90°, X = Y = 0\end{aligned}$$

Case 1: A straight line path

Table 4.2: Parameters (2) used for simulation of robot on incline

Table 4.2: System parameters (2)	
Robot wheel:	$m = 15.0kg, R = 17cm, I_{xw} = 0.0289kgm^2$
Flywheel:	$I_{xf} = 0.0063kgm^2$
Friction coeff.:	$\mu_s = 1Nm/(rad/s), \mu_g = 0.1Nm/(rad/s)$
A climbling angle:	$\varphi = 10°$

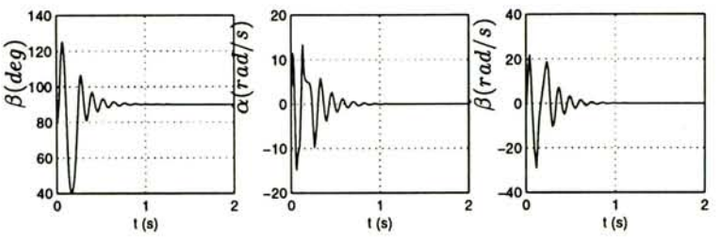

Figure 4.4: Sytem State variables $[\beta, \dot{\alpha}, \dot{\beta}]$ for straight line path

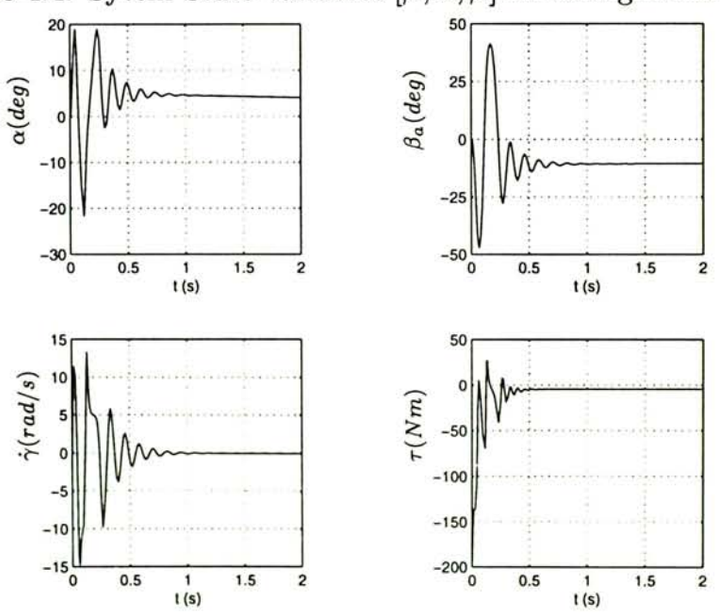

Figure 4.5: History of $\alpha, \beta_a, \dot{\gamma}, \tau$

The robot is stabilized to keep the upright position on an inclined plane, $\beta = 90°, \delta\beta_{ref} = 0°$, such that the resulting roll-up trajectory is a straight line in Figure 4.8. The lean angle β of the robot exponentially converges to 90° and the steering rate $\dot{\alpha}$ converge exponentially to zero as shown in Figure 4.4. The rolling speed of $\dot{\gamma}$ becomes -40 rad/s as shown in Figure 4.5. The trajectory of the center of the robot oscillates at the beginning and then finally is restricted to follow a

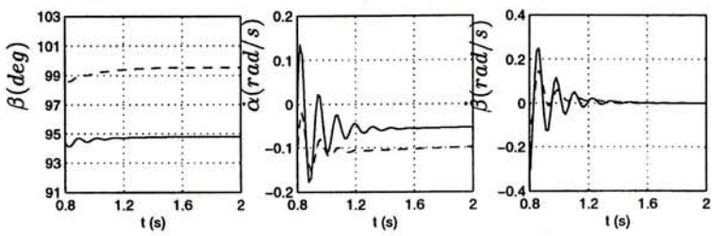

Figure 4.6: Sytem state variables $[\beta, \dot{\alpha}, \dot{\beta}]$ for $\delta\beta_{ref}$ are 5° and 10° respectively

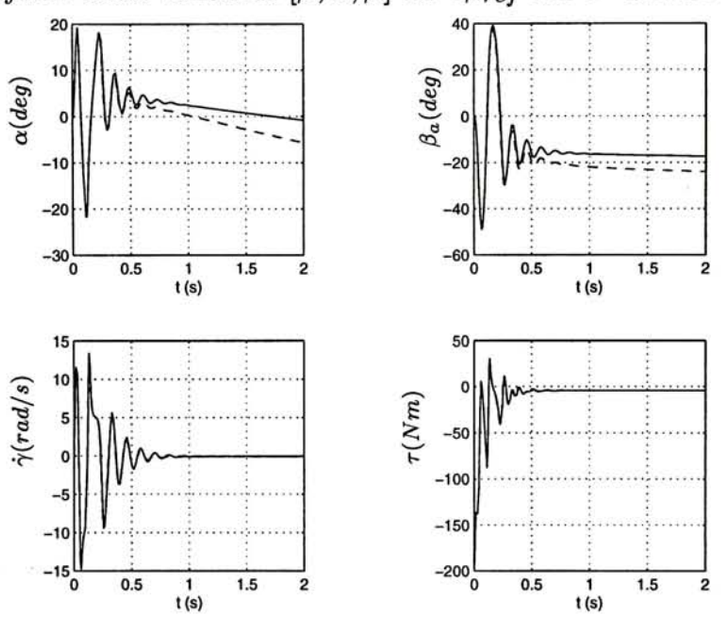

Figure 4.7: History of $\alpha, \beta_a, \dot{\gamma}, \tau$ for $\delta\beta_{ref} = 10°$ (dash line) & $\delta\beta_{ref} = 5°$ (solid line)

straight line path shown in Figure 4.8.

Case 2: A curved path

When $\delta\beta_{ref} \neq 0$, the effect of change $S_\alpha S_\varphi$ due the gravity is also investigated. The initial conditions is identical to the previous case. The robot steers right as $\delta\beta_{ref}$ are 5° and 10° respectively. The value of α decrease, meaning that the robot turns clockwise. The steady state value of α_s becomes -0.052 and -0.1 respectively as shown Figure 4.7.

The paths of the robot generated while it's lean angle converges to 90°,95° and 100° respectively as shown Figure 4.8. When the lean angle keeps at 90°, the robot tracks in a straight line path. On the other hand, the robot precesses in the direction it is leaning.

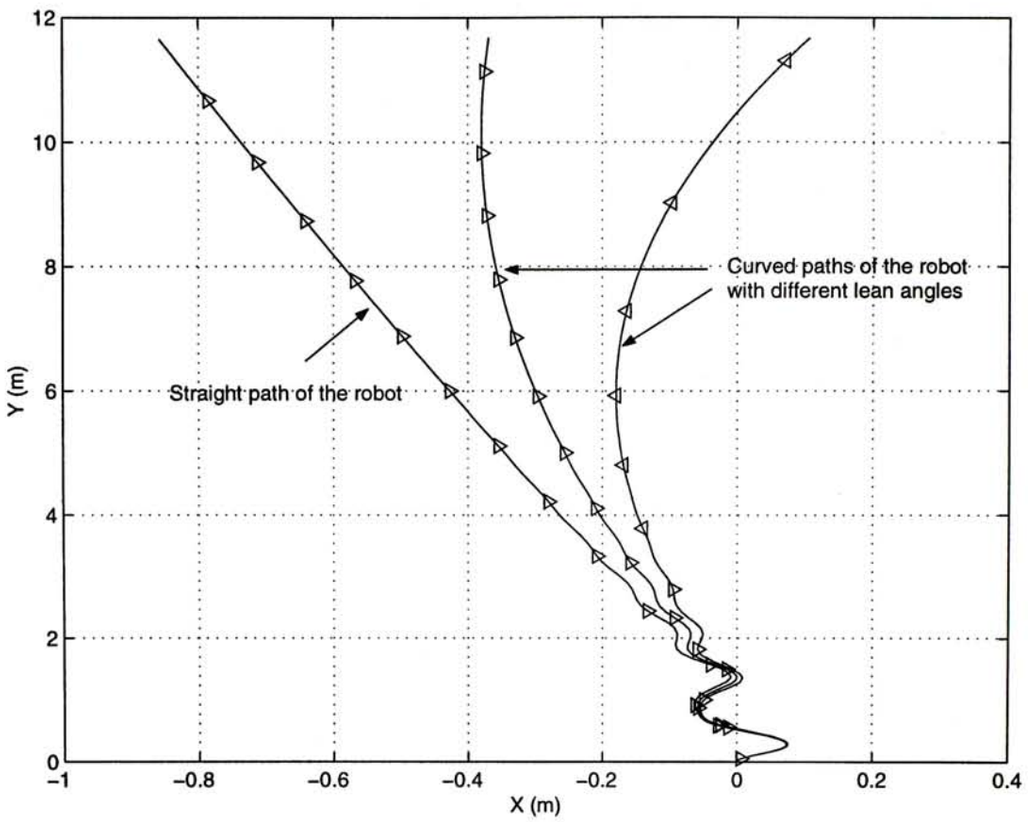

Figure 4.8: Straight path & curved paths of the robot on an inclined plane with $\varphi = 10°$

4.2.2 The effect of the spinning rate of flywheel

Now, the effect of the spinning rate of the flywheel to the robot path generated is studied. The simulation results with different spinning rates of the flywheel $\dot{\gamma}_a$, $16000rad/s$, $8000rad/s$ and $4000rad/s$ are shown in the Figure 4.9. The rate of change of velocities in yaw, pitch and roll and the convergence are investigated to validate the system performance in stabilizing the robot. Consider the system with $\dot{\gamma}_a = 16000rad/s$, the leaning angle of the flywheel β_a and the torque applied τ are small in comparison to other two different spinning rates of the flywheel. The steady state values of $\dot{\alpha}, \dot{\beta}, \dot{\gamma}$ are significantly small. The angle of steering decreases and the trajectory of the robot is more straight. It demonstrates the efficiency of stabilizing the robot with a high spinning rate of the flywheel, in comparison to that of a low spinning rate. Even when a single wheel robot is statically unstable in the roll direction, it can achieve dynamic stability by a gyroscopic force. Steering stability generally increases with a higher spinning rate due to a gyroscopic effect. The robot can balance in the flat plane, even when it stands still.

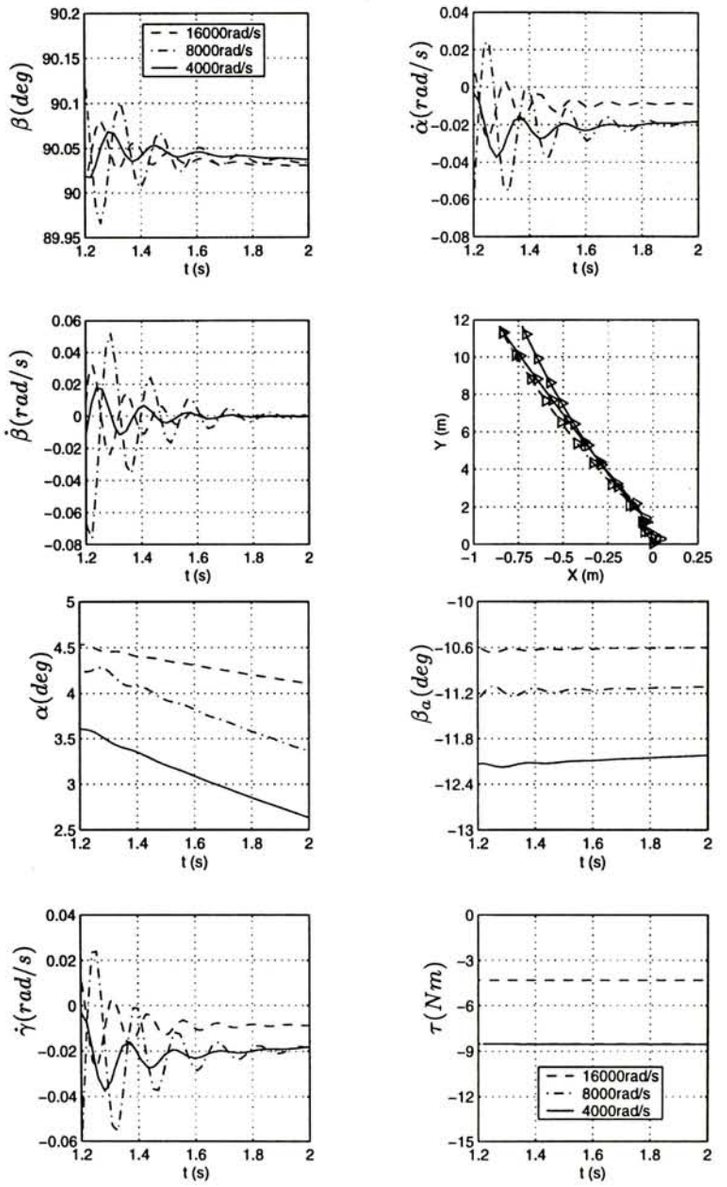

Figure 4.9: System variables for different spinning rates of flywheel

4.2.3 Simulation study

The comparison between a rolling disk and the robot on an inclined plane is studied. The initial condition in simulation study is

$$\dot{\alpha} = \dot{\beta} = 0\,\text{rad/s}, \dot{\gamma} = -15\,\text{rad/s}$$
$$\alpha = \gamma = 0°, \beta = 80°, X = Y = 0$$

4.2.4 Roll up case

Case I: Rolling up case Figure 4.10 showed the simulation of a rolling disk. It is noted that the lean angle $\dot{\beta}$ of the rolling disk decrease rapidly and the lean angle β converts to be zero. This means the disk falls over, or, its inertial matrix will become singular, which it violates the assumption of rolling without slipping. Besides, the steering rate $\dot{\alpha}$ rises up and down, and the trajectory of the rolling disk does not go up along the Y axis. The rolling disk fails to go up.

For a single wheel robot, we investigated the system when $\dot{\gamma}_a = 1600\,\text{rpm} \neq 0$. It is clear that the spinning flywheel provide a large angular momentum. We stabilize the robot to the upright position $\beta = 90°, \delta\beta_{ref} = 0°$, such that the resulting roll-up trajectory is a straight line. The feedback gains are $k1 = -30$, $k2 = -3$ and $k3 = 3$ respectively. The simulation results are shown in Figure 4.11. It shows that the lean angle β of the robot exponentially converge to 90° and the steering rate $\dot{\alpha}$ exponentially converges to zero. The rolling speed of $\dot{\gamma}$ becomes -35 rad/s and the trajectory of the center of the robot oscillates at the beginning and then finally restrict to follow a straight line path.

4.2.5 Roll down case

Case II: Rolling down case Figure 4.12 shows that a rolling disk falls down very rapidly from stationary. It is because that 5° turns in the lean angle from the vertical direction makes the disk fall down. Figure 4.13 showed the single wheel robot when rolling down. we select the feedback gains which are $k1 = 30$, $k2 = -3$ and $k3 = -3$ respectively. It is similar to the rolling up case. This implies that the single wheel robot is balanced along the vertical position by the tilting of the flywheel.

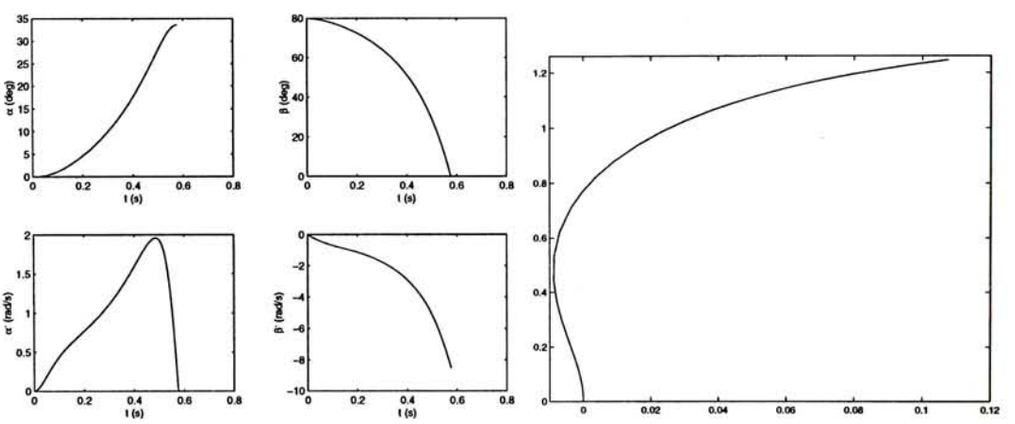

Figure 4.10: Rolling up of a disk on incline

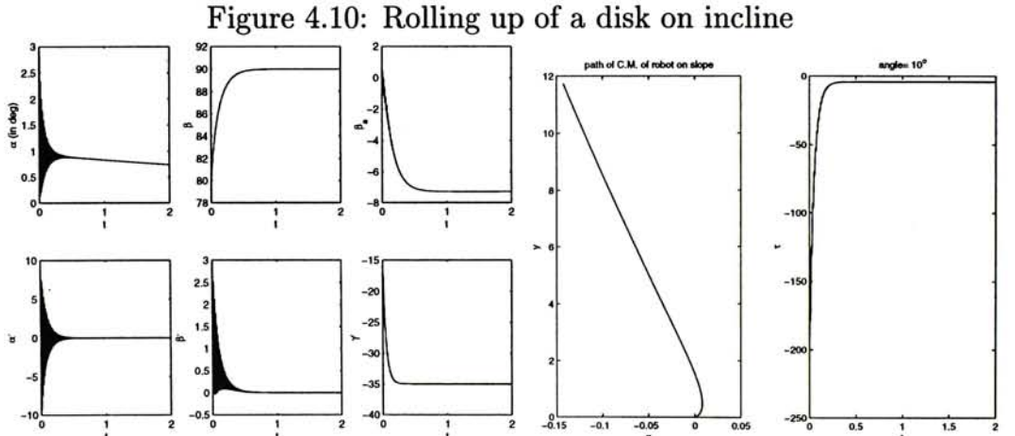

Figure 4.11: Rolling up of a single wheel robot on incline

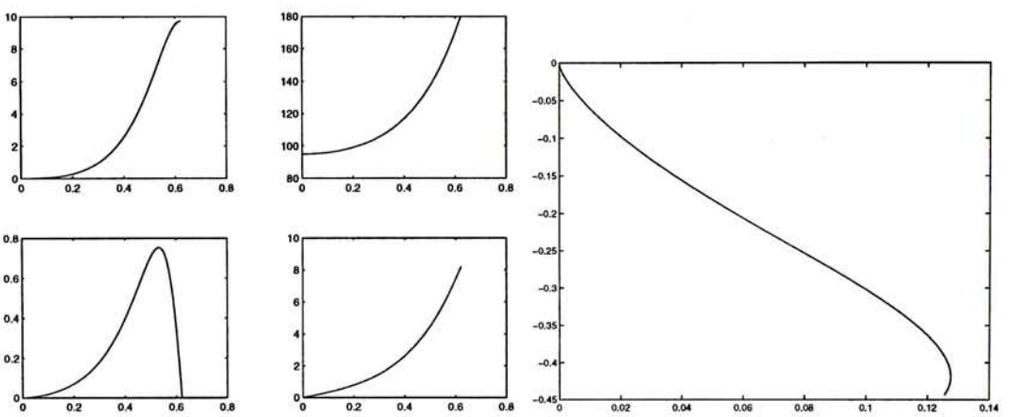

Figure 4.12: Rolling down of a disk on incline

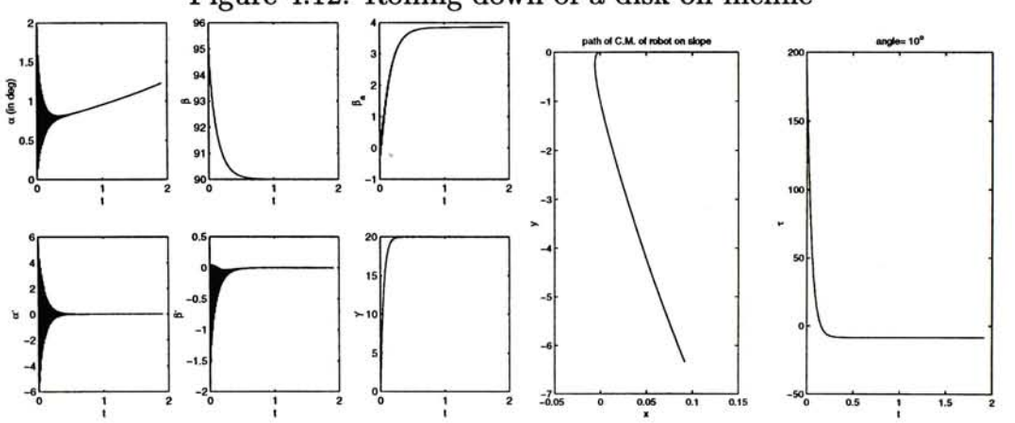

Figure 4.13: Rolling down of a single wheel robot on incline

Chapter 5

Motion planning

In this chapter, we investigate the condition of a rolling up. And then we study the ways to drive the wheel up on the inclined surface when the condition is violated. There is a strong assumption that the single wheel robot is balanced to the position perpendicular to the surface on an inclined plane. The lean angle of the robot is 90° and the rate of leaning is zero. The performance of the single wheel robot is exactly same as the rolling wheel.

5.1 Performance index

Safety Factor (SF) can be used as a performance index which measures the wheel's ability successfully to roll up a slope from stationary.

$$SF = \frac{\ddot{\gamma}_{min}(mr^2 + I)}{mgr \sin \varphi}$$

It is to measure how wheel successfully rolls up on plane quantitively. It is a dimensionless and is always larger than zero. If it becomes zero, the minimum angular acceleration of rolling wheel also becomes zero. The wheel never rolls up. The probability of rolling on plane become larger as SF increases. There are three ways to increase the value of SF. First of all is to provide a larger value of $\ddot{\gamma}_{min}$. The more the value of $\ddot{\gamma}_{min}$ is, the more the probability of wheel's rolling up i.e. larger value of SF. Secondly, if the moment of inertia of wheel increases, SF increases too. For the case that $\sin\varphi$ become less as the angle between the surface of plane and ground decrease, the chance

for rolling up is strictly larger. Therefore, the condition of wheel's roll on plane is

$$C = (SF + 1)mgr \sin\varphi$$

When SF is equal to one,

$$\ddot{\gamma}_{min} = \frac{mgr \sin\varphi}{mr^2 + I}$$
$$C = 2mgr \sin\varphi$$

For a constant of SF, φ become larger as applied torque C increases. However, there is a maximum value of φ. It was because that the condition of rolling without sliding is violated as the applied torque is greater than certain value. Since sliding occurs,

$$\begin{aligned} F &= \mu_s N \\ &= \mu_s mg \cos\varphi \qquad \text{where} \quad \mu_s \text{ is a static friction} \\ \lambda &= \mu_s mg \cos\varphi \end{aligned}$$

$$C = \frac{\left((mr^2 + I)\mu_s \cos\varphi - I \sin\varphi\right)g}{r} \tag{5.1}$$

5.2 Condition of rolling up

In this section, we determine the condition of rolling up of the wheel on an inclined plane. The linear acceleration of the rolling wheel along the plane and the angular acceleration of rolling wheel are

$$\begin{aligned} \ddot{y} &= \frac{rC - mr^2 g \sin\varphi}{mr^2 + I} \\ \ddot{\gamma} &= \frac{C - mrg \sin\varphi}{mr^2 + I} \end{aligned}$$

The conditon of rolling without slipping holds i.e., $\ddot{y} = r\ddot{\gamma}$. Initially $\dot{\gamma}, v_0$ are set to be zero. The minimum value of the angular acceleration of rolling wheel is $\ddot{\gamma}_{min}$. Therefore, the condition of wheel's roll up on an inclined plane is

$$C \geq (mr^2 + I)\ddot{\gamma}_{min} + mgr \sin\varphi$$

Let's rearrange the above equation so that φ is represented as a function of the minimum angular acceleration of rolling wheel $\ddot{\gamma}_{min}$, the moment of inertia I and the applied

torque C.

$$\sin\varphi = \frac{C - (mr^2 + I)\ddot{\gamma}_{min}}{mgr} \tag{5.2}$$

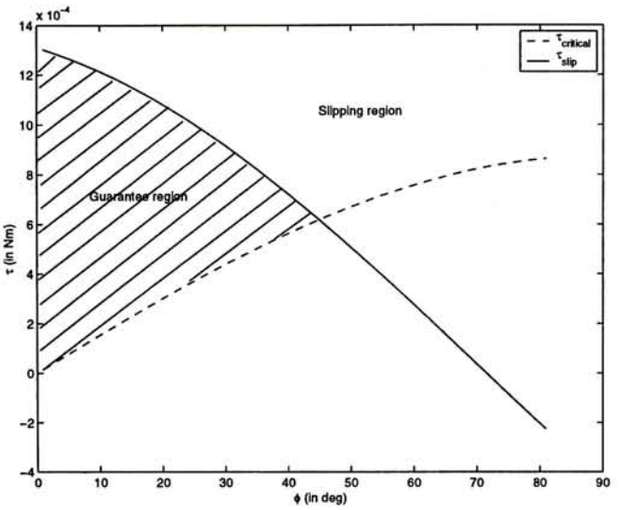

Figure 5.1: Torque applied to the coin

In Figure 5.2, for instance a rolling one dollar wheel, it shows the relationship between the torque applied and the angle of the slope. There are two curves having in the same figure. The former is called the critical torque line and the latter is the line of slipping torque. The angle between the surface of slope and the ground of the wheel at the critical torque line is called the critical angle ϕ. When the applied torque is greater than the critical torque, the wheel should roll up any slope which angle is smaller or equal to the critical angle ϕ. According to the condition of slipping, wheel impedes slip when the Equation (5.2) is hold. The applied torque is greater or equal to the torque at the line of slipping. Therefore, the Guarantee region is the area which promise the wheel can roll on specialized slope when certain torque is applied. And those equations we derived fail when it is on the region of slipping. From the Figure 5.3, the forward velocity and the acceleration of rolling determined for different angle ϕ. As the previous result, the wheel roll on the inclined plane when it's rolling acceleration is greater than a minimum acceleration. We set the value of minimum rolling acceleration is zero. Let's see Figure 5.3, when the applied torque is 0.0005 Nm, the velocities and the acceleration of wheel determined for different slopes. It is so trivial that those velocities and acceleration will increase when the angle ϕ decreases. As the default minimum rolling acceleration or the acceleration of wheel $\ddot{y}$ is set as 10 rad/s, the wheel cannot roll up the slopes with angle 34° and 35° from the Figure 5.3, according to the Equation 5.2, the critical angle of the slope for a one dollar wheel when 0.0005

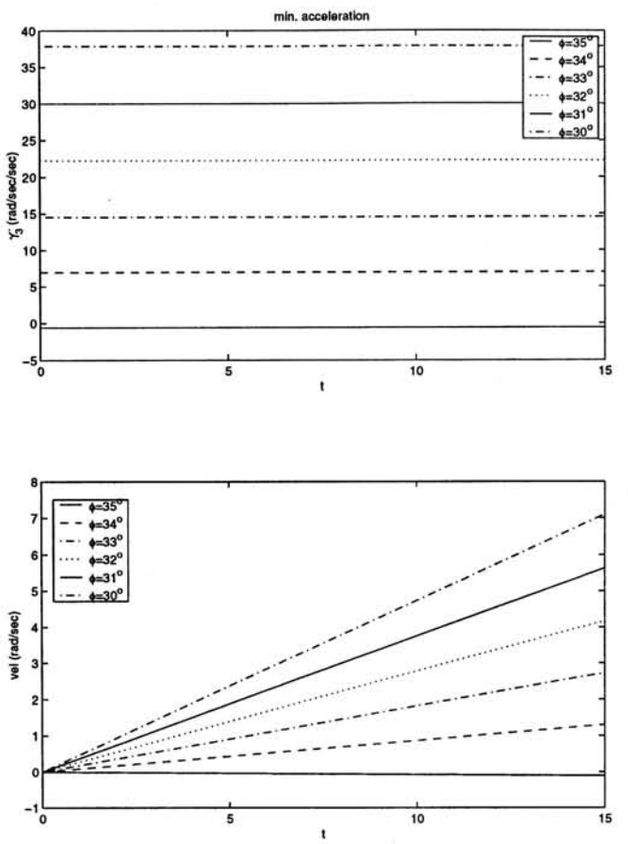

Figure 5.2: Velocity and acceleration of wheel

Nm torque applied is 33.64°.

5.3 Motion planning of rolling Up

In this section, we would like to answer a simple question. Can we still make the wheel rolls up an inclined plane φ while the condition of wheel's rolling up is failure? And how should we acquire that? Assume that the inclined plane is fixed and the trivial solution for decreasing the angle of φ is omitted. We discuss how to remedy the failure of the condition of rolling up by planning the wheel's motion in different angles.

5.3.1 Method I : Orientation change

Suppose we change the direction of heading

$$\sin\phi = \frac{y\sin\varphi}{\sqrt{x^2+y^2}} = \sin\varphi\sin\alpha$$

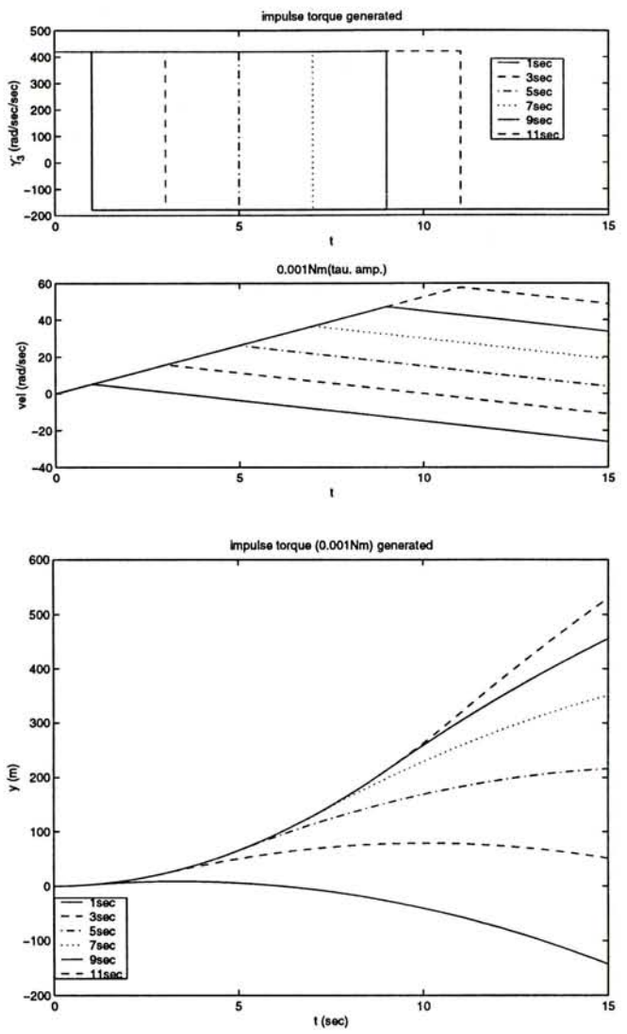

From the previous result, the condition of rolling up is

$$C \geq (mr^2 + I)\ddot{\gamma}_{min} + mgr \sin\alpha \sin\varphi$$

Now we consider the wheel rolling on an inclined plane ϕ instead of φ.

$$\begin{aligned} ds &= r d\gamma \\ dx &= -ds \cdot \cos\alpha \\ dy &= ds \cdot \sin\alpha \end{aligned}$$

On using the last equation in the former two equations, we obtain two relations amongst the differentials as

$$dx + r\cos\alpha d\gamma = 0$$

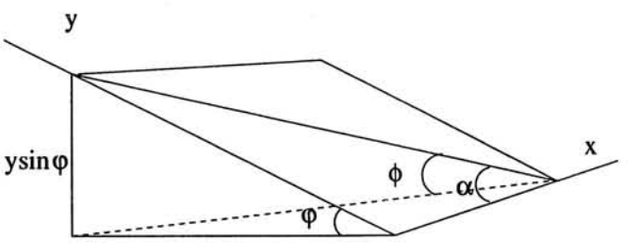

Figure 5.3: Orientation change

$$dy - r\sin\alpha d\gamma = 0$$

By the same method, Lagrange undetermined multiplier λ,

$$\lambda_1 dx + \lambda_1(r\cos\alpha)d\gamma = 0$$
$$\lambda_2 dy - \lambda_2(r\sin\alpha)d\gamma = 0$$

By the virtual work principle,

$$\delta\acute{W} = C\delta\gamma + \lambda_1 dx + \lambda_2 dy - d\gamma(\lambda_2 r\sin\alpha - \lambda_1 r\cos\alpha)$$

We may describe the configuration of the wheel in terms of four generalized coordinates: $q = [x, y, \alpha, \gamma]^T$. The Lagrange is become

$$\mathcal{L} = \frac{1}{2}m(\dot{x}^2 + \dot{y}^2) + \frac{1}{2}I\dot{\gamma}^2 + \frac{1}{2}\left(\frac{1}{2}I\right)\dot{\alpha}^2 - mg(\sin\varphi y + r\cos\varphi)$$

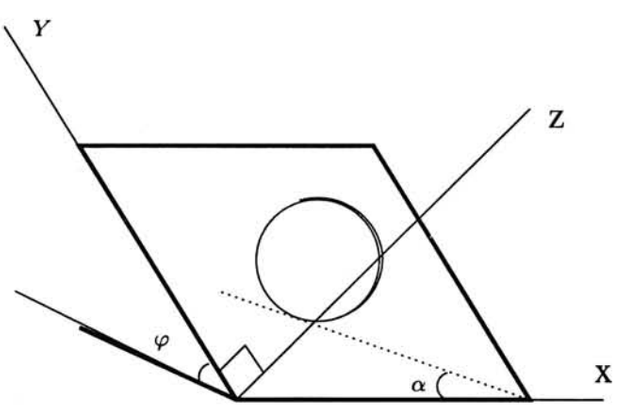

Figure 5.4: wheel rolls on plane ϕ

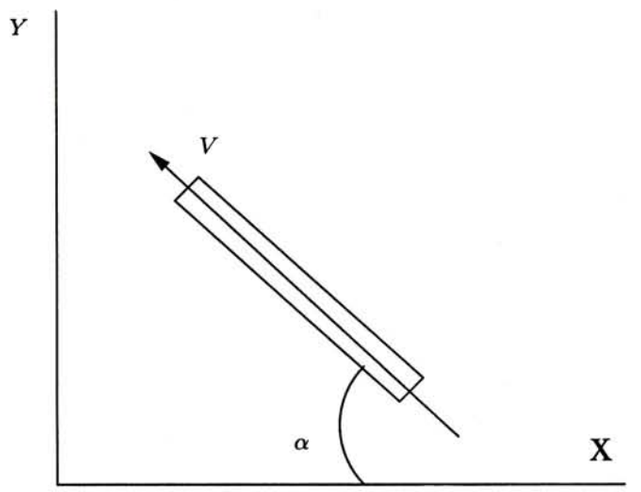

Figure 5.5: Top View

then,

$$\begin{aligned} m\ddot{x} &= \lambda_1 \\ m\ddot{y} + mg\sin\varphi &= \lambda_2 \\ I\ddot{\gamma} &= C - \lambda_2(r\sin\alpha) + \lambda_1(r\cos\alpha) \\ \left(\frac{1}{2}I\right)\ddot{\alpha} &= 0 \end{aligned}$$

These four system equations in term of the six unknowns must be solved along with the two nonholonomic constraints, which we rewrite as follows:

$$\begin{aligned} \dot{x} &= -r\cos\alpha\dot{\gamma} \\ \dot{y} &= r\sin\alpha\dot{\gamma} \end{aligned}$$

Evaluating $\ddot{x}, \ddot{y}$,

$$\begin{aligned} \dot{x} &= -r\cos\ddot{\alpha} + r\sin\alpha\dot{\gamma}\dot{\alpha} \\ \dot{y} &= r\sin\ddot{\alpha} + r\cos\alpha\dot{\gamma}\dot{\alpha} \end{aligned}$$

We may express those Lagrangian multipliers as

$$\begin{aligned} \lambda_1 &= -mr\cos\ddot{\alpha} + mr\sin\alpha\dot{\gamma}\dot{\alpha} \\ \lambda_2 &= mr\sin\ddot{\alpha} + mr\cos\alpha\dot{\gamma}\dot{\alpha} + mg\sin\varphi \end{aligned}$$

Now substituting into the equations of motion we obtain,

$$\begin{aligned} m\ddot{x} + (mr\cos\alpha\ddot{\gamma} - mr\sin\alpha\dot{\gamma}\dot{\alpha} &= 0 \\ m\ddot{y} - mr\sin\alpha\ddot{\gamma} - mr\cos\alpha\dot{\gamma}\dot{\alpha} &= 0 \\ (I + mr^2)\ddot{\gamma} + mgr\sin\alpha\sin\varphi &= C \\ \left(\frac{1}{2}I\right)\ddot{\alpha} &= 0 \end{aligned}$$

The dynamic equation of the rolling wheel is given by

$$M(q)\ddot{q} + N(q,\dot{q}) = A$$

where $M(q) \in \mathbb{R}^{4\times4} and N(q,\dot{q}) \in \mathbb{R}^{4\times1}$ are the inertia matrix and the nonlinear terms respectively.

$$N = \Big(- mr\sin\alpha\dot{\gamma}\dot{\alpha}, -mr\cos\alpha\dot{\gamma}\dot{\alpha}, mgr\sin\alpha\sin\varphi, 0\Big)^T, \quad A = (0,0,C,0)^T$$

$$M = \begin{pmatrix} m & 0 & mr\cos\alpha & 0 \\ 0 & m & -mr\sin\alpha & 0 \\ 0 & 0 & mr^2 + I & 0 \\ 0 & 0 & 0 & \frac{1}{2}I \end{pmatrix}, \quad q = [x, y, \alpha, \gamma]^T$$

Condition of rolling up:

$$C \geq (mr^2 + I)\ddot{\gamma}_{min} + mgr\sin\alpha\sin\varphi$$

Let's consider,

$$\frac{1}{2}I\ddot{\alpha} = 0 \quad \text{then} \quad \dot{\alpha} = \omega_z, \quad \alpha = \omega_z t + \alpha_0$$

If we set $\omega_z = \dot{\alpha} = 0$,

$$\begin{aligned} m\ddot{x} + (mr\cos\alpha\ddot{\gamma} &= 0 \\ m\ddot{y} - mr\sin\alpha\ddot{\gamma} &= 0 \\ (I + mr^2)\ddot{\gamma} &= C - mgr\sin\alpha\sin\varphi \end{aligned}$$

For necessary condition of rolling up,

$$C \geq mgr\sin\alpha\sin\varphi \quad \Rightarrow \ddot{\gamma} = +ve \quad \Rightarrow \ddot{x} = +ve, \quad \ddot{y} = +ve$$

The direction of forward motion is α_0 and it rolls up an inclined plane ϕ

5.3.2 Method II : Change the initial velocities

Consider a wheel rolls along a straight line and then it hits an inclined surface. Assume that the wheel does not bounce at the moment of hitting and the wheel can remain perpendicular to the surface. We increase its angular velocity and linear velocity of the wheel center. Before collide with the surface, assume that rolling without sliding occurs.

$$\begin{aligned} F &= ma \\ I\ddot{\gamma} &= C - Fr \\ &= C - mra \\ \ddot{\gamma} &= \frac{C}{mr^2 + I}, \qquad for \quad a = r\ddot{\gamma} \end{aligned}$$

Its angular velocity and the velocity of the wheel are $\sqrt{\frac{2Cs}{Ir+mr^3}}$ and $\sqrt{\frac{2Crs}{I+mr^2}}$ respectively. After it collides with the surface based on the dynamic equations derived, the initial condition must be modified because $\dot{\gamma}_0, v_0$ are nonzero in this case now. Before the hitting on the inclined surface, we have

$$\begin{aligned} \ddot{y} &= \frac{rC - mr^2 g \sin\varphi}{mr^2 + I} \\ \ddot{\gamma} &= \frac{C - mrg \sin\varphi}{mr^2 + I} \end{aligned}$$

afterward we have,

$$\begin{aligned} \dot{y} &= \frac{rC - mr^2 g \sin\varphi}{mr^2 + I} t + v_0 \cos\varphi \\ \ddot{\gamma} &= \frac{C - mrg \sin\varphi}{mr^2 + I} t + \dot{\gamma}_0 \end{aligned}$$

When $\dot{y} = \dot{y}_{min}$

$$\begin{aligned} t &= \frac{(\dot{y}_{min} - v_0 \cos\varphi)(mr^w + I)}{rC - mr^2 g \sin\varphi} \\ y &= v_0 \cos\varphi t + \frac{1}{2}\Big(\frac{rC - mr^2 g \sin\varphi}{mr^2 + I}\Big) t^2 \\ l &= \frac{(mr^2 + I)(\dot{y}_{min}^2 - v_0 \cos\varphi)}{2(rC - mr^2 g \sin\varphi)} \end{aligned}$$

$$(v_0 \cos\varphi)^2 = \dot{y}_{min}^2 - \frac{2l(rC - mr^2 g \sin\varphi)}{mr^2 + I}$$

If $\dot{y}_{min} = 0$,

$$\begin{aligned} v_0^2 &= \frac{2l(mr^2 g \sin\varphi - rC)}{\cos\varphi^2 (mr^2 + I)} \\ l &= \frac{v_0^2 \cos\varphi^2 (mr^2 + I)}{2(mr^2 g \sin\varphi - rC)} \end{aligned}$$

5.4 Wheel rolls Down

Consider a wheel of radius r rolls down at rest and no torque applied to the system. A thin wheel with a rim wide enough to prevent toppling sideways is to roll down an inclined plane. The two nonholonomic constraint equations are qiven by

$$\begin{aligned} dx - r\cos\alpha d\gamma = 0 \\ dy - r\sin\alpha d\gamma = 0 \end{aligned}$$

By the same method, Lagrange undetermined multiplier λ,

$$\begin{aligned} \lambda_1 dx - \lambda_1 (r\cos\alpha) d\gamma = 0 \\ \lambda_2 dy - \lambda_2 (r\sin\alpha) d\gamma = 0 \end{aligned}$$

We may describe the configuration of the wheel in terms of four generalized coordinates: $q = [x, y, \alpha, \gamma]^T$. The Lagrange is become

$$\mathcal{L} = \frac{1}{2} m(\dot{x}^2 + \dot{y}^2) + \frac{1}{2} I\dot{\gamma}^2 + \frac{1}{2}\left(\frac{1}{2} I\right)\dot{\alpha}^2 + mg(\sin\varphi y - r\cos\varphi)$$

then the equations of motion are derived as follow:

$$\begin{aligned} m\ddot{x} - mg\sin\varphi &= \lambda_1 \\ m\ddot{y} &= \lambda_2 \\ I\ddot{\gamma} &= -\lambda_2 (r\cos\alpha) - \lambda_1 (r\sin\alpha) \\ \left(\frac{1}{2} I\right)\ddot{\alpha} &= 0 \end{aligned}$$

In addition we still have the constraint equations.

$$\dot{x} = r\cos\alpha\dot{\gamma}$$

$$\dot{y} = r \sin \alpha \dot{\gamma}$$

Evaluating $\ddot{x}, \ddot{y}$,

$$\begin{aligned} \dot{x} &= r \cos \ddot{\alpha} - r \sin \alpha \dot{\gamma} \dot{\alpha} \\ \dot{y} &= r \sin \ddot{\alpha} + r \cos \alpha \dot{\gamma} \dot{\alpha} \end{aligned}$$

We may express those Lagrange multipliers as

$$\begin{aligned} \lambda_1 &= mr \cos \ddot{\alpha} - mr \sin \alpha \dot{\gamma} \dot{\alpha} - mg \sin \varphi \\ \lambda_2 &= mr \sin \ddot{\alpha} + mr \cos \alpha \dot{\gamma} \dot{\alpha} \end{aligned}$$

Simple substitution will eliminate λ_1 and λ_2 from the equations.

$$\begin{aligned} m\ddot{x} - mr \cos \alpha \ddot{\gamma} + mr \sin \alpha \dot{\gamma} \dot{\alpha} &= 0 \\ m\ddot{y} - mr \sin \alpha \ddot{\gamma} - mr \cos \alpha \dot{\gamma} \dot{\alpha} &= 0 \\ (I + mr^2)\ddot{\gamma} - mgr \cos \alpha \sin \varphi &= 0 \\ \left(\frac{1}{2} I\right) \ddot{\alpha} &= 0 \end{aligned}$$

Integrating this equation we obtain,

$$\begin{aligned} \dot{\gamma} &= \frac{mgr \sin \varphi \sin(\omega_z t + z_0)}{(mr^2 + I)\omega_z} \\ \gamma &= -\frac{mgr \sin \varphi \cos(\omega_z t + z_0)}{(mr^2 + I)\omega_z^2} \\ \dot{x} &= \frac{mr^2 g \sin \varphi}{2(mr^2 + I)\omega_z} \sin 2(\omega_z t + z_0) \\ \dot{y} &= \frac{mr^2 g \sin \varphi \sin(\omega_z t + z_0)^2}{(mr^2 + I)\omega_z} \end{aligned}$$

which on integration yields,

$$\begin{aligned} x &= -\frac{mr^2 g \sin \varphi}{4(mr^2 + I)\omega_z^2} (\cos 2(\omega_z t + z_0) - \cos 2z_0) + x_0 \\ y &= \frac{1}{2} \frac{mr^2 g \sin \varphi}{(mr^2 + I)\omega_z} \left(t - \frac{\sin 2(\omega_z t + z-))}{2\omega_z} \right) + y_0 \end{aligned}$$

If $\dot{\alpha}$ is not equal to zero, the wheel will not move down the incline only but sideways.

$$\omega = z_0 = 0 \quad i.e. \quad \dot{\alpha} = 0 \quad \alpha = 0$$

By L'Hospital's rule that

$$\begin{aligned} \dot{x} &= \frac{g \sin\varphi}{(1 + \frac{I}{mr^2})} t \\ \dot{y} &= 0 \\ x &= \frac{g \sin\varphi}{2(1 + \frac{I}{mr^2})} t^2 + x_0 \\ y &= y_0 \end{aligned}$$

If the elevation is h,

$$\begin{aligned} \frac{g \sin\varphi}{2(1 + \frac{I}{mr^2})} t^2 &= \frac{h}{\sin\varphi} \\ &= \sqrt{\frac{2(\frac{I}{mr^2} + 1)h}{g \sin^2\varphi}} \\ \dot{x} &= \sqrt{\frac{2gh}{\frac{I}{1+mr^2}}} \end{aligned}$$

The forward velocity of rolling down wheel at rest is $\sqrt{\frac{2gh}{\frac{I}{1+mr^2}}}$.

5.4.1 Terminal velocity of rolling body down

Consider different kinds of body, each having the same mass and the same radius, are released from rest on an incline. Determine the velocity of each body after it has rolled through a distance corresponding to a change in elevation h.

$$v = \sqrt{\frac{2gh}{1 + \frac{I}{mr^2}}}$$

The same result should be get if the conservation of energy is obtained. The kinetic energy of rolling body are

$$\begin{aligned} \mathcal{T}_1 &= 0 \\ \mathcal{T}_2 &= \frac{1}{2} m v^2 + \frac{1}{2} I \omega^2 \end{aligned}$$

Table 5.1: Different moment of inertia

Sphere	$I = \frac{2}{5}mr^2$	$v = 0.845\sqrt{2gh}$
wheel	$I = \frac{1}{2}mr^2$	$v = 0.816\sqrt{2gh}$
Hoop	$I = mr^2$	$v = 0.707\sqrt{2gh}$

$$
\begin{aligned}
&= \frac{1}{2}mv^2 + \frac{1}{2}I\left(\frac{v}{r}\right)^2 \\
&= \frac{1}{2}\left(m + \frac{I}{r^2}\right)v^2
\end{aligned}
$$

The change of potential energy of rolling body is $\mathcal{U}_{1-2} = mgh$. By the principle of work and energy,

$$
\begin{aligned}
\mathcal{T}_2 &= \mathcal{T}_1 + \mathcal{U}_{1-2} \\
\frac{1}{2}\left(m + \frac{I}{r^2}\right)v^2 & \\
v^2 &= \frac{2gh}{1 + \frac{I}{mr^2}}
\end{aligned}
$$

different moment of inertia

Now we consider a frictionless block sliding through the same distances and compare the results with the velocity attained by previous different bodies. The velocity of a block is $v = \sqrt{2gh}$. We can make a conclusion that the velocity of the body is independent of both its mass and radius. However, the velocity does depend upon the quotient $K_e = \frac{I}{mr^2}$. It measures the ratio of the rotational kinetic energy to the translational kinetic energy. Thus the hoop, which has the largest value of k_e for a given radius r, attains the smallest velocity. At the same time, sphere has largest velocity compare with other two. However, the sliding block along a frictionless same slope, which does not rotate, so the velocity of block is larger than the sphere too. The velocity of body decrease as k_e increases.

Chapter 6

Summary

6.1 Contributions

An attempt has been made in this thesis to study the modeling, dynamics and controls of a single wheel robot either in the horizontal plane or on inclines that have not yet been studied in the past. Its dynamic represents much richer dynamics and deserves attention. It provides a complete study of the fundamental dynamics characteristic of a single wheel robot in a rough terrain. Our contributions can be summarized as follows:

- We have determined the dynamics and feedback controls of a single wheel robot rolling without slipping on a horizontal plane; The general rolling single wheel robot system, when the pendulum swinging motion included, have considered. During the model developing, variable reduction of the dynamics itself was applied to get a state variables of the system. When the internal mechanism swings, the stabilizing of the robot around vertical position and the tilting up of flywheel on the robot are investigated and also compared with the cases of rolling disk and simplified model of the robot proposed by Au . The requirements for simplification of the model was addressed. The preliminary experimental results are shown for the validation of the developed model. Some important parameters for the dynamics such as the moment of inertia and the effect of friction between the robot and the surface are addressed.

- We have established the general model of the single wheel robot on an inclined plane. While the pendulum swinging motion are neglected and the vertical offset of the actuation mechanism from the axis of the whole wheel is reduced from the dynamics. If we set l_1, l_2&θ to be zero, the dynamics are exactly same as Au proposed [45]. We pay much attention for study the balancing effect of the robot

on inclined plane when augment it a high spinning flywheel and also the gyroscopical stabilization of the robot . We have derived the kinematics and dynamics of a rolling disk and single wheel robot rolling without slipping on the inclined plane respectively. The dynamic model around the position perpendicular to the surface is linearized. The state feedback controller is proposed to stabilize the robot without falling on an inclined plane and the robot rolls up on an incline. The backstepping control is designed to balance the robot following a straight path with a general heading angle. A stimulation study between the rolling disk and the robot for rolling up and rolling down on an incline is compared. The feasibility and efficiency of the method is then validated by simulation study.

- We have addressed the condition of rolling up of the robot on an inclined plane from the system dynamics itself. A performance index, Safety Factor, is used to measure the robot's ability successfully to roll up a slope from its idling. And then, we have proposed some methods for planning of rolling up by tracking the robot's motion in different motion strategies when the condition of the rolling up is violated.

6.2 Future Works

In this paper, we had concentrated to study the modeling, dynamics and controls of a single wheel robot either in the horizontal plane or on inclines, mentioned as Section 6.1. There are some extensions of the work.

1. Path Following of the Single Wheel Robot on incline. We design a controller of the system for tracking the path of the robot either in line or circle on incline. The basic idea for controller can be adopted from [17] and [18]. In [2], Au proposed a line following controller of the single wheel robot to track any desired line on the ground. However, Au and Kanayama are suffered the limitation that the system is constrained on the flat plane. The angle of inclination on the slope should not be considered. The system are become singular easily if the angle of inclination are included in the dynamics.

2. Nonlinear control of a single wheel robot. We had proposed only the linear state feedback for controlling the system of a single wheel robot on ground and on incline. The global stability of the system can not be guarantee from the linearized model. The typical nonlinear control methods for the underactuated manipulators are violated due to the no existence of the off-diagonal terms of

the inertia matrix in the system dynamics. New nonlinear control system should be designed based on the coupling effect between the yaw and pitch motions in velocity sides.

3. Perform experiments of the real robot. We perform some experimental verification of the model of the robot on an inclined plane. The proposed feedback controller to the single wheel robot Gyrover is implemented.

Bibliography

[1] H. Arai and S. Tachi, "Position control of a manipulator with passive joints using dynamic coupling," *IEEE Trans. on Robotics and Automation,* vol. 8, no. 4, pp. 528-34, 1991.

[2] K. W. Au and Y. Xu, "Decoupled dynamics and stabilizaion of single wheel robot," *Proc. IEEE/RSJ Int. Workshop on Itelligent Robots and Systems,* vol 1, pp.170-176, 1999.

[3] K. W. Au and Y. Xu, "Path Following of a Single Wheel Robot," *Proc. IEEE Int. Conf. on Robotics and Automation,* to be appear, 2000.

[4] M. Bergerman, C. Lee and Y. Xu, "A dynamic coupling index for underactuated manipulators," *Journal of Robotic Systems,* vol. 12, no. 10, pp. 693-707, 1995.

[5] A. V. Beznos, et. al., "Control of autonomous motion of two-wheel bicycle with gyroscopic stabilisation," *Proc. IEEE Int. Conf. on Robotics and Automation,* vol. 3, pp. 2670-75, 1998.

[6] A. M. Bloch, M. Reyhanoglu and N. H. McClamroch, "Control and stabilization of nonholonomic systems," *IEEE Trans. on Aut. Control,* vol. 37, pp. 1746-1757, 1992.

[7] H. B. Brown and Y. Xu, "A single wheel gyroscopically stabilized robot." *Proc. IEEE Int. Conf. on Robotics and Automation,* vol. 4, pp. 3658-63, 1996.

[8] R. W. Brockett, "Asymptotic stability and feedback stabilization", *Progress in Math.*,Vol. 27, Birkhauser, pp. 181-208, 1983.

[9] Frank S. Crawford, "Rolling and slipping down Galileo's inclined plane: Rhythms of the spheres ," *Am. J. Phys,* 64(5), May 1996.

[10] S. Dubowsky and E. Papadopoulos, "The kinematics, dynamics and control of the free-flying and free-floating space robotic systems," *IEEE Trans. on Robotics and Automation,* vol 9, no. 5, pp. 531-43, 1993.

[11] R. Fierro and F. L. Lewis, "Control of a nonholonomic mobile robot: Backstepping kinematics into dynamics," *Journal of Robotic Systems,* vol. 14, no. 13, pp. 149-163, 1997.

[12] N. H. Getz, "Control of balance for a nonlinear nonholonomic non-minimum phase model of a bicycle," *Proc. ACC,* vol. 1, pp. 148-151.

[13] N. H. Getz and J. E. Marsden, "Control of an autonomous bicycle," *Proc. IEEE Int. Conf. on Robotics and Automation,* vol. 3, pp. 1397-1402, 1995.

[14] J. Hauser and R. M. Murray, "Nonlinear controllers for non-integrable systems: the Acrobot example," *Proc. ACC,* vol. 1, pp. 669-71, 1990.

[15] R. C. Hemmings, "Improvement in velocipede", *US. Patent, 92,528,* 1869.

[16] R. C. Johnson, "Unicycles and bifurcation," *Am. J. Phys,* 66(7), July 1998.

[17] Y. J. Kanayama and F. Fahroo, "A new line tracking method for nonholonomic vehicles," *Proc. IEEE Int. Conf. on Robotics and Automation,* vol. 4, pp. 2908-11, 1997.

[18] Y. J. Kanayama and F. Fahroo, "A circle tracking method for nonholonomic vehicles," *The Fifth IFAC Symp. on Robot Control,* vol. 2, pp. 551-558, 1997.

[19] Y. J. Kanayama, "Two dimensional wheeled vehicle kinematics," *Proc. IEEE Int. Conf. on Robotics and Automation,* vol. 4, pp. 3079-84, 1994.

[20] Y. J. Kanayama, Y. Kimura, F. Miyazaki, and T. Noguchi, "A stable tracking control method for a nonholonomic mobile robot," *Proc. IEEE/RSJ Int. Workshop on Intelligent Robots and Systems,* vol. 3, pp. 1236-41, 1991.

[21] P. R. Klarer, "Recent developments in the robotics all terrain lunar explorer rover (RATLER) program," ASCE Specialty Conference on Robotics for Challenging Environments, Albuquerque, NM, 1994.

[22] I. Kolmanovsky and N. H. McClamroch, "Application of integrator backstepping to nonholonomic control problems," *Proc IFAC Nonlinear Control Syst. Des. Symp.,* pp. 747-752, 1995

[23] I. Kolmanovsky and N. H. McClamroch, "Developments in nonholonomic control problems," *IEEE Control Systems Magazine,* vol. 15, no. 6, pp. 20-36, 1995.

[24] T. McGeer,"Passive dynamic walking," *Int. Journal of Robotics Research,* vol. 9, no. 2, 1989.

[25] R. M. Murray, Z. Li and S. S. Sastry, *A mathematical introduction to robotic manipulation,* CRC Press, 1994.

[26] R. Nakajima, T. Tsubouchi, S. Yuta and E. Koyanagi, "A development of a new mechanism of an autonomous unicycle," *Proc. IEEE/RSJ Int. Conf. on Intelligent Robots and Systems,* vol. 4, pp. 3658-63, 1997.

[27] G. C. Nandy and Y. Xu, "Dynamic model of a gyroscopic wheel," *Proc. IEEE Int. Conf. on Robotics and Automation,* vol. 3, pp. 2683-88, 1998.

[28] G. Oriolo and Y. Nakamura, "Control of mechanical system with second order nonholonomic constraints: Underactuated manipulators," *Proc. IEEE Conf. on Decision and Control,* vol. 3, pp. 1682-87, 1996.

[29] A. Palmer, "Modern Mechanix and Inventions," June 1935.

[30] E. Papadopoulos and S. Dubowsky, "Failure recovery control for space robotic systems," *Proc ACC,* vol. 2, pp. 1485-90, 1991.

[31] C. Rui and N. H. McClamroch, "Stabilization and asymptotic path tracking of a rolling disk," *Proc IEEE Int. Conf. on Decision and Control,* vol 4, pp. 4294-4299, 1995.

[32] F. Saito, T. Fukuda, and F. Arai, "Swing and locomotion control for two-link brachiation robot," *IEEE Control Systems Magazine,* vol. 14, no. 1, pp. 5-12, Feb., 1994.

[33] C. Samson, "Time-varying feedback stabilization of car like wheeled mobile robot," *Int. Journal of Robotics Research,* vol. 12, no. 1, pp. 55-64, 1993.

[34] N. Sarkar, X. Yun, and V. Kumar, "Control of mechanical systems with rolling constraints: Application to dynamic control of mobile robots," *Int. Journal of Robotics Research,* vol. 13, no. 1, pp. 55-69, 1994.

[35] A. Schoonwinkel, "Design and test of a computer stabilized unicycle," Ph.D. dissertation, Stanford Univ., 1987.

[36] Z. Sheng and K. Yamafuji, "Postural stability of a human riding a unicycle and its emulation by a robot," *IEEE Trans. on robotics and automation,* vol. 13, no. 5, pp. 709-20, 1997.

[37] S. J. Singh and D. H. Shin, "Position based path tracking for wheeled mobile robots," *Proc. IEEE/RSJ workshop on the Intelligent Robots and Systems,* vol. 1, pp. 386-91, 1989.

[38] M. W. Spong, "The swingup control problem for the acrobot," *IEEE Control Systems Magazine,* vol. 15, no. 1, pp. 49-55, 1995.

[39] A. Tayebi, M. Tadjine and A. Rachid, "Discontinuous Control Design for the Stabilization of Nonholonomic Systems in Chained Form Using the Backstepping Approach ," *Proc IEEE Int. Conf. on Decision and Control,* vol 5, pp. 3089-3090, 1997.

[40] S.J. Tsai, Enrique D. Ferreira, Christiaan J.J. Paredis, " Control of the Gyrover: A single-Wheel Gyroscopically Stabilized Robot," *IEEE/RSJ International Conference on Intelligent Robots and Systems,* vol. 1, no.1, pp. 178-184, 1999.

[41] D. W. Vos and A. H. von Flotow, "Dynamics and nonlinear adaptive control of an autonomous unicycle: theory and experiment," *Proc. IEEE Conf. on Decision and Control,* vol. 3, pp. 2670-75, 1989.

[42] K. Waldron, *The adaptive suspension vehicle,* MIT Press, 1989.

[43] Bong Wie, *Space vehicle: Dynamics and Control,* AIAA Education Series, 1998

[44] Y. Xu, K. W. Au, G. C. Nandy and H. B. Ben, "Analysis of actuation and the dynamic balancing for a single wheel robot," *Proc. IEEE/RSJ Int. Conf. on Intelligent Robots and Systems,* vol. 4, pp. 3658-63, 1998.

[45] Y. Xu, H. B. Ben and K. W. Au, "Dynamic mobility with single-wheel configuration," *Int. Journal of Robotics Research,* vol. 18, no. 7, pp. 728-738, 1999.

[46] Y. Xu and H. Y. Shum, "Dynamic control and coupling of a free-flying space robot system," *Journal of Robotic Sytems,* vol. 11, no. 7, pp. 573-89, 1994.

[47] Y. Xu and L. W. Sun, "Stabilizaton of A Gyroscopically Stabilized Robot on Inclined Plane," *Proc. IEEE Int. Conf. on Robotics and Automation,* to be appear, 2000.

[48] W. K. Yu, "Learning and Input Selection of Human Strategy in Controlling a Dynamically Stabilized Robot ," *MPhil Thesis,* The Chinese University of Hong Kong, 2000.

[49] X. Yun, "State Space Representation of Holonomic and Nonholonomic Constraints Resulting from Rolling Contacts," *IEEE international Conference on Robotics and Automation*, vol. 2, pp. 2690-2694, 1995.